A Comparative Palynofacies Study of Two Methods Used for Source Rock Validation

A Case Study From a Mississippian Succession on Spitsbergen

Master of Science Thesis

Tone Stoddart Hetland Hansen

Department of Earth Science

University of Bergen

June 2017

Abstract

This study is conducted on the analysis of twenty-nine kerogen slides of Tournasian and Visean age. The outcrop samples were collected from the Hoelbreen and Birger Johnsonfjellet Members in the Birger Johnsonfjellet section on Spitsbergen, Svalbard. The main aim of this study was to test two different methods for palynofacies analysis using the scheme after Bujak *et al.* (1977): point counting and a relative area measurement method using the free image analysis software ImageJ. A secondary minor aim was to evaluate the hydrocarbon source rock potential of the organic matter from the studied samples. All five kerogen types defined for this study (hylogen, melanogen, phyrogen, AOM and pseudoAOM) were present in the twenty-nine samples, and most of the material was dark brown in colour. A pre-study to assess the validity of visual estimation of relative areas was first conducted. The number of fields of view that should be analysed to get a reliable result was estimated and concluded leading to that 60 frames were analysed per sample. Images captured with a camera connected to a transmitted light microscope were analysed using both methods, and a total of 1789 frames and 16 266 particles were counted, and their area measured. Fluorescence analysis was also conducted in order to clarify the presence of *Botryococcus*. The kerogen groups hylogen and pseudoAOM dominates the samples, with an increased amount of phyrogen recorded towards the top of the studied succession. The kerogen groups melanogen and Amorphous Organic Matter (AOM) were both poorly represented in these samples which all were terrestrially derived. An increasing amount of *Botryococcus* was observed in the upper part of the succession in the Birger Johnsonfjellet Member. This is also observed in previous studies of this formation.The average result based on the 29 slides studied herein did not reveal any significant difference between the two tested methods, however, analysis of each individual kerogen group revealed important differences: this included variations within the individual kerogen groups as well as between the different groups. Based on the results obtained in this study area measurement is recommended to be a more accurate method than point counting for palynofacies analysis. The preliminary hydrocarbon estimation indicates that the Hoelbreen Member is predicted to have produced gas, and the Birger Johnsonfjellet Member, is regarded as oil prone.

Acknowledgements

This study is part of a project carried out by the University of Bergen and the FORCE industry consortium funded by AkerBP, Chevron, DEA, Faroe, Shell and VNG.

First and foremost, I want to thank my main supervisor Professor Gunn Mangerud, Head of Department of Earth Science at UiB, for all her guidance, motivation and for introducing me to palynology. Especially the kindness and understanding she has shown me in the last couple of weeks. I am also very grateful that she managed to fund the conference-trip to Houston, Texas. I also want to thank my co-supervisor Dr. Gilda Lopes for her invaluable assistance providing excellent guidance, advice, valuable discussions, and for helping me get settled in Dublin. Her door was always open which I am very grateful for. A special thank you goes out to co-supervisor, Emeritus Professor Geoffrey Clayton, visiting professor at the university of Sheffield, for teaching me Organic Petrology, Palynology & Palaeobotnay, as well as how to properly carry out a laboratory project, and making me feel welcome as a visiting student at Trinity College.

I would also like to thank Frank, for showing me his palynological lab, and teaching me how to prepare palynological slides, as well as providing a roof over my head, and first class suppers when visiting Dublin.

I also want to thank CIMP for the Student Travel Award to help offset the cost of attending the AASP meeting in Houston, Texas.

Many thanks to my family for all support and patience during this period.

Last, but not least, a huge thank you goes out to all my fellow geology students, especially everyone at "Midtrommet". All the hours spent studying together, and the fieldtrips are all moments which have given me friends for life, and I will be forever grateful.

Tone Stoddart Hetland Hansen
Bergen, June 2017

This thesis is dedicated to my mentor, hero and best friend, Karl Stoddart Hansen

"If a job's worth doing, it's a job worth doing well"

Table of contents

1. Introduction

The study of organic matter is, according to Tyson (1995), focusing on the interaction between the geosphere and the biosphere and has proven to be fundamental in the process of characterizing source rock potential and determining depositional palaeoenvironments (Mendonça Filho *et al*., 2012). Estimation of relative proportions of the various organic constituents of shale is a routine method for both the assessment of hydrocarbon source rock potential (petrographic kerogen typing) and the interpretation of palaeogeographic setting and depositional environments (palynofacies analysis). Several palynological methodologies can be used to estimate the different organic matter (OM) types for palynofacies analysis. Point counting and measurement of relative areas are frequently used methods in the industry and academic research. Point counting is the most commonly employed proxy method due to its speed and low cost. However, a major problem is that some common organic constituents, woody debris and amorphous organic matter, disintegrate easily both during natural transport and laboratory processing, potentially leading to serious over-representation in point count. Accurate measurement of relative areas of organic constituents provides a more precise approximation to relative volumes than point counting but it is more time consuming and requires relatively expensive equipment.

The hypothesis tested in this study considers whether the method of the measurement of relative areas based on image analysis is a more accurate method than point counting for estimation of relative proportions of organic matter (OM). This hypothesis already takes into account that visual estimation can introduce more errors, all the area measurement analysis is therefore done recurring to photographs of the fields of view.
The project involves estimation of relative proportions of organic particles in twenty-nine outcrop samples collected from Spitsbergen using both the point count and image analysis methods in photographed fields of view.

1.1 Aim of Study

This study is part of a larger partly industry funded research project at the University of Bergen, under the FORCE initiative. The project focuses on the Early Carboniferous biostratigraphy of the Barents Sea. Dating and reliable correlation tools are essential in every aspect of geological mapping and palaeogeographic reconstructions. The larger project is aimed at dating and correlating the clastic Mississippian (Early Carboniferous) Billefjorden Group using palynology, which has proven to be the only applicable paleontological technique in this part of the succession.

The Barents Sea has been open for exploration for more than 30 years, yet only two fields are producing today (NPD, 2016). There has been an increasing interest in the area, and since 2000, a total of 71 exploration wells have been spudded, and over 30 discoveries have been made (NPD, 2016).

According to the NPD (2016), the amount of standard cubic meters of oil equivalent related to sub Triassic undiscovered resources in the North- and Norwegian Sea is very small. However, there is a considerable amount of recoverable undiscovered resources of Sub Triassic age in the Barents Sea. Gaining a better understanding of the early Carboniferous succession can be beneficial for future hydrocarbon exploration (Fig. 1.1). The clastic-dominated Mississippian succession in the Barents Sea area contains palynological assemblages suitable for dating and correlation that can also serve as proxies for palaeoclimatic and paleogeographic interpretations.

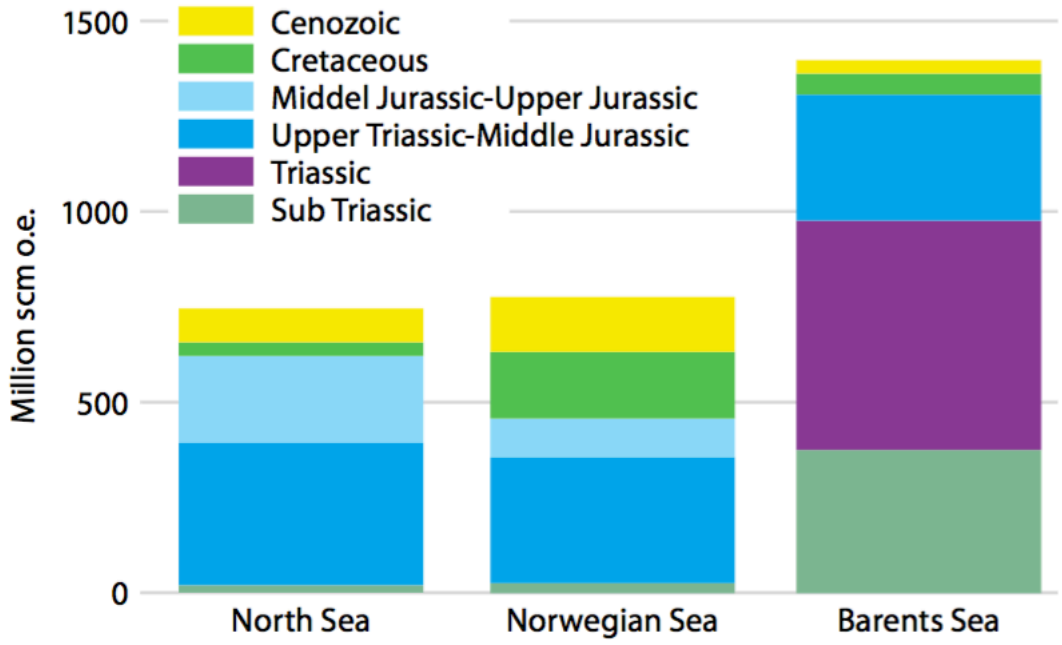

Figure 1. 1: Undiscovered resources for the different areas of the Norwegian Continental Shelf by geological stratigraphic level (From NPD, 2016).

This thesis aims at comparing two different methods of estimation of relative proportions of organic particles: point counting in the photographed field of view, where all particles are counted manually and assigned to a kerogen group, and relative area measurements where the area of each particle is measured in pixels through image analysis in the photographed field of view, using the software ImageJ. The software is not automatic, and the analysis is done by the interpreter. The samples are captured with a camera connected to the microscope, and each image is analysed manually using both methods. Visual estimation is a common method among geologists in the industry due to its low cost and high speed but errors in the estimation might lead to erroneous results. Visual estimation can also be too inaccurate because the method depends on the analyst experience.

1.2 Palynology

Palynology is the study of acid-resistant organic-walled microfossils (Traverse, 2007). When Hyde and Williams first introduced the term, in 1944, it was to describe the study of spores and pollen (Jansonius and McGregor, 1996; Traverse, 2007). Today the term is no longer restricted to spore and pollen analysis but concerns palynomorphs, a collective term introduced by Tschudy in 1961, to include all acid-resistant, organic-walled microfossils and acid resistant organic matter. Palynomorphs includes pollen, spores, algae, acritarchs and other groups with walls made of highly resistant organic molecules like sporopollenin, chitin or 'pseudochitin', which can endure palynological maceration (Traverse, 2007).

The material studied in this thesis is of Tournaisian and Visean age. The Barents Sea region moved from around 15 ° to 40 ° north during the Carboniferous, crossing several climatic zones. These changes in paleolatitudes and paleoclimates are reflected in the sedimentological succession and the palynological/paleobotanical record (Worsley and Nøttvedt, 2008). At the beginning of the Carboniferous, Spitsbergen and the Barents Sea were located near the equator, and due to the humid and warm climate in this area the vegetation developed rather rapidly. The fauna and flora developed immensely during the Devonian and Carboniferous time interval and typical huge forests with lycopodiophytes and euphyllophytes such as spermatophytes and monilophytes developed during the Carboniferous (Willis and McElwain, 2014). These dense forests covered much of the vast continental areas, and the remains of all this vegetation are part of most of today's coal deposits (Worsley and Nøttvedt, 2008).

Spores are unicellular reproductive parts of lower vascular plants such as Bryophytes (mosses) and Pteridophytes (ferns) (Jansonius and McGregor 1996; Traverse, 2007). Like other palynomorphs, spores are classified based on morphology. Spores of most plant groups are formed in fours, 'tetrads'. According to the tetrads configuration, a single spore will typically show a mark indicating where it was in contact with the other members of the tetrad. The mark can be 'y' shaped, commonly called 'trilete mark', or it can be a monolete spore which only include an "I" shaped mark (Traverse, 2007).

The palynomorphs range in size from 5-500 microns (μm), but mostly they occur within the range of 20-60 μm (Traverse, 2007). This is within the silt fraction (3.9-62 μm), and why palynomorphs are found embedded within sedimentary rocks. Due to their resistant wall structure, palynomorphs can endure palynological maceration and are very resistant to degradation during transport and diagenesis (Traverse, 2007). Palynomorphs are useful index fossils due to their high diversity, rapid evolution and widespread distribution. Also, they are the only fossil group that can be used to correlate both marine and terrestrial strata as they often are wind or water transported and therefore are deposited in both environments (Traverse, 2007).

1.3 Palynofacies and Kerogen Studies

Muller (1959) discovered that studying the particulate organic matter (POM) such as palynomorphs, cuticles or woody tissue present in organic rich sedimentary rocks, remaining after palynological preparations, could provide valuable information in the interpretation of facies, as well as palaeoenvironmental and palaeogeographic reconstruction (Muller, 1959; Tyson, 1993, 1995; Batten and Stead, 2005).

Muller's work on the correlation between the distribution of palynomorphs and depositional facies led Combaz to introduce the concept of palynofacies as an area of expertise in 1964 (Tyson, 1993, 1995; Batten and Stead, 2005). Initially, the term regarded all organic material present in palynological preparations but ever since, new authors have developed the definition and classification of the concept (Ercegovac and Kostić, 2006). Tyson (1995) established the modern concept of palynofacies, stating that it included all organic matter found in sediment which reflects a certain environment or process (Batten and Stead, 2005). Today, it is agreed upon that, palynofacies analysis is the study of the total particulate organic matter (POM) present after maceration and mounting using standard palynological preparation methods, without oxidation (Tyson, 1993, 1995; Ercegovac and Kostić, 2006; Mendonça Filho *et al.,* 2012).

Organic matter (OM) is found in most modern sediments, as well as in old sedimentary rocks. According to Durand (1980), OM can be divided into two constituents, kerogen and bitumen. Kerogen includes both terrestrial and marine derived OM and will therefore have different chemical compositions depending on the source type. Kerogen is the organic matter that is insoluble in the usual organic solvents, while the soluble part of the OM is called bitumen (Durand, 1980).

The classification of kerogen is based upon morphology and state of preservation (Tyson, 1995; Batten and Stead, 2005; Mendonça, Filho *et al.,* 2012). Several classification systems have been developed, and may be applied in this work, but it is important to choose a classification scheme which provides information about all the variables needed to respond to the main aims of the study (Mendonça, Filho et al., 2012). In the following paragraphs, some of the most known kerogen classification systems are presented, including the one used in this study.

One of the earlier publications on palynological kerogen classifications is Staplin (1969). He divided the organic matter into two categories; 'primary materials' and 'modified materials' (Tyson, 1995). Primary materials comprise cuticles, sporomorphs, lignified wood fragments, charcoal, resins, freshwater phytoplankton and marine organisms (Tyson, 1995). The second group included 'unorganized amorphous sapropelic' material which is commonly known as amorphous organic matter (AOM), 'platey translucent brittle amber' and reworked 'platey nearly inert modified cuticular remains' (Tyson, 1995). This classification scheme also distinguishes 'thermal transformation products' (heat-darkened particles analogous to the other materials) (Tyson, 1995). A big flaw with this classification is the interpretation of all AOM as 'sapropelic', without being able to distinguish the origin of the AOM (Tyson, 1995).

Another palynological kerogen classification is the one after Combaz (1980) which is a more detailed scheme (Tyson, 1995). The palynomorph and amorphous components are described in greater detail and the structured kerogen is divided into 19 different sub-groups with amorphogen being divided into 5 sub-groups (Tissot and Welte, 1984; Tyson, 1995). According to Tyson (1995) the description of the amorphous groups is not complete, lacking well-defined criteria, and fluorescence observations.

Batten and Stead (2005) concluded that the terminology for palynomorphs recognisable in reflected light is generally agreed upon, the problem, however, is for the non-palynomorph components. They distinguished between palynomorphs and non-palynomorph components in their scheme. The non-palynomorph group divides between structured organic matter (STOM) and unstructured organic matter (USTOM). STOM includes phytoclasts and zooclasts, while USTOM comprises amorphous organic matter (AOM) of both terrestrial and aquatic origin, gelified matter, resins and solid bitumen (Batten and Stead, 2005). The phytoclasts group covered material such as wood, charcoal, cuticles, filaments and fungal hyphae, while zooclasts are used for egg cases and parts of beetle carapaces (Batten and Stead, 2005). This classification scheme is used frequently in coal petrology (Batten and Stead, 2005).

One of the most used palynofacies schemes was presented by Tyson (1993, 1995). The classification system can be used to determine the origin of the organic matter, relative percentages of different constituents and their state of preservation, the organic matter potential for hydrocarbon generation, the depositional palaeoenvironments, as well as, the degree of thermal alteration of the organic matter. Tyson (1993, 1995) divides the particulate organic components into three main categories that can be recognised in transmitted white light microscopy presented in figure 1.2. The palynomorph group includes organic-walled constituents that can endure palynological preparation, the phytoclast group includes structured organic matter derived from higher plants or fungi, and the amorphous organic matter (AOM) group, which refers to all structureless matter derived from non-fossilizing algae (Fig. 1.2) (Tyson, 1993, 1995). The results from palynofacies analysis using Tyson's (1993, 1995) scheme is normally plotted in ternary diagrams that can be adapted according to the main aim of the study. One of the most used ternary diagrams is the AOM-Phytoclast-Palynomorph (APP) ternary plot where kerogen assemblages have been divided into nine marine depositional environments, as shown in figure 1.3.

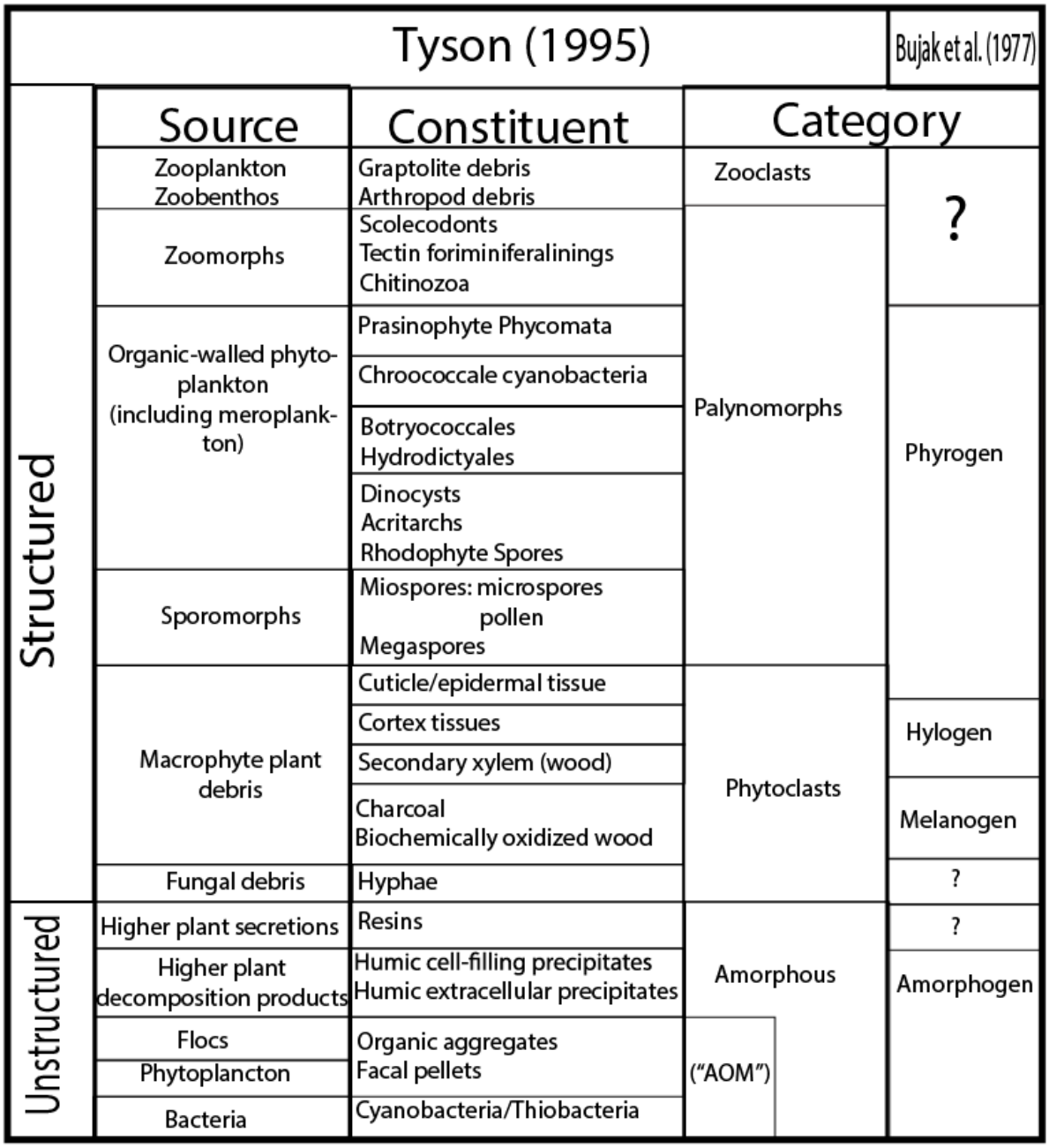

Figure 1. 2: Correlation between published kerogen classification after Tyson (1993) and Bujak *et al*. (1977). The classification scheme is also indicating biological source. The question marks in the classification after Bujak *et al*. (1977) represents constituents not included in this scheme (Modified from Tyson, 1993).

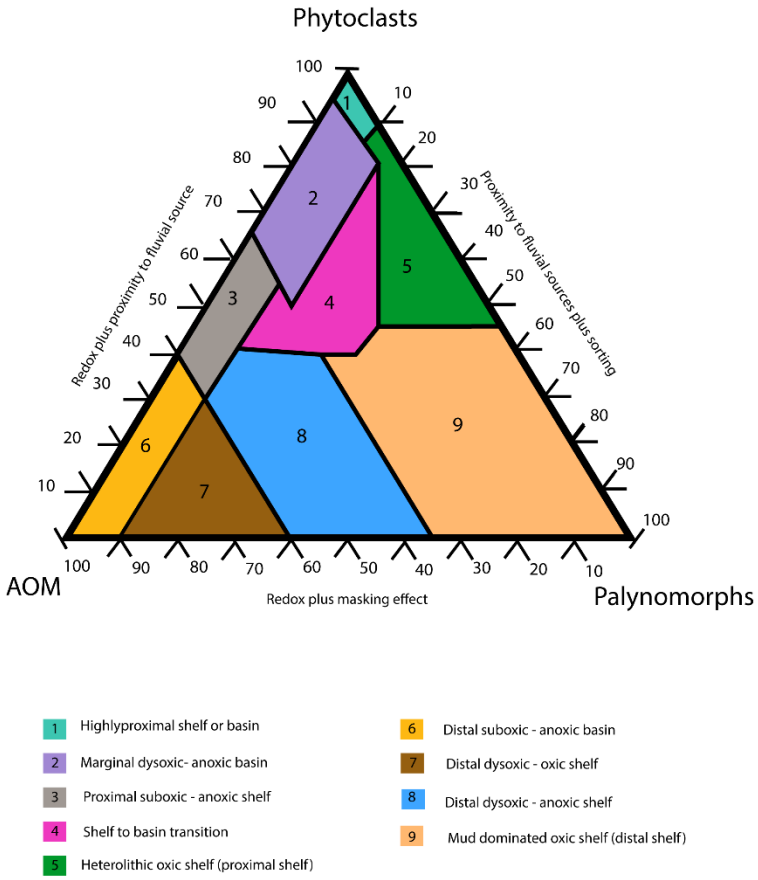

Figure 1. 3: APP Ternary plot showing nine different shallow-marine facies. Adapted from Tyson (1993, 1995).

In this project, the kerogen classification scheme of Bujak *et al.* (1977) was used with minor modifications (Fig. 1.4). The classification of Bujak *et al.* (1977), has been widely used to study hydrocarbon source rock potential. One advantage with this scheme is that the OM categories used do not depend on identification of the biological affinities of the particles but only on the shape, colour and size of the different components, which will minimize the risk of subjective errors by the interpreter. Also, it is a very simple scheme to use, with a reduced number of categories that use palynological kerogen slides.

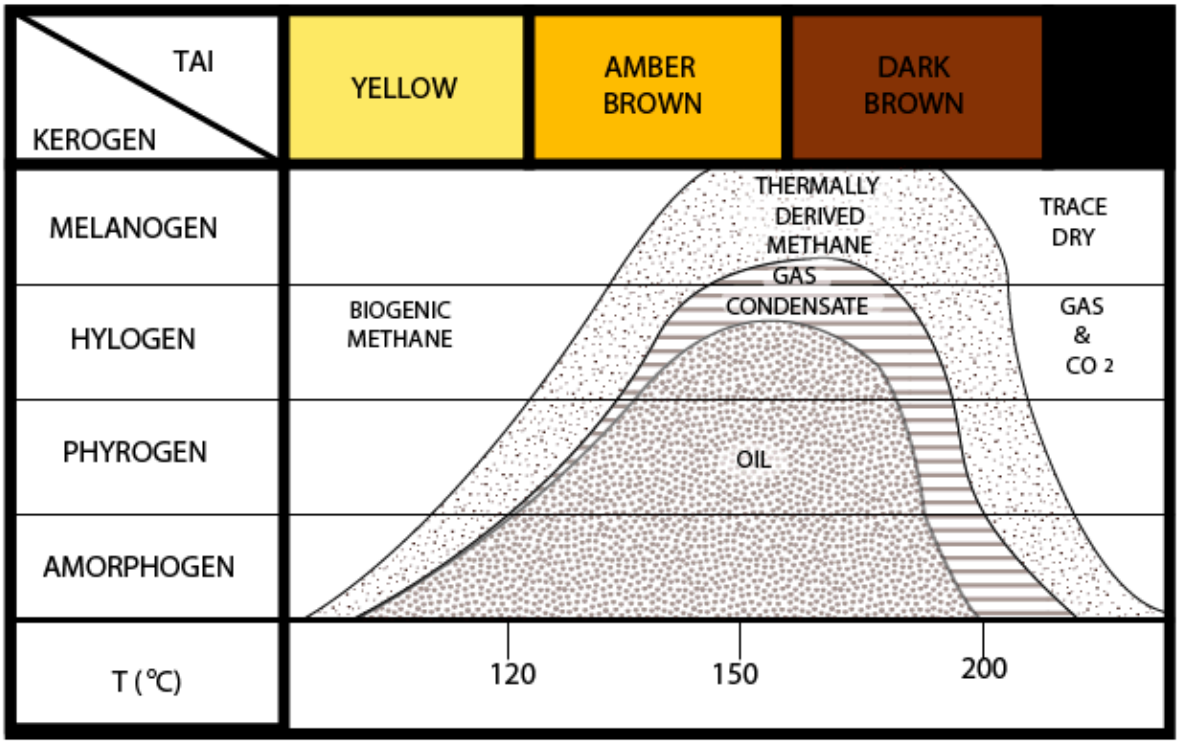

Figure 1. 4: Illustration of the relationship between kerogen type, spore colour, hydrocarbon generation and temperature. (Modified from Bujak *et al.* 1977). TAI – Thermal alteration index. T – Temperature.

The original classification divides the kerogen into four groups based on morphology: Melanogen, Hylogen, Phyrogen, and Amorphogen. Melanogen covers all the opaque material seen in transmitted light and has almost no hydrocarbon source potential (Fig. 1.4). The hylogen group includes non-opaque organic matter with a woody origin and is regarded as gas prone (Fig. 1.4) (Bujak *et al.,* 1977). Phyrogen comprises all non-opaque plant material, which is not of a woody origin, such as spores, plant cuticles and pollen (Fig. 1.5) (Bujak *et al.,* 1977). Depending on the pressure and temperature conditions the OM comprised in this group can be either gas or oil prone (Fig. 1.4). Amorphogen, also referred to as "amorphous organic matter" (AOM) is used to refer to all the organic matter lacking any form of structure (Fig. 1.5). This kerogen group is according to Bujak *et al.* (1977) mostly oil prone (Fig. 1.4).

For this project, a fifth kerogen group was introduced - pseudoAOM (pseudo amorphous organic matter). This term has previously been used in the literature by Tyson (1993). According to this author, this material corresponds to degraded OM that could originally have been either hylogen or phyrogen, and thus it can be both oil and gas prone (Fig. 1.4). PseudoAOM differs from AOM because it is not truly amorphous, and some structure can

still be observed (Fig.1.5). The distinction between AOM and PseudoAOM can often be difficult. However, classifying these is possible with the use of microscopes with UV-fluorescence.

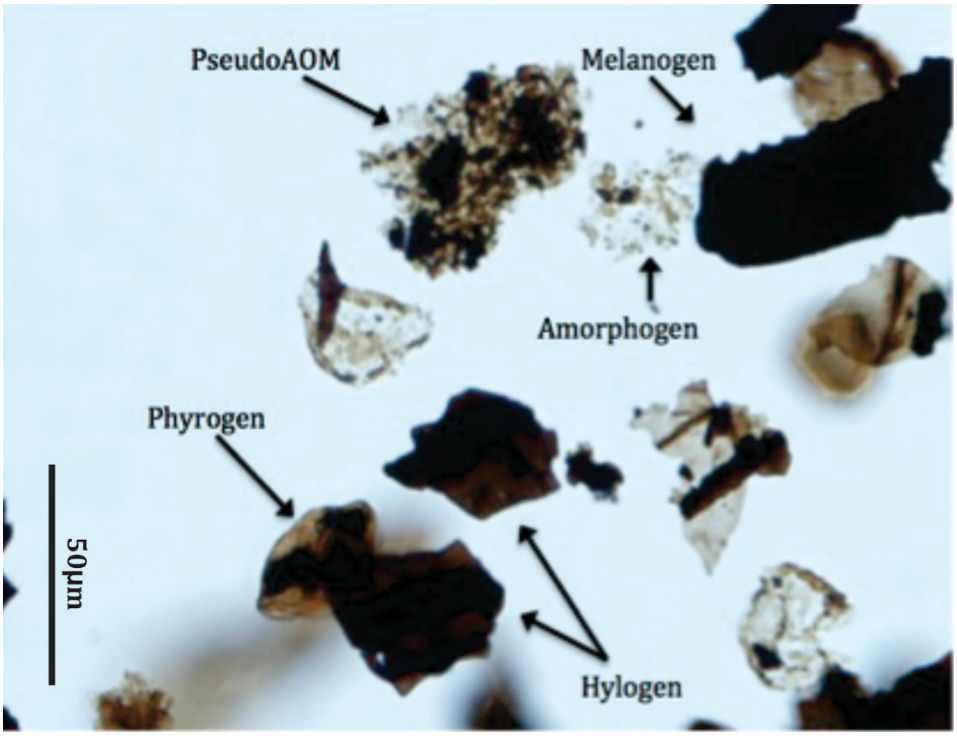

Figure 1. 5: The five different kerogen groups after Bujak *et al.* (1977).

2. Geological Framework

2.1 Spitsbergen and the Barents Sea Geological and Geographic Context

The Barents Sea continental shelf is located in the north-western corner of the Eurasian plate. In the west, the shelf is bordered by the Norwegian-Greenland Sea, it extends up to Svalbard and Franz Josef Land in northwest and northeast, is bound by the Russian island Novaya Zemlya in the east, and extends down to the Russian and Norwegian coast in the south (Fig. 2.1) (Faleide *et al.,* 1984; Doré, 1991, 1995; Worsley, 2008). The entire shelf covers an area of approximately 1.3 million km^2 with the average depth of the shelf sea being 230 m (Sakshaug *et al*., 1994). The Svalbard archipelago is comprised of uplifted and exposed areas covering 62 700 km^2 of offshore area, representing less than 5 % of the entire Barents Sea area (Worsley *et al*., 1986; Mørk *et al*., 1999; Worsley, 2008). The archipelago has proven to be a good analogue of the offshore geology in the surrounding basins (Mørk *et al*., 1999). The largest island of the archipelago, Spitsbergen is located in the north-western corner of the Barents shelf and has proven to be an important location for understanding the late Paleozoic history of the Barents Sea (Cutbill and Challinor, 1965).

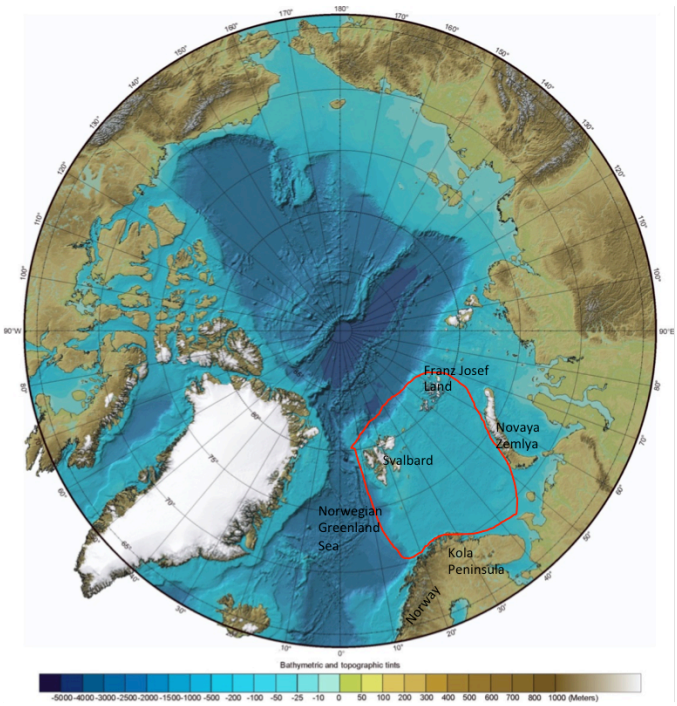

Figure 2. 1: Simplified bathymetric and topographic map of the Barents Sea (Indicated by red square). Modified from Jakobsson *et al*., 2008.

The Barents Shelf can be divided into two main geological provinces, the western province is dominated by several smaller basins and platforms, while the eastern province is made up of two large basins known as North- and South Basin (Fig.2.2) (Faleide *et al.*, 1984; Worsley, 2008). As mentioned in chapter 1.1 there are considerable amounts of recoverable undiscovered resources of sub-Triassic age in this area. Gaining a better understanding of these basin structures and their hydrocarbon potential is therefore important.

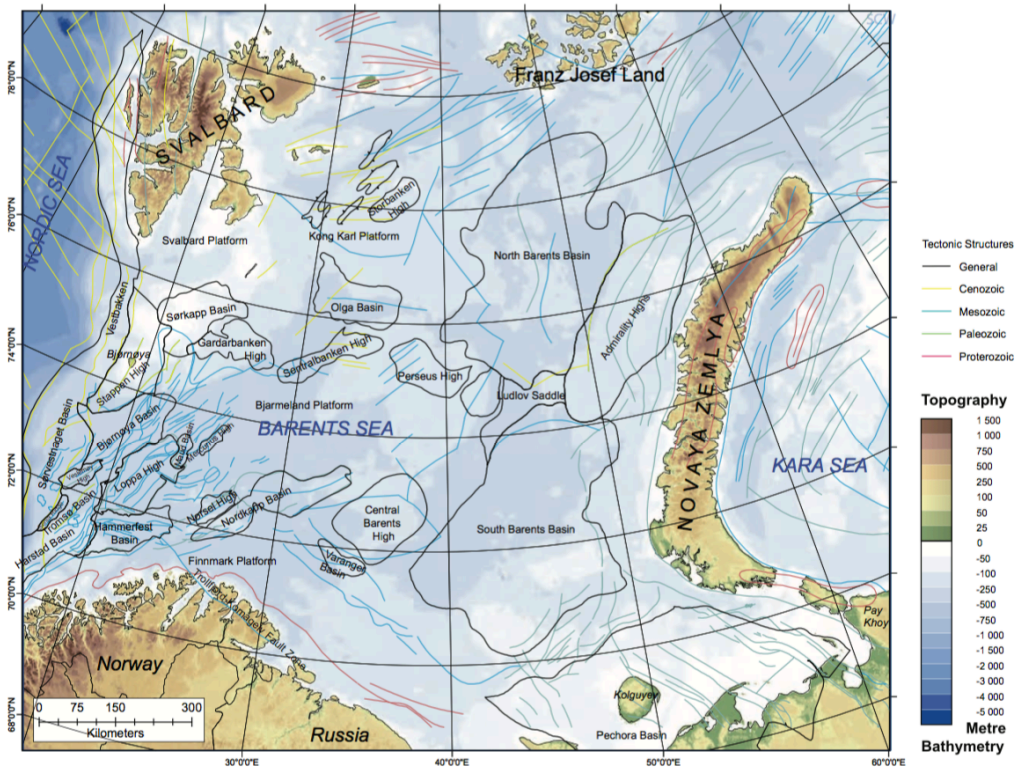

Figure 2. 2: Illustration of the two main geological provinces from the Barents Sea; the eastern province consisting of the North- and South Barents Basin, and the western region comprised of several smaller basins and platforms (From Smelror *et al.*, 2009).

2.2 Tectono-Statigraphic Context, Palaeoclimates and Palaeogeography During the Carboniferous

The siliciclastic succession studied in this project comprises Tournaisian and Visean rocks, of the Mississippian period. Published paleoenvironmental studies such as Van der Zwan (1981), Van der Zwan *et al*. (1985) and Jäger and McLean (2008) have provided valuable information in the reconstructing of palaeoenvironments in the Visean. At the beginning of the Carboniferous, Spitsbergen and the Barents Sea areas were located near the equator, on the northern part of the Euramerica continent (Fig.2.3). During this time, this region was under humid and warm climates that led to the development of luxurious vegetation. The fauna and flora developed immensely in the transition between the Devonian and Carboniferous. Typical huge forests with lycopodiophytes and euphyllophytes such as spermatophytes and ferns developed during the Carboniferous (Willis and McElwain, 2014). As described in chapter 1.2, it was the remains of these dense forests, covering most of the continental areas that forms most of today's coal deposits (Worsley and Nøttvedt, 2008). *Botryococcus* algae is colonial freshwater algae, indicative of a terrestrial environment which spans from Carboniferous to present day. The algae have a high lipid content, and is therefore regarded as oil prone (Tyson, 1995; Mendonça Filho *et al.,* 2012). The Barents Sea region moved during the Carboniferous from around 15 ° to 40 ° north, crossing several climatic zones. These changes in paleolatitudes and paleoclimates are reflected in the sedimentological succession and the palynological/paleobotanical record. Accordingly, the study of these records can provide important information about the palaeoenvironments, hydrocarbon potential and depositional settings for this region (Worsley and Nøttvedt, 2008).

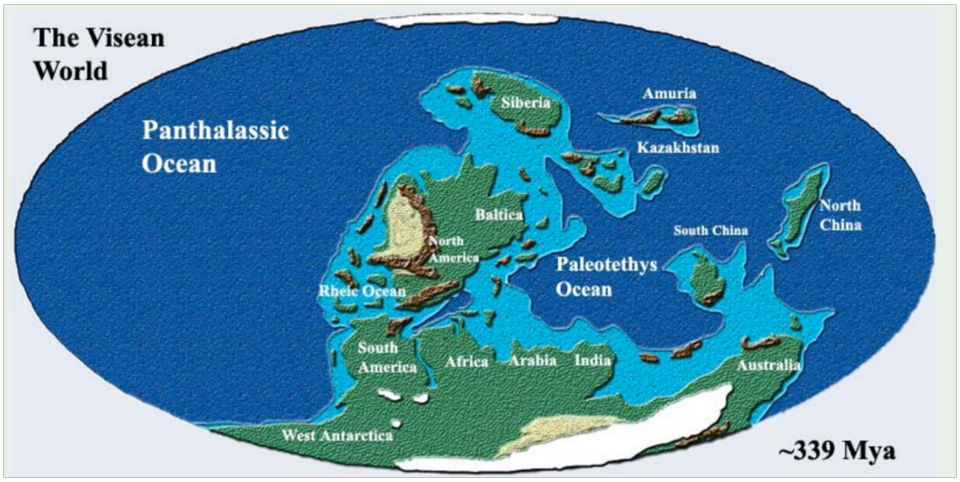

Figure 2. 3: Paleogeographic map, of the Visean, Mississippian, Carboniferous. (From Palaeos, 2002).

From early to mid-Carboniferous the region was under an extensive regime which resulted in the development of several basins with a half-graben geometry (Samuelsbeg & Pickard, 1999; Worsley & Nøttvedt, 2008). The Barents Sea region was part of a large E-W oriented intracratonic basin located on the northern part of Euroamerica (Worsley *et al*., 1986; Samuelsberg & Pickard, 1999; Larssen *et al*., 2005) (Fig. 2.4). In Spitsbergen, the basins are NNW-SSW oriented and follow older "Caledonian" basement structures (Pickard *et al*., 1996; Samuelsberg & Pickard, 1999; Worsley *et al*., 2008). The structure of these tectonic depressions varies from large, deep basins during the early Carboniferous to narrow, subsided basins which developed during Mid-Carboniferous (Worsley & Nøttvedt, 2008).

The Carboniferous deposits show a similar development in different parts of the Barents Sea. This development reflects the changes in crustal movement, climate and sea level changes during this period, which resulted in distinctive deposits. The early Carboniferous sandstones, shales, local coals and conglomerates, are followed upwards by mid-carboniferous red sands and mudstones, which are capped by limestones and evaporites formed in late Carboniferous and early Permian (Worsley & Nøttvedt, 2008) (Fig. 2.4).

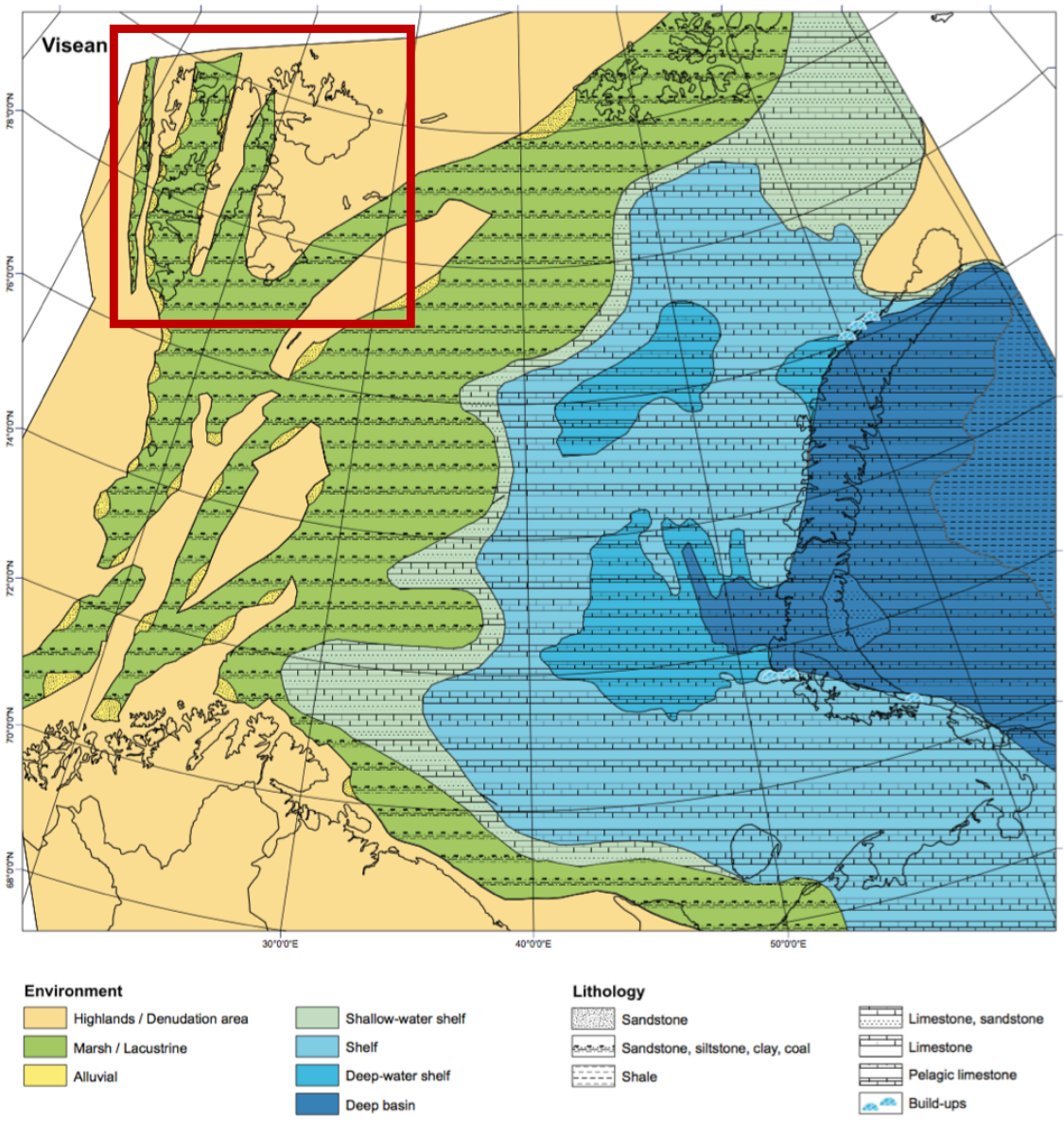

Figure 2. 4: Palaeogeographic map illustrating the depositional environments from Visean, Carboniferous. Spitsbergen is located within the red square. Modified from Smelror *et al.* (2009).

The studied section is represented by the Billefjorden Group. This continental siliciclastic succession was first described by Cutbill & Challinor in 1965. The deposition of this succession started during the Upper Devonian and continued during the Tournaisian and Visean, being interrupted only at the beginning of the Serphukovian, where a regional unconformity is known (Dallmann *et al.,* 1999).

In the Billefjorden area, the group has been divided into the Hørbyebreen and Mumien formations. The Hørbyebreen Formation comprises the Triungen and Hoelbreen members. In the studied section, the Triungen Member unconformably overlies folded basement strata and consists of lacustrine and flood-basin shales interbedded within fluvial sandstones and conglomerates (Fig. 2.5) (Mørk *et al.* 1999). Following upwards, a stratigraphic break separating the Triungen Member from the overlying Hoelbreen Member was recognized, mainly due to palynological data (Nøttvedt *et al.,* 1992). Playford (1962, 1963) described two different palynomorph assemblages within the formation that was observed in a close by section, and the transition between them occurs within the Hoelbreen Member. This transition is, however, not reflected in the lithology (Fig. 2.5) (Cutbill *et al.* 1976). Existing formation boundaries within the Billefjorden Group are not easy to map, and lacks major lithological changes.

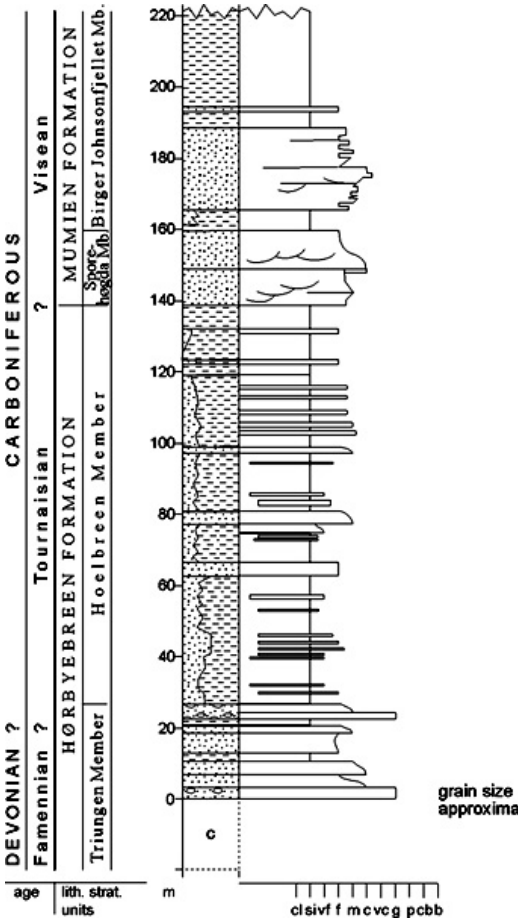

Figure 2. 5: Stratigraphic succession of the Billefjorden Group. Stratotype for Hørbybreen Formation, Hoelbreen Member Locality: Ferdinandbreen (Mumien NE) from: Gjelberg, J.G. (unpubl.). http://nhm2.uio.no/norges/litho/svalbard/paleo.htm

The overlying Hoelbreen Member is comprised of shales and mudstones, interbedded with thin sandstone layers, coals, coaly shale and clay ironstones representing floodplain to flood basin deposits. Some thicker sandstones units are also present, these represent fluvial channels (*Mørk et al.* 1999). Overlying the Hørbyebreen Formation lies the Mumien Formation. The Formation is divided into two members: Sporehøgda and Birger Johnsonfjellet members. The base of the Mumien Formation comprises several trough cross-stratified sandstone levels of the Sporehøgda Member (Fig. 2.5). Units within the member can be bound by a curved erosion surface that represents braided stream deposits (Gjelberg and Steel, 1981; Mørk *et al.,* 1999)

The boundary between the Sporehøgda Member and the overlying Birger Johnsonfjellet Member is placed below the first shale level that overlies the braided stream deposits of the Sporehøgda Member (Fig. 2.5) (Mørk *et al*., 1999). This part of the succession is dominated by dark shales, coaly shales and dark grey claystones interbedded with thin siltstones and thin coal layers, and plant root horizons have been reported. According to Abdullah *et al.* (1988) the coal seams are mostly composed of algal material and could potentially be a good source rock for oil and gas. Birger Johnsonfjellet Member sediments deposition was done in a flood basin and lake deposits environment (Mørk *et al*., 1999). The top of Birger Johnsonfjellet Member is truncated by the unconformably overlying Gipsdalen Group.

3. Materials and Methods

A brief description of the samples and how they were collected are included in this chapter. This is followed by a sub-chapter with a brief explanation of how the kerogen slides were processed, as well as the microscopy settings used, before the point counting method is explained. A pre-study was preformed previously to this study, the motivation for this and the findings from the pre-study are presented in this chapter. The complete workflow of how to do the area measurement by using the image analysis software ImageJ is thoroughly presented. The assessment of how many field of view which should be analysed is explained together with some general description and challenges during the analysis of the slides.

3.1 Samples Collection

The samples used in this study were collected in Birger Johnsonfjellet area, Spitsbergen, by scientists from the University of Copenhagen, Denmark. The material was obtained as part of a collaboration between the Department of Earth Science, University of Bergen and the University of Copenhagen and the Natural History Museum in Denmark. These samples are also being used as a part of a PhD-project at the University of Copenhagen, where other organic parameters are being evaluated. The samples are outcrop material collected approximately at 78°44'38"N, 16°18'35"E. Twenty-nine samples were collected in an interval between 58.5 m to 255 m, above basement rocks. The standard precautions were carefully followed to avoid contamination. Each sample contained 50-100 grams of either shale or siltstone from the Hørbyebreen and Mumien formations (Fig. 3.1). No samples were collected from the sandstone levels. Due to partial scree cover, the material from the upper part of the section was difficult to collect. A stratigraphic log was made at the location and the samples were measured accordingly (Fig. 3.1).

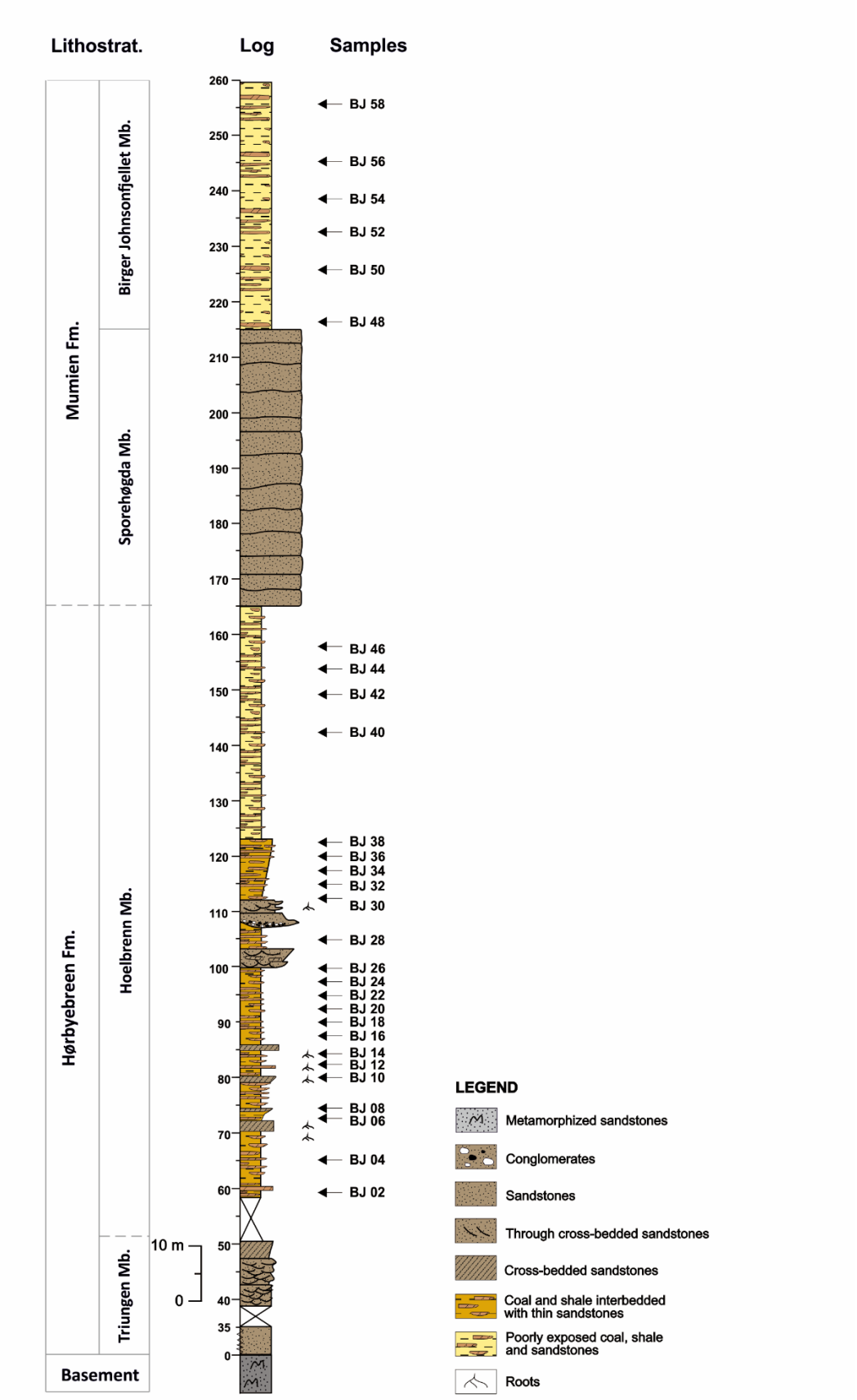

Figure 3.1: Lithostratigraphic log indicating the stratigraphy and the location of the different samples. Courtesy of Gilda Lopes and adapted from Kristensen (personal comm.).

3.2 Kerogen Slides Preparation

The Palynological Laboratory Services Ltd, United Kingdom, processed the samples using standard palynological preparation techniques after Doher (1980). The samples were not prepared by the author, however, in one of the exchange courses taken during the first year of this master in Trinity College, University of Dublin, the author went through all the preparation process in the palynological laboratory (Fig. 3.2).
The following summarized procedure was applied:

The preparation process can be divided in two phases. The first phase is to chemically dissolve the minerals of the matrix in the sample, so that the organic matter can be extracted, and the next step includes the oxidation of the material so that it can be better identified in transmitted light microscopy (Jansonious and McGregor, 1993; Traverse, 2007). In this study two sets of slides were made: one set of kerogen slides and one set of palynological slides. The first was used in this thesis where the total organic matter in the slide is studied without altering the chemical and physical properties of the material. The second set of slides were used in the larger palynostratigraphic project referred to in chapter 1.1.

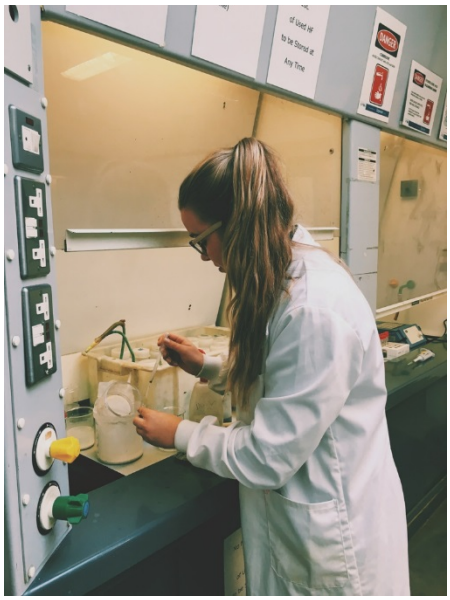

Figure 3. 2: Palynological preparation process at Trinity College, University of Dublin.

The first step in the preparation process is to clean the surface of the material; this can be done by cleaning it in running water using a brush to scrub before blowing it with compressed air. The sample can also be scraped with a knife or it can be placed in distilled water for 10 minutes, while stirred occasionally (Doher, 1980). After the initial cleaning the sample is dried, crushed into smaller fragments and weighed (Doher, 1980). The next step in the preparation process is carbonate removal, which is done by adding 10 % hydrochloric acid (HCl) to the sample in a beaker, this step needs to be repeated if it failed to remove all the carbonate (Brown, 1960; Doher, 1980; Traverse, 2007) (Fig. 3.3). It is important that all the carbonate is dissolved in this step because it removes the Ca^{+} ions, which could form calcium fluoride (CaF_2) if reacted with Hydrofluoric acid (HF), which is

added in the next step of the preparation. Before HF is added, the sample containing HCl is neutralized by using distilled water to remove all acid. The next step is to remove Silicates and for this purpose HF is used. Again, the sample is neutralized using distilled water, it is especially important that this is done with great care, as HF is extremely corrosive (Brown, 1960; Doher, 1980; Traverse, 2007).

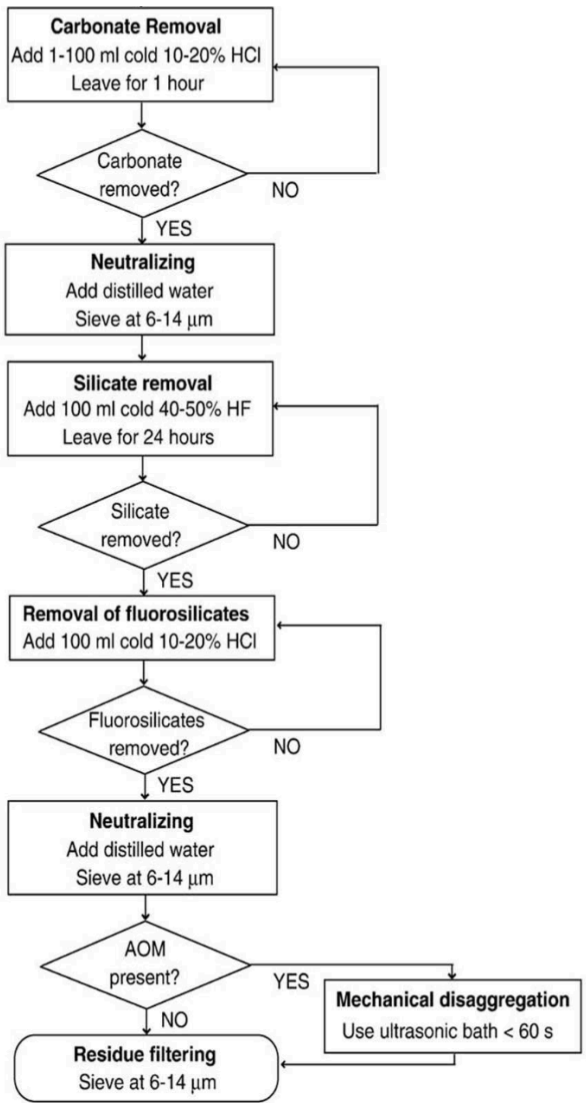

Figure 3. 3: Flow chart of the standard palynological preparation technique, modified from Mertens *et al*. (2009).

The final step is to sieve the sample at ideally 6-14 µm, before it is mounted onto a glass slide (Fig. 3.3).

There are additional treatments such as ultrasonic bath to ease the sieving and to prevent organic matter to block the sieve, centrifuging to remove unwanted organic material and heavy minerals, and staining to aid the observation of palynomorphs, none of which was done on the slides used in this study. The treatments mentioned above could potentially break down or destroy the organic matter, and are therefore, never performed on kerogen slides that will be used for palynofacies analysis.

3.3 Microscopy Setting

All frames were photographed using an AxioCam ERc 5s camera mounted to a Zeiss Axioplan transmitted light microscope (Fig. 3.4). The images of the organic matter were obtained using the Zeiss Zen software (2012, blue edition). A 40x objective, giving a 400x magnification was used for all images.

Figure 3. 4: The Zeiss Axioplan transmitted light microscope used to analyse the samples in this study. The AxioCam 5s camera used to capture all the images that were analysed is indicated with a red arrow.

A Leica fluorescence microscope with orthoplan UV light was also used to analyse the slides (Fig.3.5). This was done on all the frames analysed in this study, mainly to distinguish pseudoAOM from AOM, as AOM is of bacterial or algal origin and will therefore fluoresce a yellow colour (McPhilemy, 1988; Tyson, 1995). The fluorescence microscope was also used to tell the difference between pseudoAOM and the algae *Botryococcus* as the latter will also fluoresce a bright yellow colour when exposed to fluorescence light (McPhillemy,1988; Mendonça Filho *et al*., 2012).

Figure 3. 5: The Leica microscope with orthoplan UV light used for this study.

3.4 Point Counting Method

Images used in the point counting method were captured with a AxioCam ERc 5s camera as described in subchapter 3.3. The point counting method is a quantitative approach, where all the objects present in a frame were identified manually, counted and assigned to one of the five kerogen groups modified after Bujak *et al.* (1977). An example of how the point counting was carried out by category, in frame 10 in slide BJ42 is illustrated in figure 3.6 and table 3.1. Each particle was counted manually and assigned to one of the five kerogen groups. In this example, there are two particles split between two frames, the PseudoAOM particle in figure 3.6 was counted in the presented frame (Fig. 3.6), as it covers a bigger area in this frame. The particle within the red square was counted and assigned to frame 9 (the previous frame) since the particle covered a larger area in that frame.

Table 3.1 illustrates how the results from point counting were treated for each frame. Relative amounts were calculated by dividing the counts of a kerogen group (A) on the total count for that frame (B), this number was multiplied by one hundred, so that the relative amounts were presented as percentage, as indicated by the red arrow (Table 3.1) (as indicated by the red arrow). All the data can be consulted in the appendix. Presenting the results in percentages allows comparison between the two different methodologies being tested as the results will have different units.

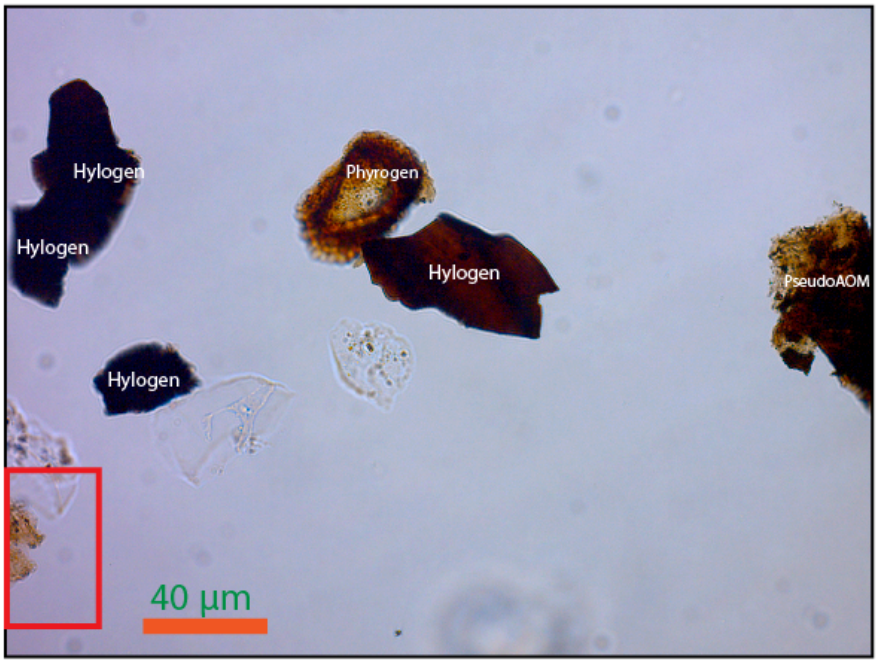

Figure 3. 6: Point counting illustrated in frame 10_B from slide BJ42. Each particle has been assigned to a kerogen group as shown in table 3.1. The particle within the red square is an example of how particles can be split between to frames.

Table 3. 1: Illustration of how point counting was carried out in frame 10 from slide BJ42 (Fig3.6). How the results were plotted in Excel is shown for frame 10 to 14 in slide BJ42. The table also demonstrates how the relative amounts of each kerogen group was calculated by dividing the counts for a kerogen group (A) on the total counts in the frame (B), this number was multiplied by a hundred so that the relative amounts were presented as percentage (as indicated by the red arrow).

			Point counting			
10	Melanogen	Hylogen	Phyrogen	Amorphoger	Pseudo AOM	Total
Counting		A 4,00	1,00		1,00	B 6,00
%	0,00	66,67	16,67	0,00	16,67	100,00
11	Melanogen	Hylogen	Phyrogen	Amorphoger	Pseudo AOM	Total
Counting		1,00			7,00	8,00
%	0,00	12,50	0,00	0,00	87,50	100,00
12	Melanogen	Hylogen	Phyrogen	Amorphoger	Pseudo AOM	Total
Counting		2,00			2,00	4,00
%	0,00	50,00	0,00	0,00	50,00	100,00
13	Melanogen	Hylogen	Phyrogen	Amorphoger	Pseudo AOM	Total
Counting		3,00			2,00	5,00
%	0,00	60,00	0,00	0,00	40,00	100,00
14	Melanogen	Hylogen	Phyrogen	Amorphoger	Pseudo AOM	Total
Counting		3,00	1,00		3,00	7,00
%	0,00	42,86	14,29	0,00	42,86	100,00

3.5 Pre-study: Visual Estimation

The Russian sedimentologist Shvetsov stated as early as 1954 that people tend to overestimate when using visual estimation methods (Terry and Chilingar, 1955). Shvetsov published a study where fellow geologists were asked to visually estimate the percentages of a variety of elements in unmarked sections (Terry and Chilingar, 1955). He discovered that people had different results, and both over- and underestimations were done, but overestimations occurred more frequently, up to seven times the original values (Terry and Chilingar, 1955).

In order to assess the validity of visual estimation of relative areas, a survey was made to determine people's perception of relative areas in a false-coloured image (Fig. 3.7). This was a preliminary study carried out in the Spring of 2016, where staff and students from both Trinity College, Dublin and UiB were asked to estimate the relative area of five particle types, each represented by a different colour. 53 people, all with a scientific background, completed the survey. The results of the survey are presented in Fig 3.8. and revealed that most people tend to overestimate some of the values, however some also underestimates greatly. In the case shown for the yellow tab, the lowest score was 7 %, which is 21 % less than the real proportion. This survey shows the spread in how different persons estimate relative proportions. For both pink and yellow, there is 25 % range interval that differs from the highest to the lowest answer. This preliminary study illustrates how important it is to use a good technique for palynofacies analysis. Either point counting or the use of software to estimate the relative areas in photographed frames, can be more accurate and provide better results. The aim is to try to determine which of these two methods is better.

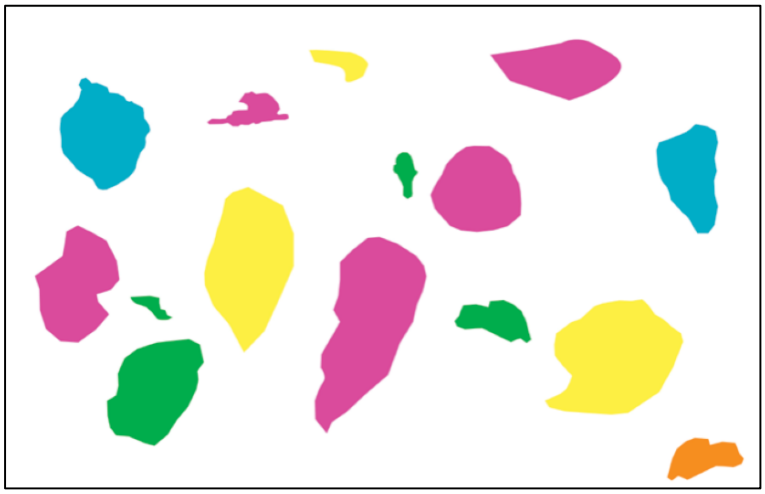

Figure 3. 7: Image from survey to assess the validity of visual estimation of relative areas.

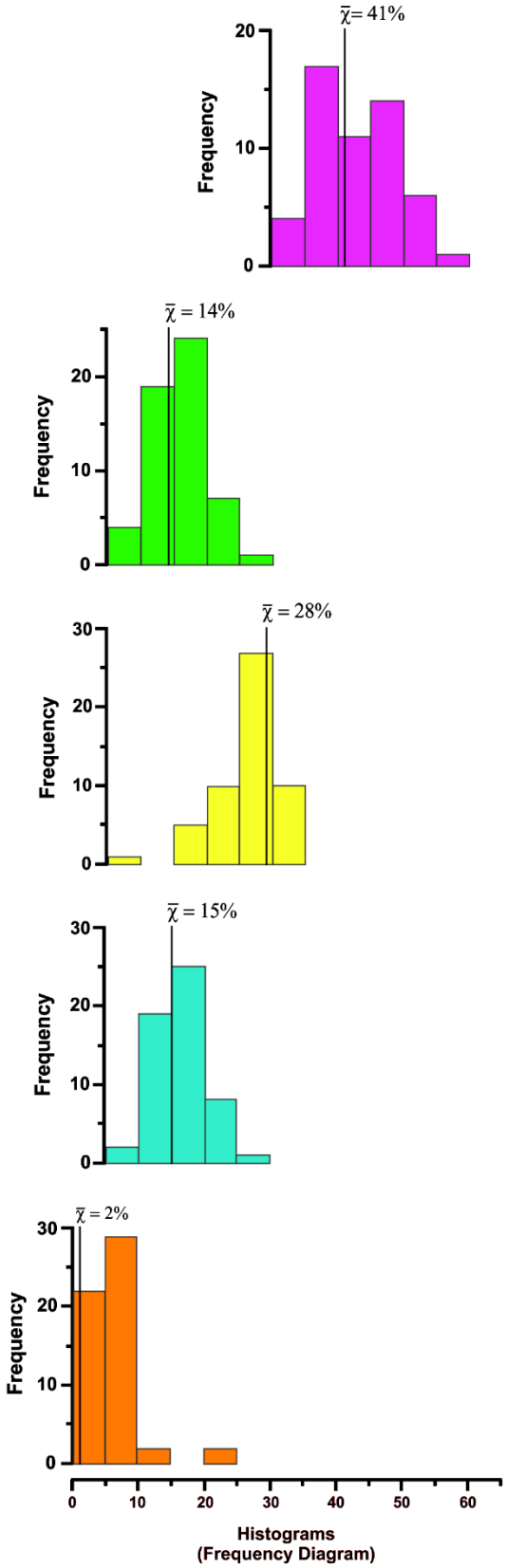

Figure 3. 8: The results from the survey presented as histograms. The colour of the histogram represents the particle colour in figure 3.7. The actual relative proportions for the image were measured using ImageJ, and are included as vertical black lines on each histogram.

3.6 Area Measurement by Image Analysis

For the measurements of relative areas in the photographed frames, the open source image analysis software ImageJ was downloaded and used (https://imagej.nih.gov/ij/). This is an image processing program which can process, edit and analyse scientific images. The particles were manually identified in the photographs, before the area of each individual particle was measured in pixels by the help of the ImageJ software.
All the results were plotted in an excel spreadsheet, an example of this is shown in table 3.2, where the results from the area measurement of the first five frames of the slide BJ02 is presented. The full table of all twenty-nine samples are included in the appendix. The results from the area measurement was calculated into relative percentages following the same procedure as described in the point counting methods (Sub-chapter 3.4), dividing the area measured for each category (marked with a red A in table 3.2) on the total area, which is the sum of all five kerogen groups, marked with a B in table 3.2. The relative area is then multiplied by one hundred to present the relative area measurement in percentage, plotted in the bottom row in the "%" category (Table 3.2). The reason for presenting the relative amounts of both methods is to ease the comparison between the two tested methods as the original results is presented in two different units, number of counts and the area in pixels.

Table 3. 2: The table illustrates how the results from the area measurement method was plotted in Excel. Presented in this table are the results from the area measurement of the first five frames of slide BJ02, and the relative percentages of each kerogen group. Relative area was calculated by dividing the measured area of a kerogen group (A) on the total measured area for that frame (B), this number was multiplied by one hundred so that the relative amounts were presented as percentage (as indicated by the red arrow).

			Area measurement			
1	Melanogen	Hylogen	Phyrogen	Amorphoger	Pseudo AOM	Total
Area		A 2262				B 2262
%	0	100	0	0	0	100
2	Melanogen	Hylogen	Phyrogen	Amorphoger	Pseudo AOM	Total
Area		1729	1012			2741
%	0	63,079168	36,920832	0	0	100
3	Melanogen	Hylogen	Phyrogen	Amorphoger	Pseudo AOM	Total
Area					685	685
%	0	0	0	0	100	100
4	Melanogen	Hylogen	Phyrogen	Amorphoger	Pseudo AOM	Total
Area		954			4638	5592
%	0	17,060086	0	0	82,939914	100
5	Melanogen	Hylogen	Phyrogen	Amorphoger	Pseudo AOM	Total
Area		803			558	1361
%	0	59,000735	0	0	40,999265	100

The following is a step-by-step instruction on how the software was used to measure areas:

1. The first action to be done includes the calibration of the system. To set the scale, an image of a calibrated graticule (Fig.3.9) was captured with the camera using the same settings as for all the subsequent palynofacies frames. The scale was then added to the figure based on the chosen magnification. The microscope already had pre-established scales, which was 20 µm since the 40x magnification "lens" was being used.

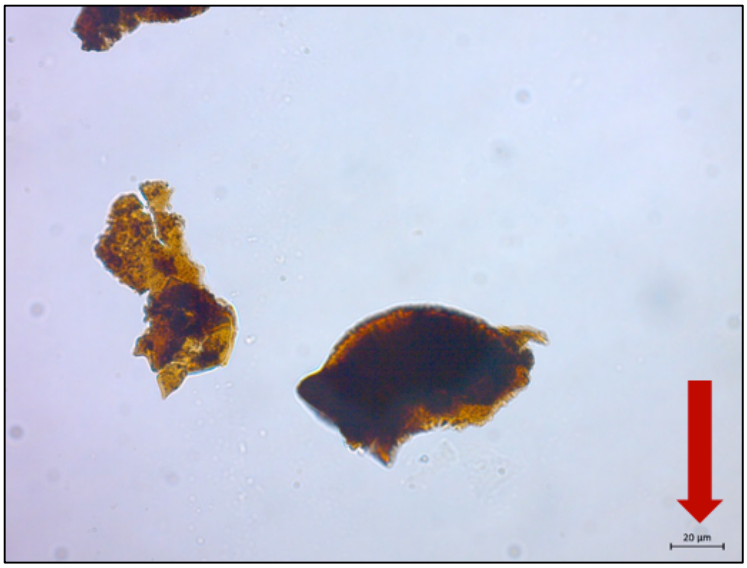

Figure 3. 9: Image of a frame illustrating the scale of 20 µm that was used.

2. The length of the scale is then measured in pixels using the *Straight line* function (button within the red square figure 3.10). To enter the values for the scale, go to the *Analyse* tab, and then press *Set scale.*

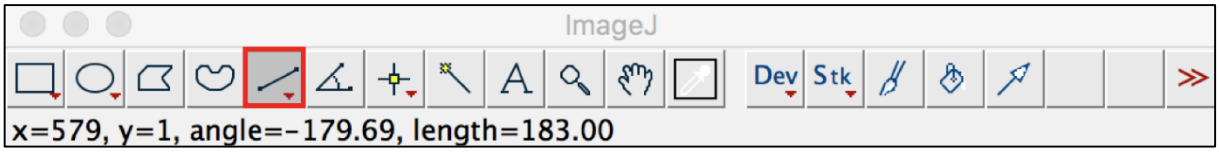

Figure 3. 10: The red square indicates the straight line function used to measure the length of the scale in the image.

Table 3.3 shows the input parameters used to calibrate the images. It is important to tick the box saying that the scale will be global, so that the scale will remain constant for all the images to be analysed.

Table 3. 3. Table with input parameters used to calibrate the scale.

Distance in pixels	183
Known distance	20
Pixel aspect ratio	1.0
Unit of length	Micron
Scale	9,15 pixels/micron

3. Upload a photo to the ImageJ. The easiest way to do this is to drag the file over to the program. The software accepts several file formats; the files used for this project were TIFF files due to their good resolution.

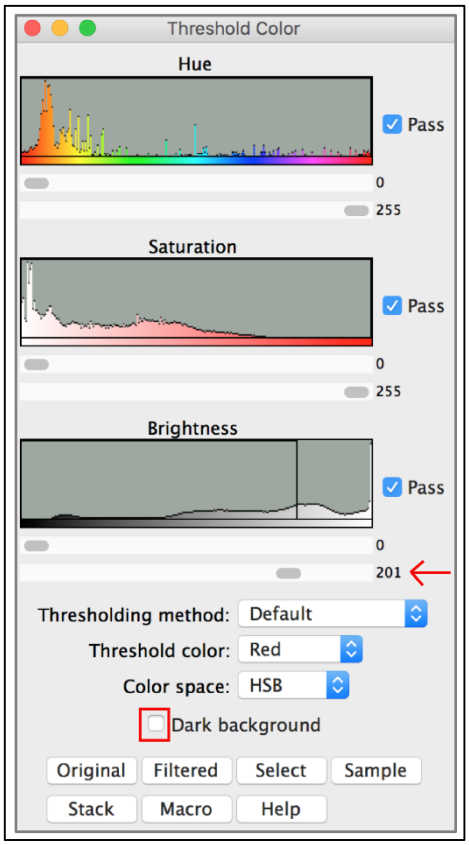

Figure 3. 11:The threshold colour setting window, where the brightness is changed so that the particle area can be coloured.

4. To adjust the colour on the image click on the *Image* tab.

→ *Adjust*

→ *Threshold*

The only pre-set setting that needs to be changed is the "*Dark background".* Toggle this off (Fig. 3.11).

→ Change the brightness until the coverage of the area to be measured is satisfying (Fig. 3.11). An example of the processed image sided with the unprocessed version of the image is shown in figure 3. 12.

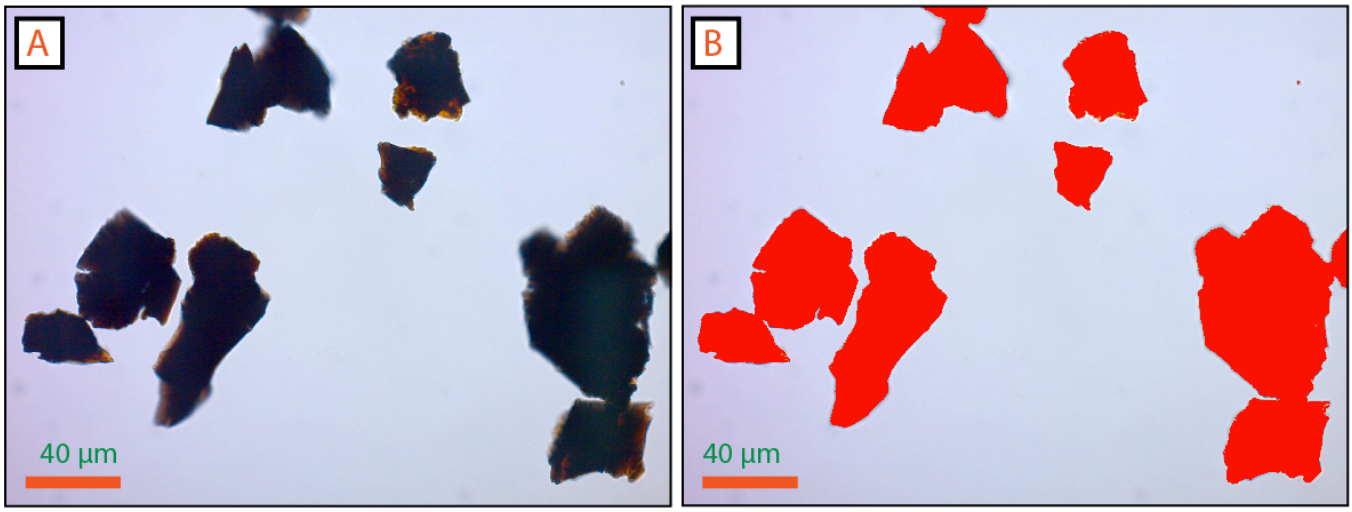

Figure 3. 12: Image A is illustrating the unprocessed version of frame 45 in slide BJ44, Image B is showing the processed version of the same frame.

→ For the particles lacking a continuous edge, or with a weaker contrast to the background, the border needs to be drawn by hand. Press the *Freehand selections* in the task bar, and draw the border manually (The button is marked with a red square in figure 3.13).

Figure 3. 13: The red square indicates the freehand selections command used to draw the border around the particles manually.

5. From the task bar click on the *Analyze* tab.

→ *Tools*

→ *ROI Manager*

A window will open with commands such as add, delete and measure (Fig. 3.14).

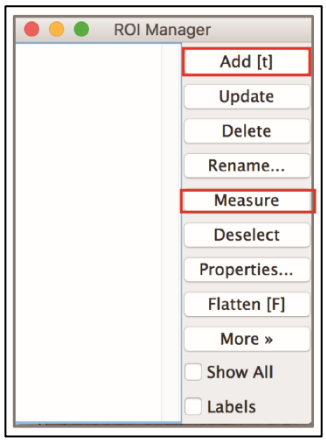

Figure 3. 14: The ROI Manager window where areas are added, then measured.

6. Press the "wand (tracing tool)" on the task bar (Marked with a red square Fig. 3.15). Then click on the object/objects that is to be measured. A yellow border will appear around the chosen object/objects as illustrated in figure 3.16. To measure several objects at the same time, as is done in figure 3.16 simply hold the shift button while using the wand to mark all the chosen objects.

Figure 3. 15: The red square indicates the wand, or tracing tool used to mark the object that needs to be measured.

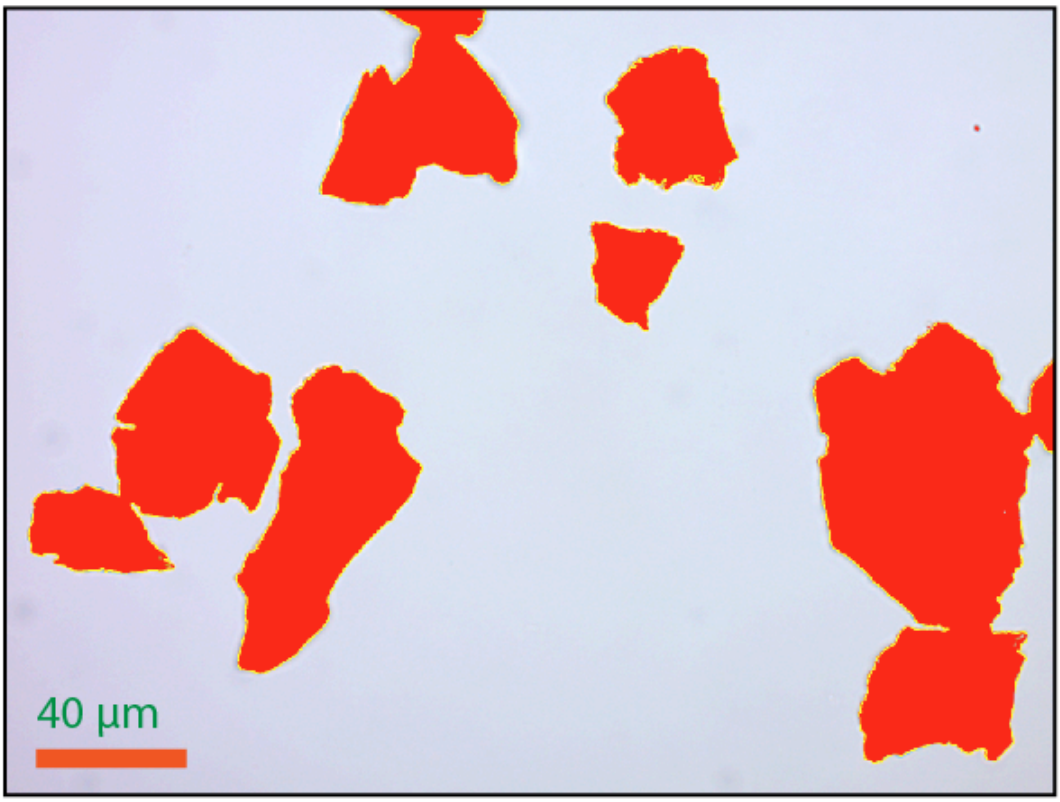

Figure 3. 16: Illustration of a frame where the object that is to be measured has been highlighted using the wand (Fig.3.15).

→ *Add*

A file will appear on the list in the ROI Manager (Fig 3.14). Click on the file to make it active.

→ *Measure*

When choosing the *measure command*, a new window with the results will appear (Fig. 3.17). As shown in Fig. 3.17 the scale for the area measurement will be pixels/micron.

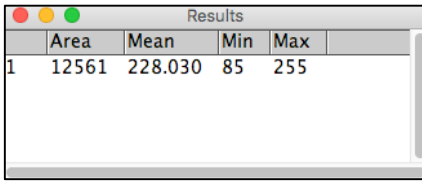

Figure 3. 17: The results window which appear when the measure command is applied. The area is measured in microns/pixel.

The values from the area measurement (Fig. 3.17) was copied and added to an excel spreadsheet so that the results could be analysed. All the results are included in the appendix.

3.7 Fields of View Assessment

There are several suggested protocols regarding the number of particles that should be counted for palynofacies analysis. Tyson (1995) suggested a count of 500 particles with additional counts of specific categories with special interest if occurring in low numbers, while Mendonça Filho (2012) stated that a minimum of 300 counted particles per sample was enough to obtain a representative result. Since the aim of this study was to compare two methods and photographed fields of view were the used protocol, palynological slide BJ40 was analysed using both methods, in order to establish a recommendation of the number of fields of view needed to analyse to produce a representative result. This sample was chosen due to its good representation of all five kerogen groups. A total of 109 non-overlapping images of the slide were captured along a horizontal transect of the cover slip, from one edge to the other (Fig. 3.18). This same assessment was carried out as a part of the pre-study at Trinity College, Dublin. The images for that assessment was photographed with a Nikon, DXm1200C digital camera connected to a Nikon Eclipse transmitted light microscope with a 50 x objective lens. Since the camera used in this study had a 40 x objective lens the process was repeated, to eliminate any sources of error that could be related to the magnification of the images. Cumulative curves (Figs. 3.20, 3.21) were plotted for the relative area results and the point count results so that the minimum number of fields of view that should be analysed could be estimated. The point where the curve flattens, has been taken as an indication on the number of frames needed to be counted per slide, before the results will not be affected by the number of frames analysed. This is indicated with a black line in both figures.

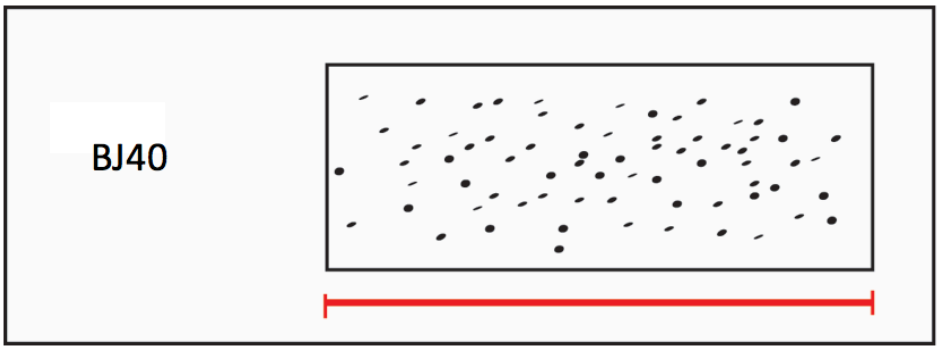

Figure 3. 18: Sketch of slide BJ40. The red line shows the horizontal transect where the 109 frames were captured along.

The results based on the cumulative curves for both methods are presented in figures 3.19 (point counting) and 3.20 (area measurement using the software ImageJ). According to the cumulative curve from the point counting (Fig. 3.19), 60 frames need to be analysed to get a reliable outcome for each slide. The cumulative curve for point area measurement (Fig.3.20) shows that 55 frames are enough to get an accurate result from one slide (marked with a black line). Based on the results expressed in figures 3.19 and 3.20, 60 fields of view per slide was the protocol used in this study. This was the same results from the pre-study at Trinity College, Dublin, suggesting that the magnification used does not affect the study.

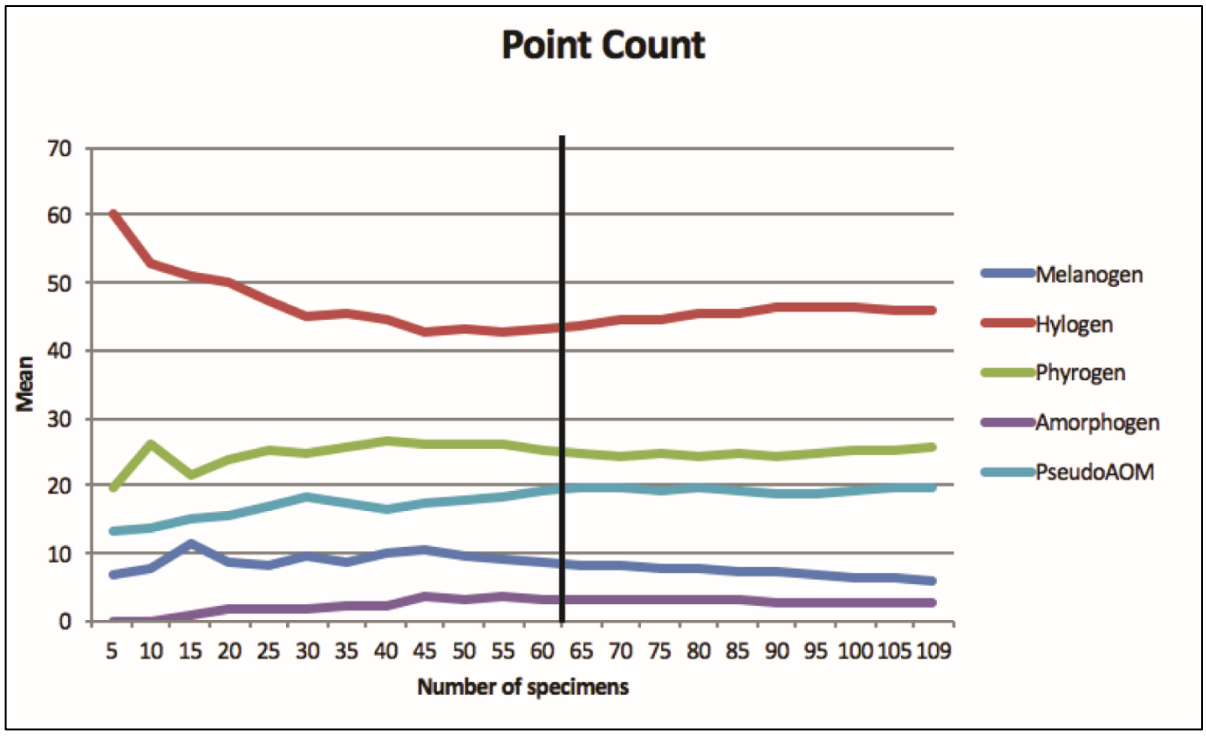

Figure 3. 19: The results from the point counting of slide BJ40 presented as cumulative curves. The black line indicates how many slides which needs to be analysed to get a reliable result.

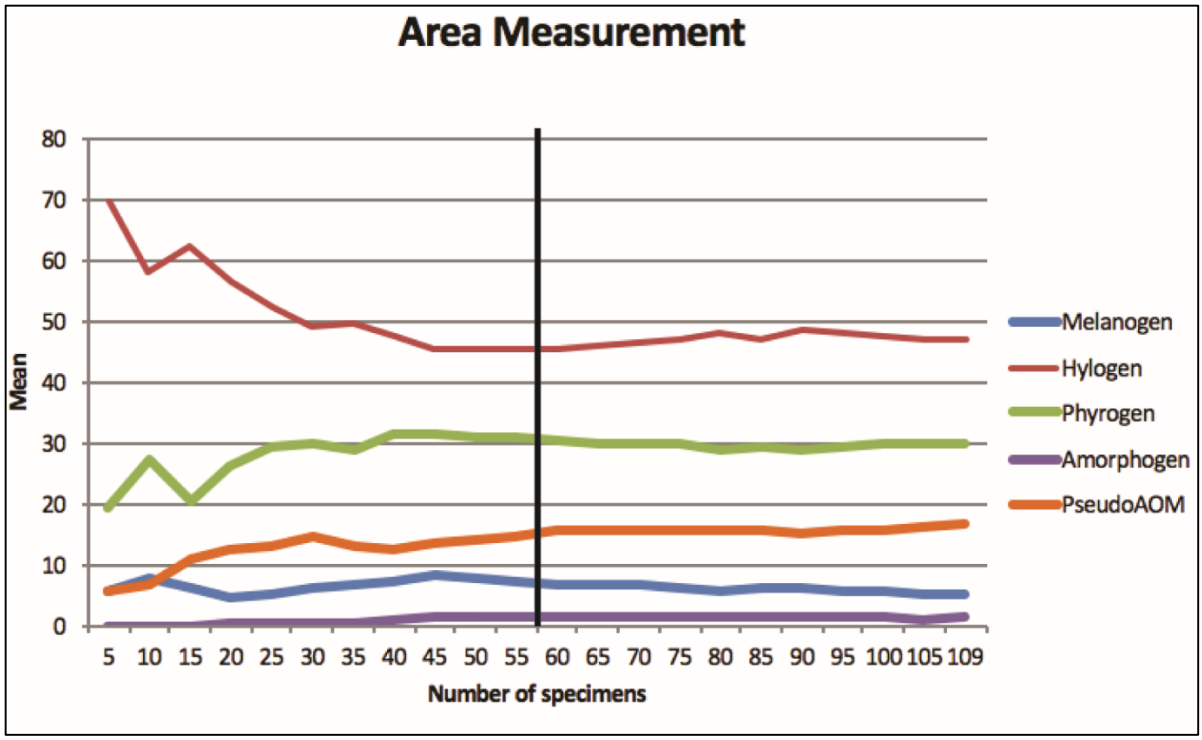

Figure 3. 20: The results from the area measurement of slide BJ40 presented as cumulative curves. The black line indicates how many slides which needs to be analysed to get a reliable result.

3.8 General Description and Challenges During the Analysis of the Slides

The twenty-nine kerogen slides studied were all productive. The organic material was dominantly dark brown in colour when analysed in transmitted light; some of the phyrogen could occasionally be of brown to dark yellow colour. In some of the samples, there was a lot of debris which was difficult to separate from AOM. In these cases, particles were only included in the study when large enough to be recognised by the software. Overlapping of particles occurred frequently and was resolved by taking pictures of the same frame at several levels, so that all material was captured while in focus (Fig. 3.21). When a particle was split between two frames the area was measured in both frames, but it would be counted only once. Both the area and count would be recorded for the frame where the particle covered a larger area, as explained in sub-chapter 3.4.

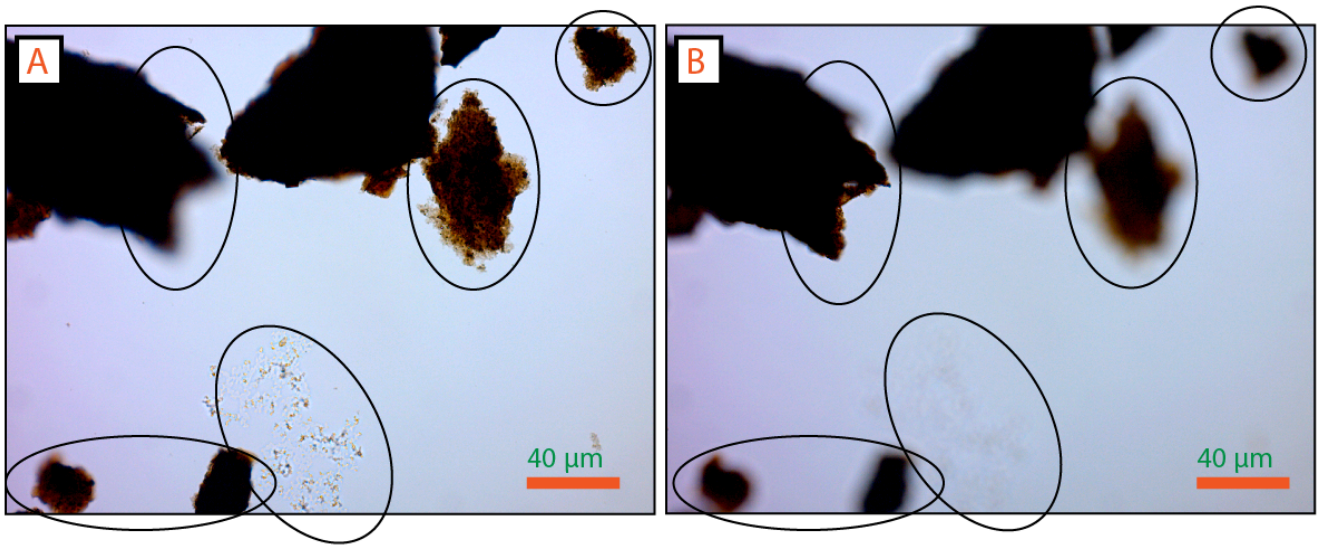

Figure 3. 21: Two images from the slide BJ24, frame 57, illustrating the focus issue in many of the frames analysed in this study.

4. Results

The results from both methods are presented below; first a brief presentation of the main observations grouped in 4 groups based on the difference in relative percentage between the methods. This is followed by a comparison of the two methods for each kerogen group, to test the hypothesis that the image analysis method gives the most reliable result. All the data gathered for this project including the tables presenting the results of both the point counting and area measurement can be found in the appendix. The results from this study have also been used for hydrocarbon source rock preliminary assessment and the results will be presented in this chapter.

4.1. Point Counting Results

Based on the 29 samples studied (see chapter 3.1) 1789 frames were captured and 16266 particles were counted following the kerogen categories described in chapter 2. Relative proportions (%) were calculated for each category in all 1789 frames. The conversion of the numbers was done to ease the comparison of the two methods, because point counting and area measured in pixels have different annotations. The relative proportion (%) from the point counting method is presented in table 4.1. The original counts of each slide per category, together with the standard deviation is presented in the appendix. The total average values for each category have been plotted in a pie chart, see figure 4.1. When comparing the values from the pie chart in figure 4.1 with the average values for each slide in table 4.1 it demonstrates that a global average value might not be the best way of portraying the results since there can be up to 86 % difference within the same kerogen group between two slides as is the case for hylogen when comparing for example BJ26 with BJ44 (table 4.1).

Table 4. 1: The global results from the point counting presented as average values for each frame. SD – Standard Deviation.

Point counting						
%	Melanogen	Hylogen	Phyrogen	Amorphogen	Pseudo AOM	Total
BJ02	2	29	8	2	59	100
BJ04	1	67	19	0	13	100
BJ06	1	10	2	6	81	100
BJ08	1	51	24	3	20	100
BJ10	3	23	15	6	52	100
BJ12	11	50	17	1	22	100
BJ14	1	14	19	2	64	100
BJ16	0	17	35	10	38	100
BJ18	2	24	14	13	47	100
BJ20	0	65	20	0	14	100
BJ22	1	19	9	17	55	100
BJ24	2	38	11	19	30	100
BJ26	1	6	31	20	42	100
BJ28	6	45	34	2	12	100
BJ30	4	70	1	0	26	100
BJ32	12	37	42	1	8	100
BJ34	1	17	5	1	76	100
BJ36	6	55	27	0	12	100
BJ38	5	28	14	0	53	100
BJ40	6	46	26	3	20	100
BJ42	5	43	15	0	37	100
BJ44	6	92	1	0	1	100
BJ46	1	27	13	0	59	100
BJ48	4	59	11	2	23	100
BJ50	6	21	8	0	65	100
BJ52	3	12	59	0	26	100
BJ54	0	11	14	3	72	100
BJ56	1	21	8	5	65	100
BJ58	1	65	6	1	27	100
Total Count	**558**	**5766**	**3016**	**636**	**6250**	**16226**
Average	**3**	**37**	**17**	**4**	**39**	**100**
SD	**6**	**20**	**14**	**7**	**1**	

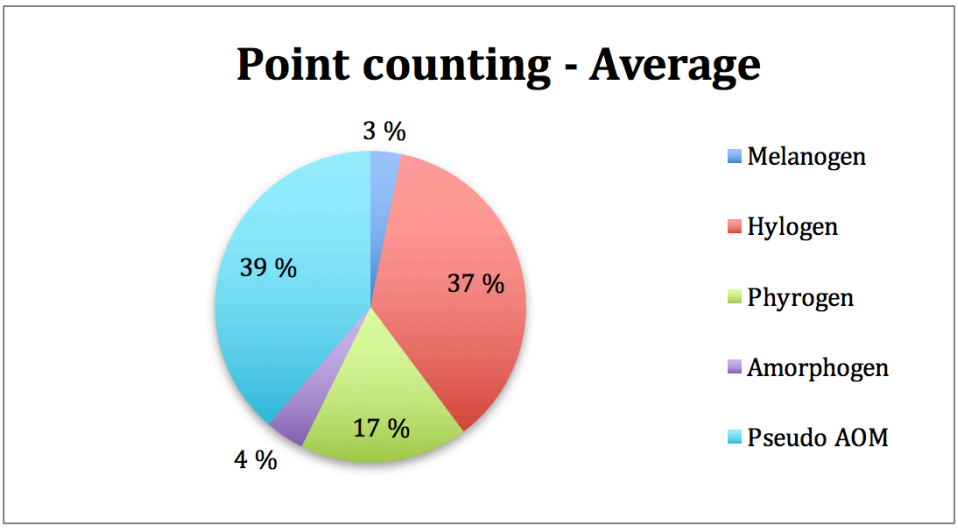

Figure 4. 1: The average global results of point counting presented in a pie chart. All values have been rounded to the nearest whole number.

4.2. Area Measurement Results

Based on the same set of 29 samples and the same 1789 frames, the relative area (in pixels) covered by each kerogen group was measured and calculated using the ImageJ software. As explained previously, only the areas recognized by the software were measured, excluding some background debris that the software could not identify due to the lack of contrast between the object and the background. Overlapping particles and objects split between two frames was handled as described (chapter 3.8). The results from the image analysis for all 29 slides is presented in table 4.2. The full table with the area measurements of all frames together with the standard deviation for each slide can be found in the appendix. The global average values of the area measurements have been plotted in a pie chart, see figure 4.2.

Table 4. 2: The Global results from the area measurement method presented as average values for each frame. SD-Standard Deviation.

Area measurement						
%	Melanogen	Hylogen	Phyrogen	Amorphogen	Pseudo AOM	Total
BJ02	2	26	8	1	62	100
BJ04	1	71	19	0	9	100
BJ06	0	10	3	4	82	100
BJ08	2	51	24	2	21	100
BJ10	3	20	15	3	60	100
BJ12	14	56	12	1	17	100
BJ14	1	12	19	0	68	100
BJ16	0	19	39	4	38	100
BJ18	3	27	13	9	47	100
BJ20	0	67	21	0	12	100
BJ22	1	21	7	9	63	100
BJ24	3	55	9	3	29	100
BJ26	1	7	33	6	53	100
BJ28	7	46	34	1	12	100
BJ30	4	71	1	0	25	100
BJ32	13	37	38	1	10	100
BJ34	2	20	4	0	74	100
BJ36	6	53	30	0	12	100
BJ38	4	27	13	0	56	100
BJ40	5	47	30	1	17	100
BJ42	4	44	14	0	37	100
BJ44	7	91	1	0	1	100
BJ46	2	22	13	0	64	100
BJ48	4	65	11	0	18	100
BJ50	4	22	8	0	65	100
BJ52	3	12	54	0	31	100
BJ54	0	12	9	1	78	100
BJ56	1	24	5	2	68	100
BJ58	1	72	4	0	23	100
Total area	**648894**	**47825570**	**3068744**	**256596**	**7316857**	**58393120**
Average	**3**	**38**	**17**	**2**	**40**	**100**
SD	**8**	**23**	**15**	**4**	**22**	

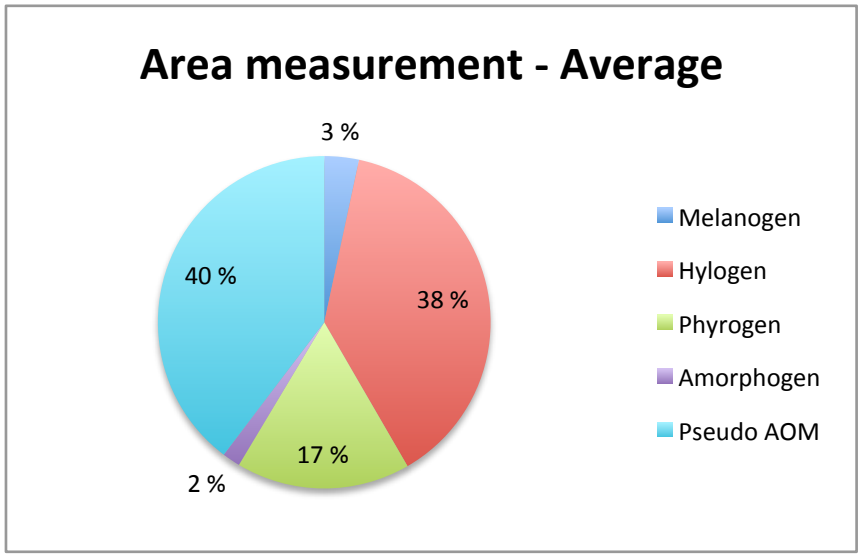

Figure 4. 2: The average global results of area measurement using the software ImageJ presented in a pie chart. All values have been rounded to the nearest whole number.

When comparing the average values from the two pie-charts in figures 4.1 and 4.2 for each category, almost no difference in the values are observed. The greatest change is seen in the amorphogen category where only a 2% difference is observed in the area measurement between the two methods. For pseudoAOM and hylogen, only 1 % difference are seen between the two methods. As discussed previously, the study of the total statistical parameters for both methods are not the best way to compare the methods. Much of the information can be concealed and that can lead to erroneous interpretations. To avoid this situation the data are analysed in sample groups, in the following sub-chapter.

4.3 Sample Groups Results

The results from both the point counting (table 4.1) and the area measurement (table 4.2) are presented in figure 4.3. The software Stratabugs was used to create the chart, and it illustrates the relative percentages of both methods for all five kerogen groups based on the classification scheme after Bujak et al. (1977). In the case where a kerogen group lacks a symbol it indicates that the value is less than 0.5 %. By comparing the average values for each slide one can see that the two methods differ considerably more than the global average values showed (see chapter 4.1 and 4.2. To gain a better comprehension of the data, the slides were grouped according to the difference in the percentages (table 4.3) between the two methods tested. Some of the larger differences between the two methods for certain kerogen groups are indicated with a red circle.

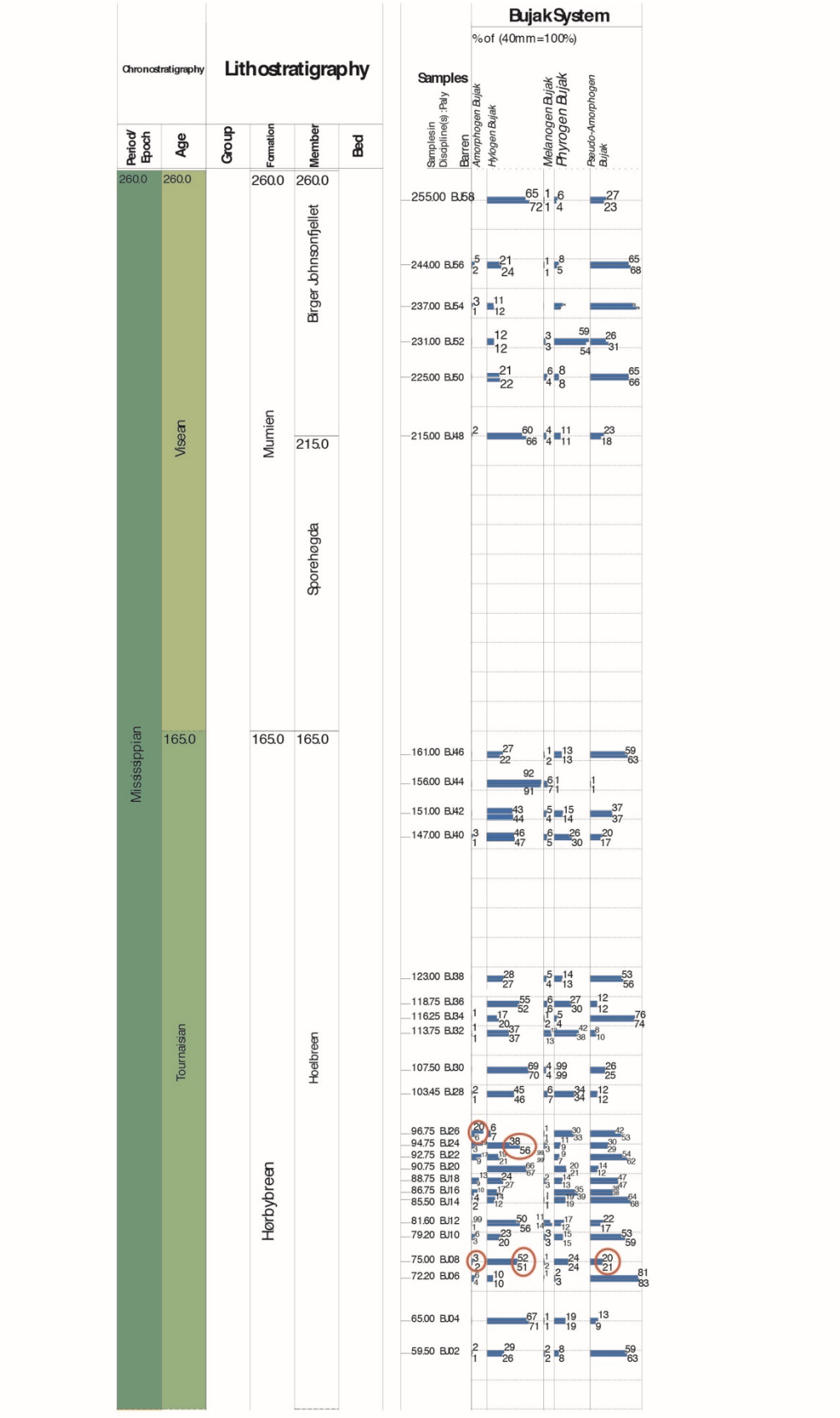

Figure 4. 3: Chart illustrating the relative percentages of both methods for all five kerogen groups after Bujak et al. (1977). The red circles indicate some frames where there is a bigger difference between the two tested methods, for certain kerogen groups.

- Group 1: Palynological slides showing a difference ranging from 0 to 2 % between the two methods tested. They comprehend the following palynological slides: BJ006, BJ008, BJ020, BJ028, BJ030, BJ042, BJ044, BJ050, see the log presented in figure 3.1 for stratigraphically position for the slides. 28 % of the slides fall within group 1, marked with a purple colour in table 4.3 and in figure 4.4.

- Group 2: Palynological slides showing a difference from 3-5 % between the results from the point counting versus the area measurement. A total of 41 % of the palynological slides falls within this group which comprehend the following slides: BJ002, BJ004, BJ014, BJ018, BJ032, BJ034, BJ036, BJ038, BJ040, BJ046, BJ052, BJ056, see the log presented in figure 3.1 for stratigraphically position for the slides. Group 2 is marked with a green colour in table 4.3 and in figure 4.4.

- Group 3: Palynological slides showing a 6-9 % difference between the results from point counting and area measurement. Group 3 comprehend the following palynological slides: BJ010, BJ012, BJ016, BJO22, BJ048, BJ054, BJ058, which is 24 % of all the samples. See the log presented in figure 3.1 for stratigraphically position for the slides. Group 3 is marked with a blue colour in table 4.3 and in figure 4.4.

- Group 4: Palynological slides showing a difference in the results between area measurement and point counting exceeding 9 %. The group comprehend the palynological slides BJ024, BJ026 which represents 7% of the material studied. Group 4 is marked with a red colour in table 4.3 and in figure 4.4.

Table 4. 3: The groups and the associated slides according to the difference in the percentages.

Group number	Difference (%)	Slide #
1	0-2	BJ06, BJ08, BJ20, BJ28, BJ030, BJ42, BJ44, BJ50
2	3-5	BJ02, BJ04, BJ14, BJ18, BJ32, BJ34, BJ36, BJ38, BJ40, BJ046, BJ52, BJ56
3	6-8	BJ10, BJ12, BJ16, BJ22, BJ48, BJ54, BJ58
4	>9	BJ24, BJ26

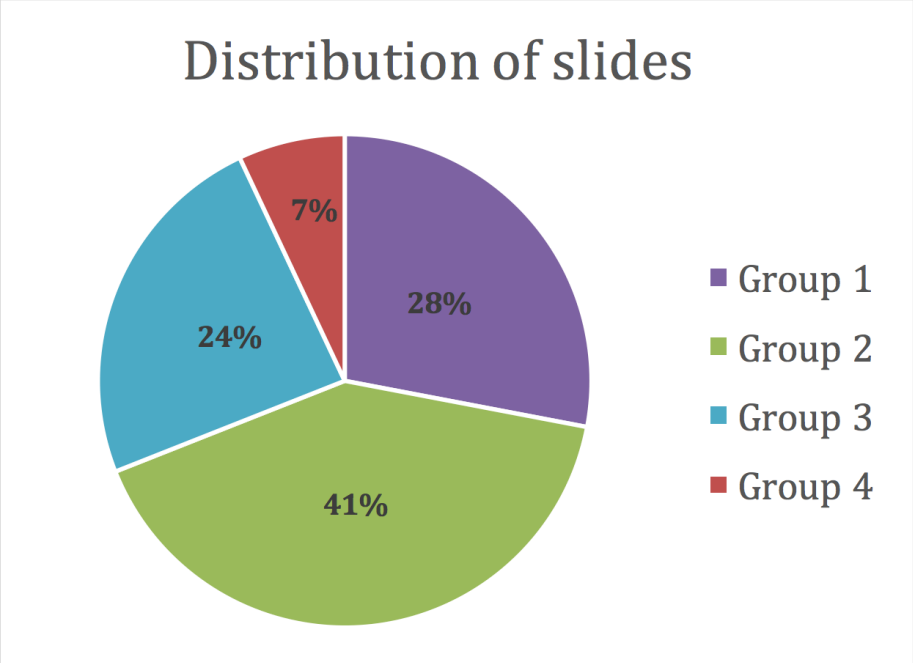

Figure 4. 4: Pie chart displaying the distribution of the slides within the 4 groups presented in table 4.3.

4.3.1 Group 1

All slides results for this group are presented in table 4.3 (page. 59). Slide BJ44 was analysed as a representative slide due to its abundance in organic matter, giving a good illustration of the size distribution of the material within this group. The slide shows a maximum difference of 1 % between the two analysis methods (table 4.4). Hylogen is the dominant kerogen group, as shown in table 4.4 the kerogen group covers over 90% in both the analytical methods. Figure 4.5 shows the consistent particle size dominating this slide.

Table 4. 4: The results (%) from both point counting and area measurement for slide BJ044.

BJ044	Melanogen	Hylogen	Phyrogen	Amorphogen	Pseudo AOM	Total
Count (%)	6	92	1	0	1	100
Area (%)	7	91	1	0	1	100

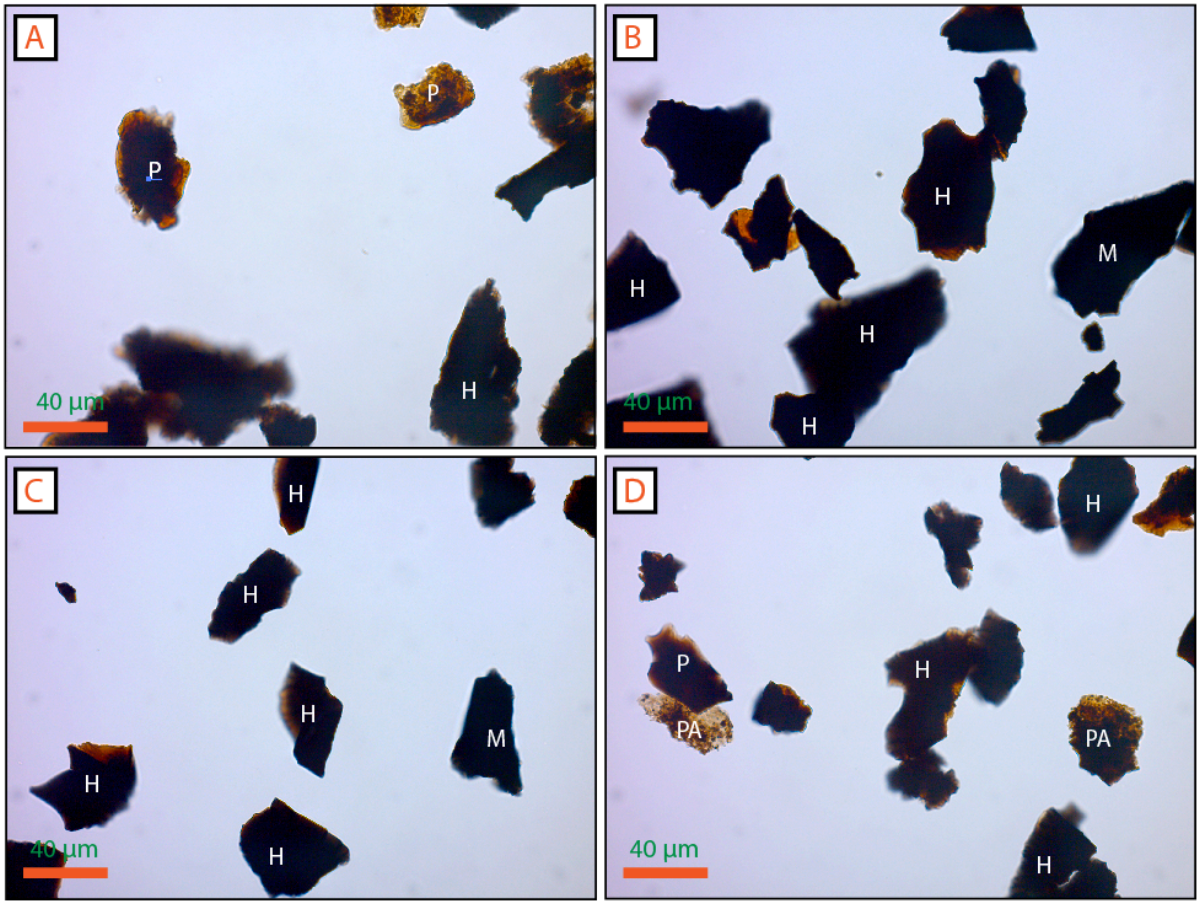

Figure 4. 5: A: Slide BJ44 Frame 18, B: BJ44 frame 14, C: BJ44 frame 25, D: BJ44, frame 54. H-Hylogen, M- Melanogen, P-Phyrogen, PA- PseudoAOM.

4.3.2 Group 2

Group 2 consist of slides showing a difference of 3-5 % in the results, between the two tested methods. All slides in this group are presented in table 4.3 (page 59). BJ38 was chosen to be analysed as a representative for group 2 due to the well demonstrated variation in the material. This slide does not show any significant difference between the two methods, the greatest difference observed is 3 % in the pseudoAOM kerogen group, between the methods applied. Figure 4.6 shows a selection of frames from slide BJ38 where the particles are of similar size and pseudoAOM particles differentiates in sizes are also shown.

Table 4. 5: The results (%) from both point counting and area measurement for slide BJ038.

BJ038	Melanogen	Hylogen	Phyrogen	Amorphogen	Pseudo AOM	Total
Count (%)	5	28	14	0	53	100
Area (%)	4	27	13	0	56	100

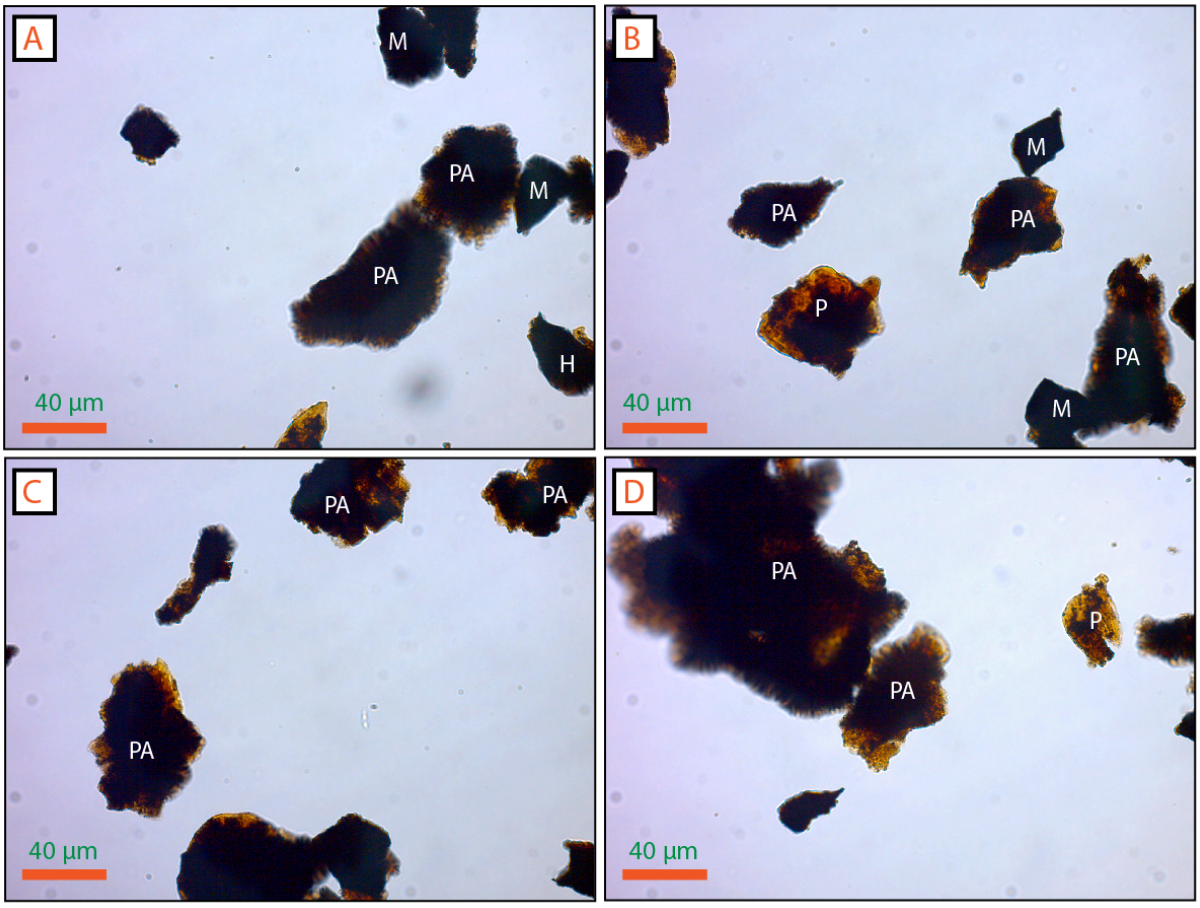

Figure 4. 6: Image A: Slide BJ38, frame 9, Image B: Slide BJ38, frame 11, Image C: Slide BJ38 frame 19, Image D: Slide BJ38, frame 23. H-Hylogen, M- Melanogen, P- Phyrogen, PA- PseudoAOM.

4.3.3 Group 3

All slides in this group are presented in table 4.3. The slide BJ48 was analysed as a representative for this group. The biggest difference can be seen for hylogen where there is a 6 % difference between the two methods, while PseudoAOM have a 5 % difference (Table 4.6). By observing figure 4.7 it is clear that the size differs quite a lot within the same kerogen group, this is especially applicable for the hylogen group.

Table 4. 6 The results (%) from both point counting and area measurement for slide BJ048.

BJ048	Melanogen	Hylogen	Phyrogen	Amorphogen	Pseudo AOM	Total
Count (%)	4	59	11	2	23	100
Area (%)	4	65	11	0	18	100

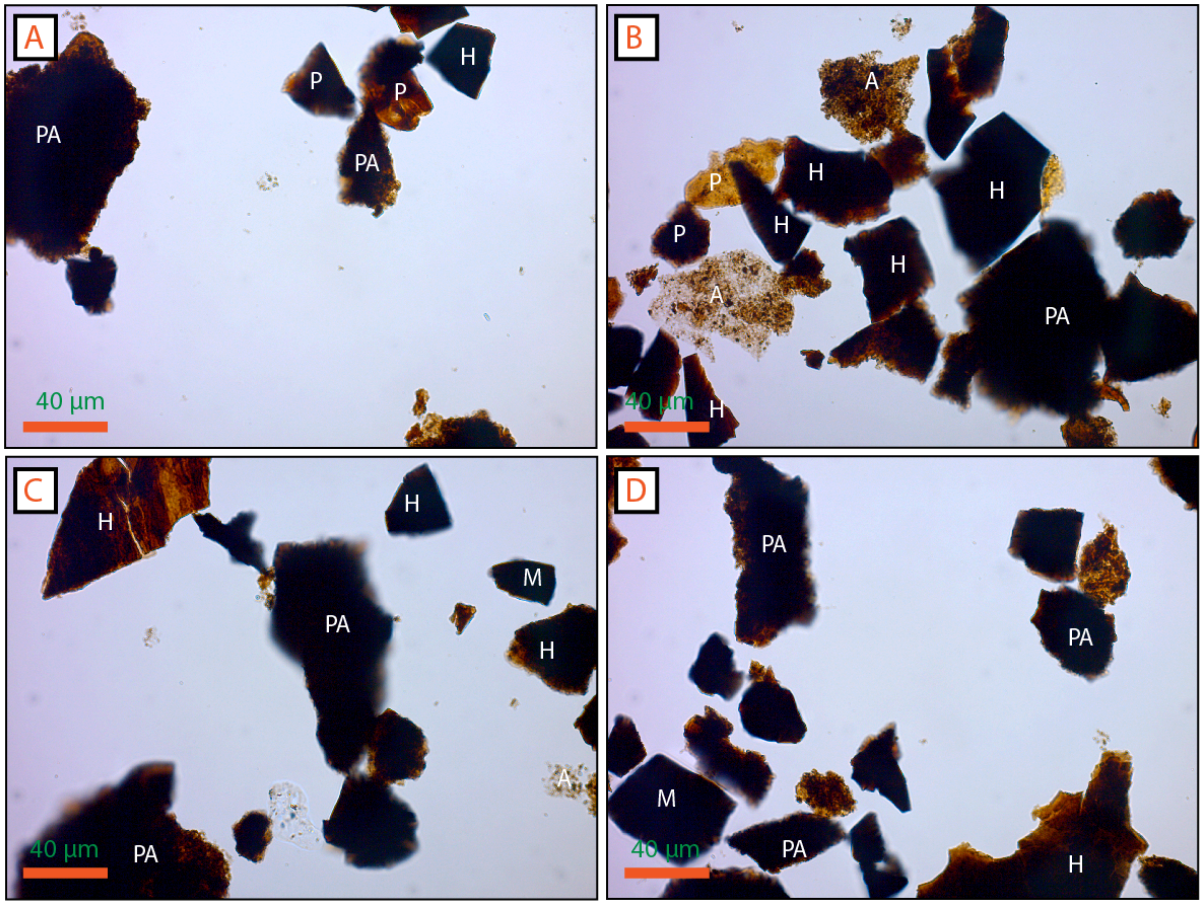

Figure 4. 7: Image A: Slide BJ48, frame 15, Image B: Slide BJ48, frame 20, Image C: Slide BJ48, frame 39, Image D: Slide BJ48, frame 43. A- AOM (amorphous organic matter), H-Hylogen, M- Melanogen, P- Phyrogen, PA-PseudoAOM.

The slide BJ22 is another representative slide from group 3. Maximum difference between point counting and area measurement is 8 % for both the amorphogen group and the PseudoAOM group (Table 4.7). This slide contained a lot of debris not recognized by the software, which was therefore not included in the study. From the frames illustrated in figure 4.8 it looks like pseudoAOM is dominating the slide.

Table 4. 7 The results (%) from both point counting and area measurement for slide BJ22.

BJ022	Melanogen	Hylogen	Phyrogen	Amorphogen	Pseudo-AOM	Total
Count (%)	1	19	9	17	55	100
Area (%)	1	21	7	9	63	100

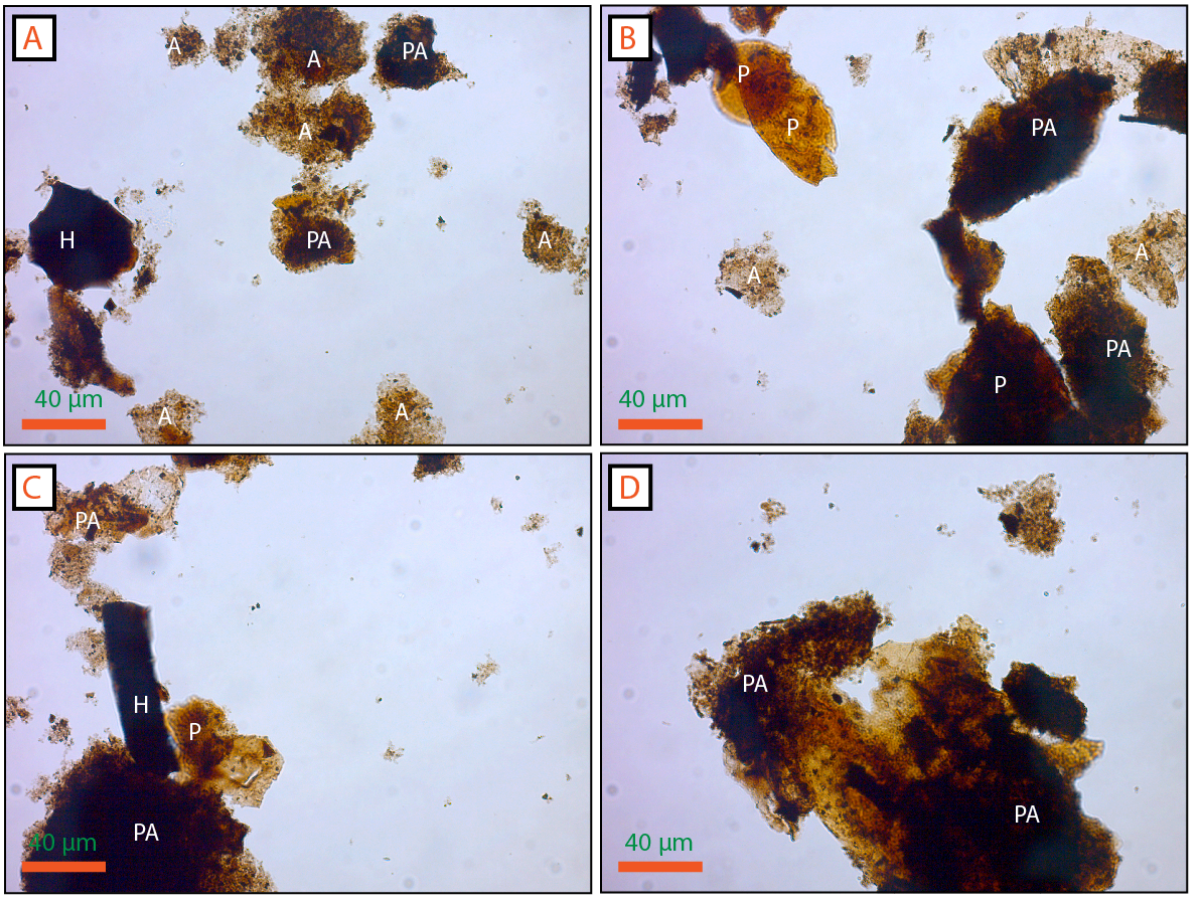

Figure 4. 8: Image A: Slide BJ22, frame 40, Image B: Slide BJ22, frame 45, Image C: Slide BJ22, frame 49, Image D: Slide BJ22, frame 54. A- AOM (amorphous organic matter), H-Hylogen, M- Melanogen, P- Phyrogen, PA-PseudoAOM.

4.3.4 Group 4

The slides within this group are presented in table 4.3 (page 59). The slide BJ24 was interesting to analyse since it represents the slide out of the entire dataset the greatest average difference between the two methods. In slide BJ024 there is a 17 % difference between the two methods when Hylogen is measured. For Amorphogen there is a 16 % difference (Table 4.8). Figure 4.9 show a random selection of frames. By observing these figures there is clearly a great difference in the size of the particles. For example, the Pseudo-AOM particles differ quite a lot in size, as well as the hylogen particles.

Table 4. 8: The results (%) from both point counting and area measurement for slide BJ24.

BJ024	Melanogen	Hylogen	Phyrogen	Amorphogen	Pseudo AOM	Total
Count (%)	2	38	11	19	30	100
Area (%)	3	55	9	3	29	100

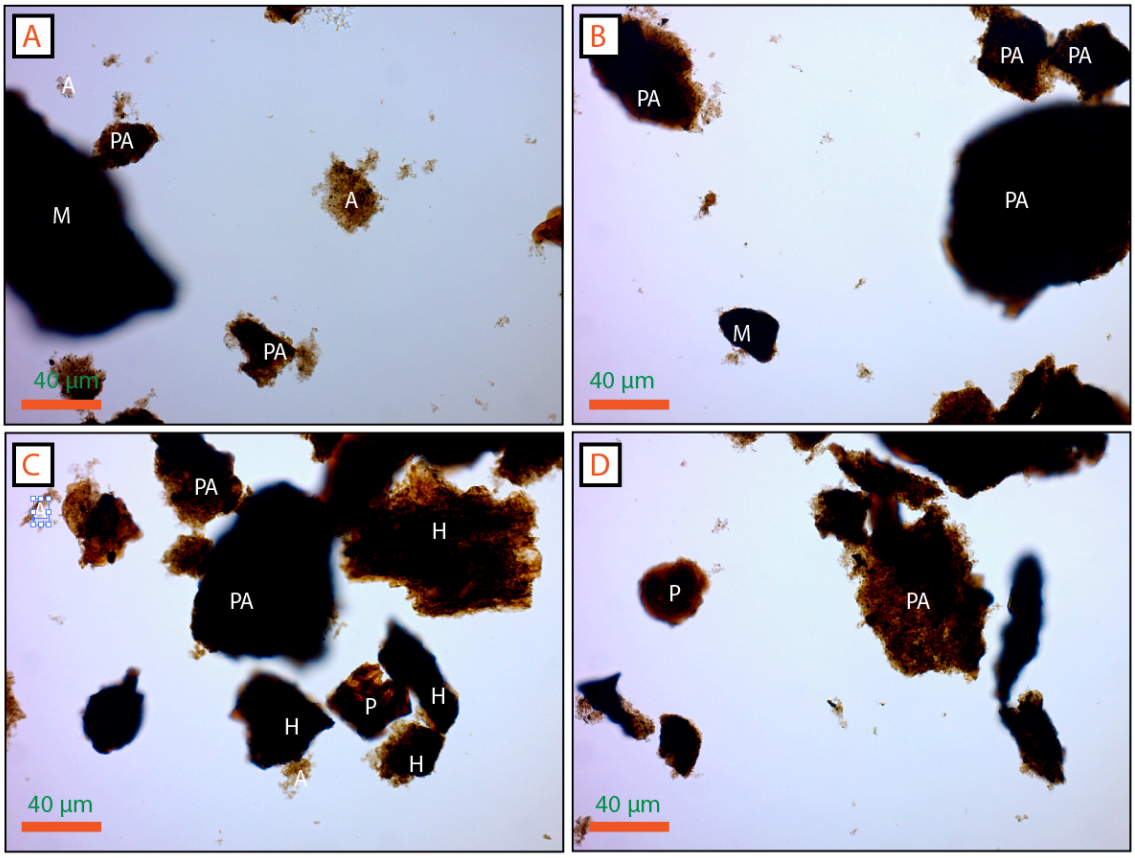

Figure 4. 9: Image A: Slide BJ24, frame 12, Image B: Slide BJ24, frame 14, Image C: Slide BJ24, frame 36, Image D: Slide BJ24, frame 45. A- AOM (amorphous organic matter), H-Hylogen, M- Melanogen, P- Phyrogen, PA- PseudoAOM.

The difference between the two methods is surprisingly large for certain single frames, as demonstrated by the results from the analysis of frame 24 in slide BJ24, presented in table 4.9. In this frame, the two methods differ with 50 %, for both the hylogen and amorphogen kerogen groups. Slide BJ24 contained a lot of AOM, but the particles were very small and scattered through the frame. As explained in sub-chapter 3.8 particles are included only when they were recognized by the ImageJ software. This situation can introduce some small statistical errors related to the software precision and analyst perception.

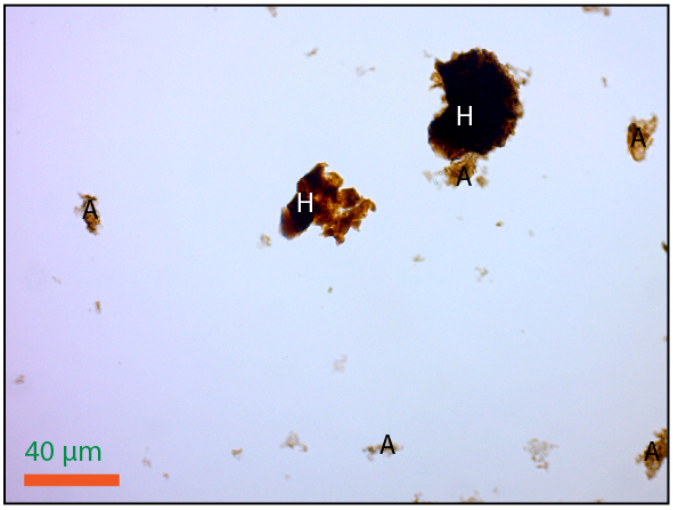

Figure 4. 10: Frame 24 from slide BJ24, illustrating the large difference between the two methods within certain frames.

Table 4. 9: The results (%) from both point counting and area measurement for frame 24, slide BJ024.

BJ024 #24	Melanogen	Hylogen	Phyrogen	Amorphogen	Pseudo AOM	Total
Count (%)	0	29	0	71	0	100
Area (%)	0	79	0	21	0	100

4.4 Kerogen Group Results

4.4.1 Melanogen

Based on the results from the point counting and area measurement presented in table 4.1 and 4.2, the variation in quantity of melanogen is not large between the two methods. The average representation of melanogen in the 29 slides is, regardless of the method, only 3 % (figures 4.1 and 4.2). The maximum difference between the two methods within a single frame is also just 3 % (Slide BJ12, listed in appendix). Presented in figures 4.11 and 4.12, are diagrams illustrating the average values for each slide with associates standard deviation (SD) values. It is worth noting that the maximum result for one slide is 17 % when using the area measurement method in the kerogen slide BJ12, and 3 % difference in the results between the two methods. Except for the results from slide BJ12 when point counting is the applied method, the SD exceeds the average results in all the kerogen slides. In the point counting results for BJ12 the SD is equal to the average value of melanogen, 11 %. Due to its sparse representation throughout the kerogen slides and the huge spread within the measured values as indicated by the SD values, statistically melanogen is not the best kerogen group to base the results on which is why this kerogen group was not analysed as thoroughly as the other kerogen groups.

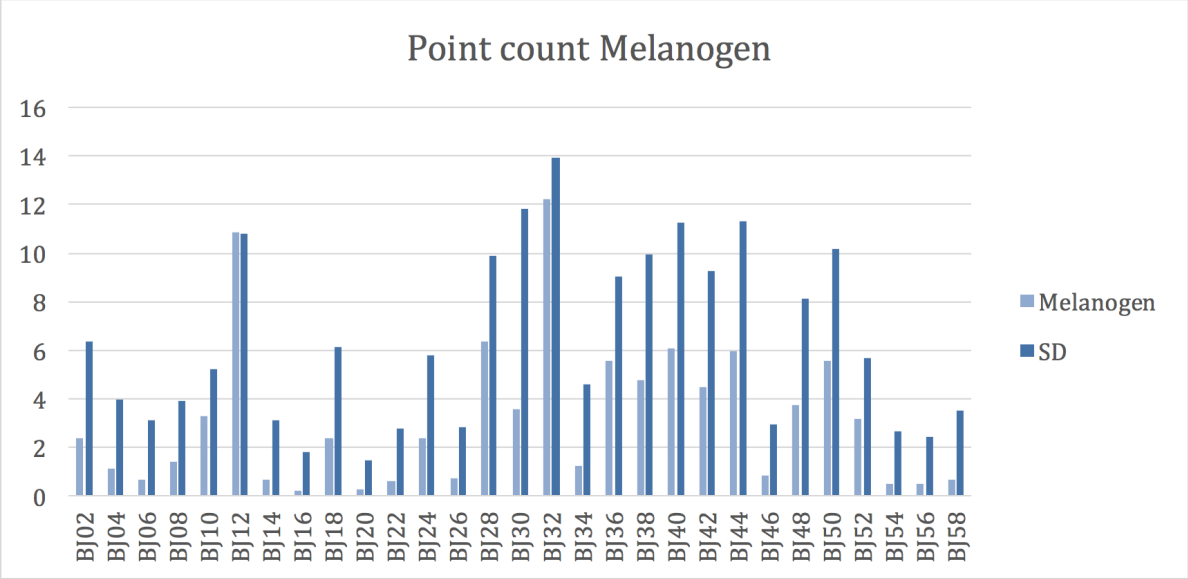

Figure 4. 11: Relative percentage of the average values of melanogen for each slide using the point counting method. The average values of the point count (blue) have been collected from table 4.1 in chapter 4, while the standard deviation (SD, dark blue colour) are presented in the appendix.

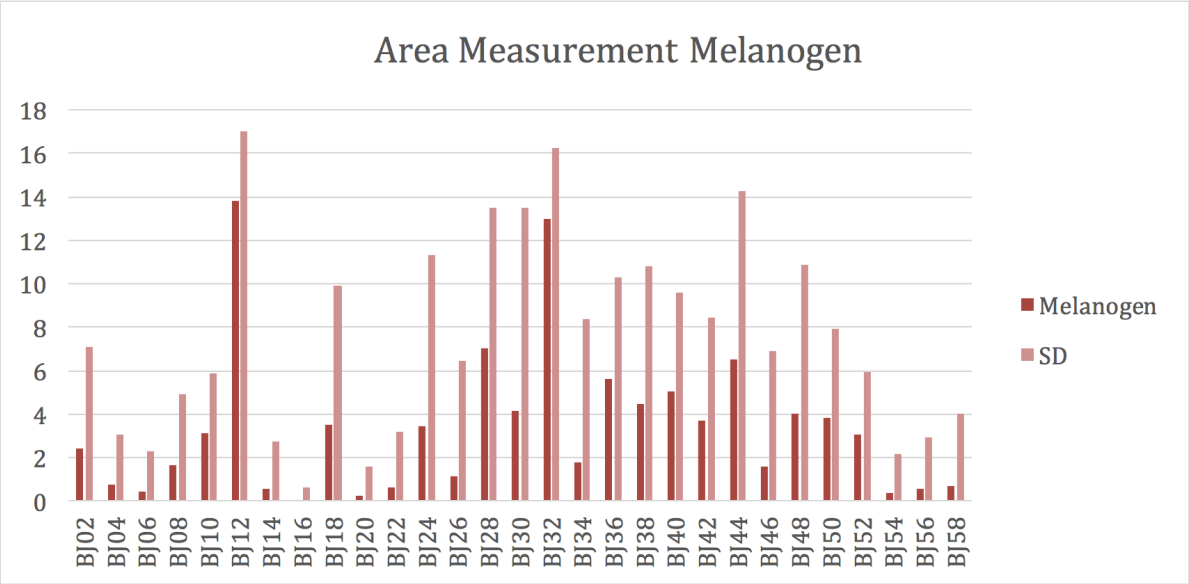

Figure 4. 12: Relative percentage of the average values of melanogen for each slide when using the area measurement method (red) together with the calculated standard deviation(SD) values for each slide (pink). The values from the area measurement are presented in table 4.2 while the standard deviation values are included in the appendix.

4.4.2 Hylogen

As stated previously Hylogen is one of the five kerogen groups showing the largest difference between the two methods, despite that the difference of the average values only being 1 % (pie charts figs. 4.1, 4.2 chapter 4). Figure 4.13 presents the point count for each frame, and associated standard deviations for the hylogen category. In 7 of the slides; BJ06, BJ14, BJ16, BJ22, BJ26, BJ34 and BJ54 the standard deviation exceeds the point count, indicating a large spread in the results. Other slides such as BJ04, BJ08, BJ12, BJ20, BJ30, BJ44 and BJ48 have a relatively low SD, meaning that the number of hylogen particles is consistent in most of the frames throughput those slides. When studying the standard deviation results of both point count and area measurement (figs. 5.1, 5.2) the spiking SD values shows that there is a wide range of results not being portrayed when the average values are calculated, such as for the pie charts in figs. 4.1 and 4.1 where the maximum difference between the methods is 2 %.

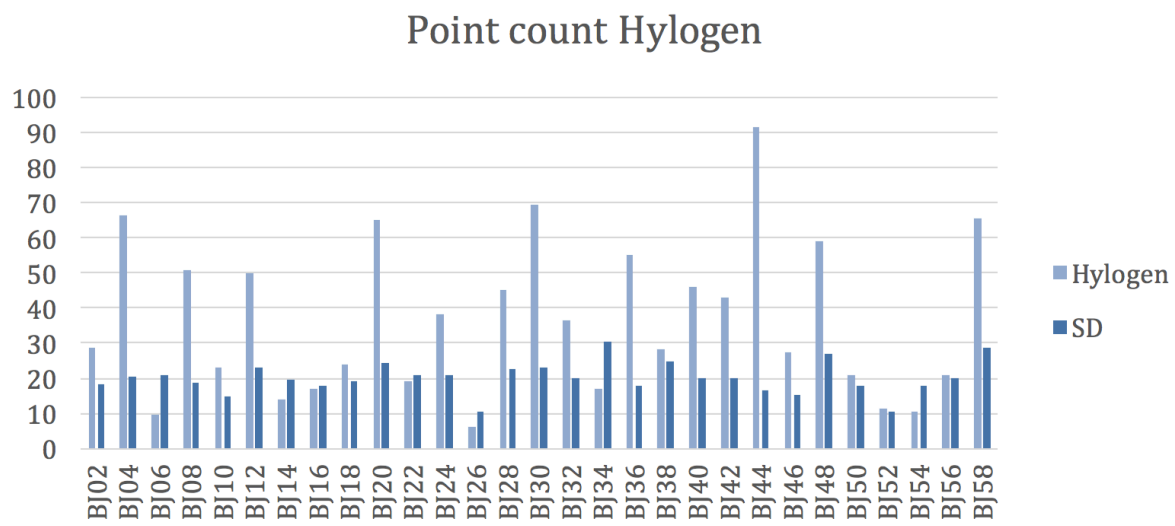

Figure 4. 13: Relative percentage of the average values of hylogen for each slide using the point counting method. The average values of the point count (blue) have been collected from table 4.1 in chapter 4, while the standard deviation (SD, dark blue colour) are presented in appendix.

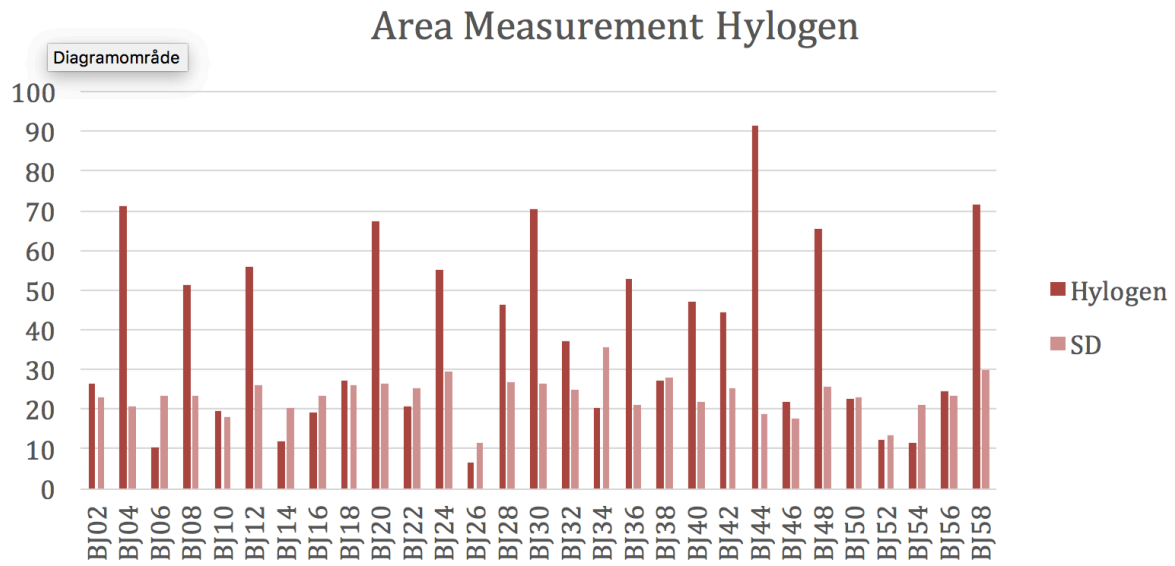

Figure 4. 14: Relative percentage of the average values of hylogen for each slide when using the area measurement method (orange) together with the calculated standard deviation(SD) values for each slide (pink). The values from the area measurement are presented in table 4.2 while the standard deviation values are included in the appendix.

When comparing figures 4.13 and 4.14, the peaks with low SD relative to the point count/area measurement seems to coincide, but with an additional 3 peaks of slides with low SD for the area measurement (Fig. 4.14): BJ02, BJ04, BJ08, BJ10, BJ12, BJ18, BJ20, BJ24, BJ28, BJ30, BJ32, BJ36, BJ38 BJ40, BJ44, BJ48, BJ50, BJ52, BJ54, BJ56 and BJ58. For the area measurement method, 10 slides have SD values exceeding the area measurement average value, indicating a great variety of size within the frame. Figure 4.13 illustrates that the SD exceeds the point count results in 5 slides: BJ06, BJ14, BJ16, BJ22, BJ26, BJ34 and BJ54. The SD exceeds the area measurement in the following 10 slides: J06, BJ14, BJ16, BJ22, BJ26, BJ34, BJ38, BJ50, BJ52 and BJ54.

The largest difference recorded in this dataset between the two methods for the same slide is recorded in slide BJ24 which was presented in group 4. In this slide, there is a 17 % difference between point counting and area measurement for hylogen, as shown in figure 4.3 and tables 4.1 and 4.2 Within a single frame there can be as much as 50 % difference between the two methods (BJ24, frame 24, page 65). As previously described in material and methods, 60 frames per palynological slide were captured along a horizontal transect along the middle of the slide. In frame 24, half way to the centre of the slide, the possible error regarding less material along the edges is removed.

4.4.3. Phyrogen

The average values presented in the pie charts in figures 4.1 and 4.2 in chapter 4 suggest that there is no distinct difference between the two methods when it comes to the relative amounts of phyrogen. From the 29 slides analysed, only small differences are observed, with the maximum difference between the two methods being 5 %. This is confirmed by the similarities of the values in figures 4.15 and 4.16 illustrating the point count and area measurement with adjacent SD values for this kerogen group. The Values of both the phyrogen and SD are close to identical in both methods. The slides showing some difference between the two methods are: BJ12, BJ16, BJ32, BJ36, BJ40, BJ52, BJ54 and BJ56, where the maximum difference measured was 5 % between the two methods.
Regarding the point counting method the SD exceeds the point count 14 times in the following palynological slides: BJ02, BJ06, BJ18, BJ20, BJ22, BJ24, BJ30, BJ34, BJ42, BJ44, BJ48, BJ50, BJ56 and BJ58.

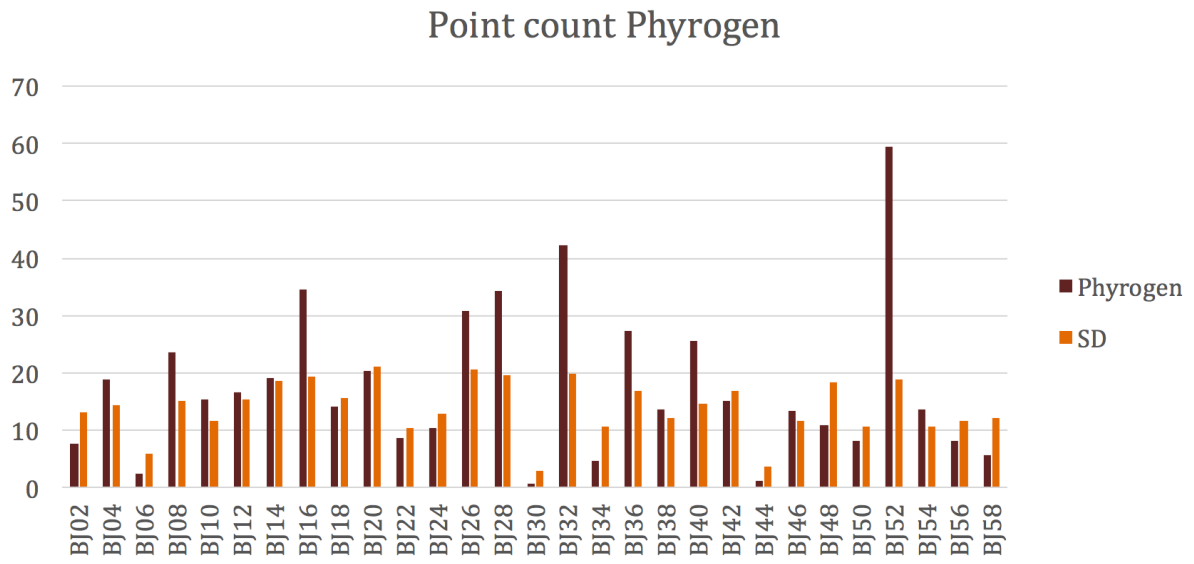

Figure 4. 15: Relative percentage of the average values of phyrogen for each slide using the point counting method (brown) together with adjacent standard deviation (SD) values for each slide (orange). The values from the point counting are presented in table 4.1, while the standard deviation values are included in the appendix.

The SD exceeds the area measurement values in 18 palynological slides, - all the ones where the SD exceeded the point counting value, and then 4 additional slides: BJ12, BJ14, BJ38 and BJ54.

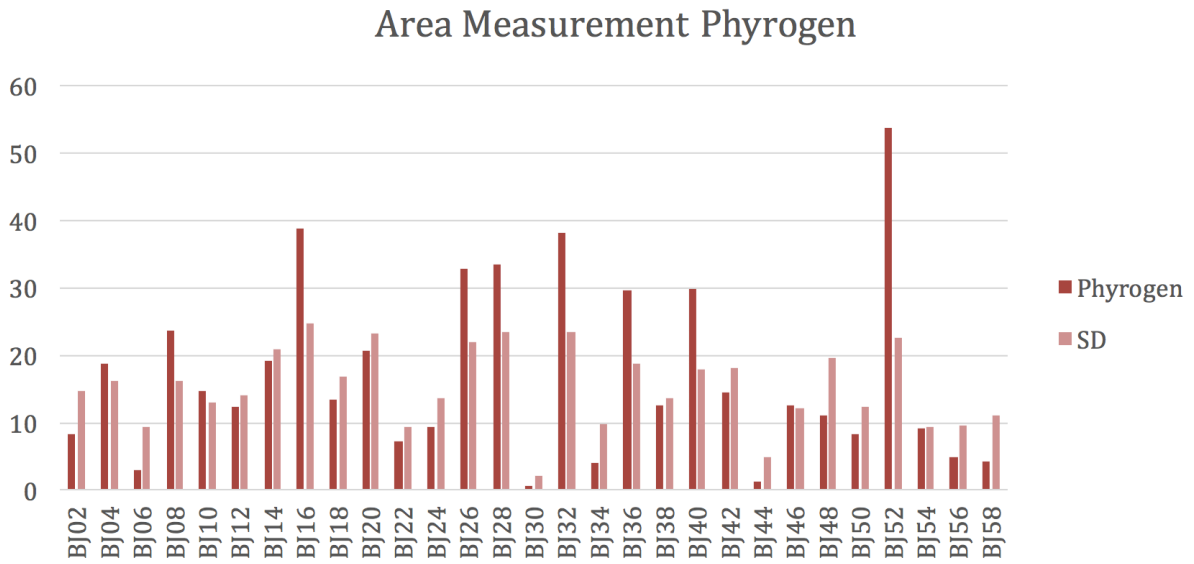

Figure 4. 16: Relative percentage of the average values of phyrogen using the area measurement method (red) together with the calculated standard deviation(SD) values for each slide (pink). The values from the area measurement are presented in table 4.2 while the standard deviation values are included in the appendix.

4.4.4. Amorphogen

As was the care for melanogen, the analysed data for this kerogen group is relatively finite due to its sparse representation in the samples. Amorphogen is the kerogen group with the lowest representation when using the area measurement method with its 2 %, while the average value is doubled to 4 % for this kerogen group when point counting is conducted (Figs. 4.1 and 4.2). When comparing the two figures displaying the standard deviation (Figs. 4.17 and 4.18) the maximum difference between the two methods within a single frame is 16 % (Slide BJ24, also see table 4.3). Figure 4.17 shows that in all but two of the palynological slides: BJ24 and BJ26 point counting is surpassed by the SD values, indicating a great amount of variation in the number of amorphogen particles present in the slides. The results from the area measurement in figure 4.18 reveals that the SD exceeds the average value in all the analysed slides, and in some palynological frames e.g. BJ18 the SD value is twice the value from the area measurement. This is illustrating the huge spread in size of the amorphous particles that were described in chapter 4.3.4.
Despite the sparse representation of amorphogen in the dataset, it is interesting to see these large differences between the two methods tested within single frames, and how the size of the particles can vary.

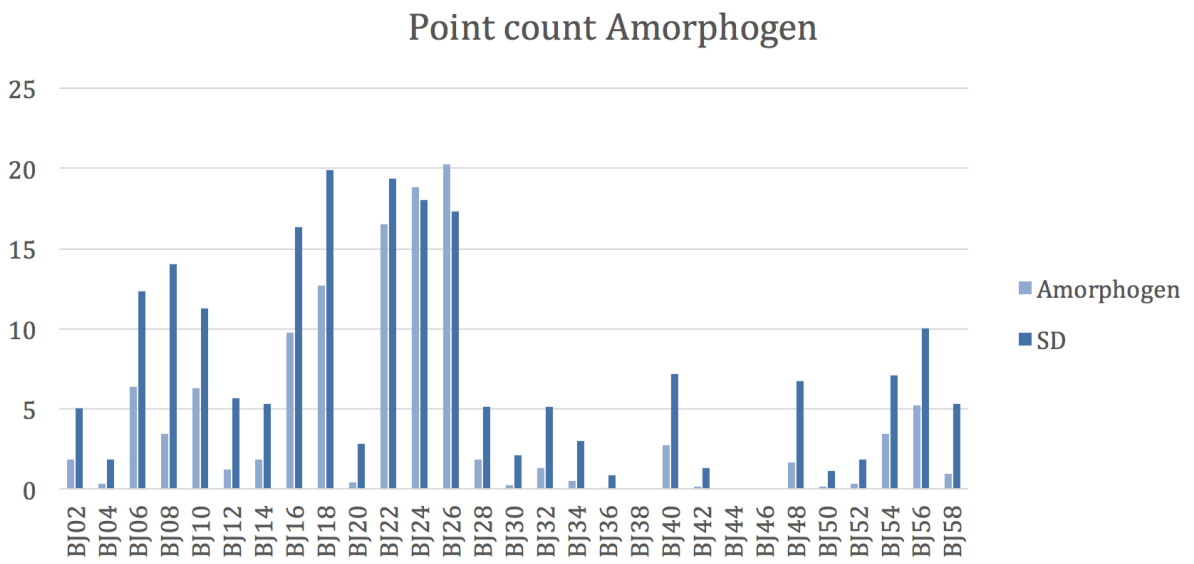

Figure 4. 17: Relative percentage of the average values of amorphogen for each slide using the point counting method (light blue) together with adjacent standard deviation (SD) values for each slide (blue). The values from the point counting are presented in table 4.1, while the standard deviation values are included in the appendix.

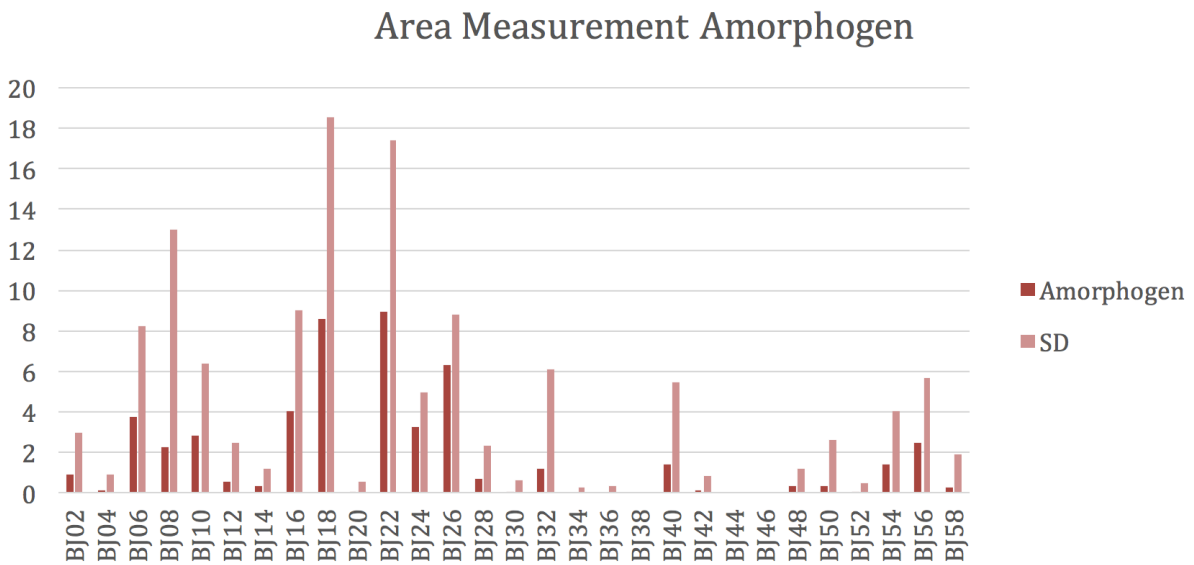

Figure 4. 18: Relative percentage of the average values of Amorphogen using the area measurement method (red) together with the calculated standard deviation(SD) values for each slide (pink). The values from the area measurement are presented in table 4.2 while the standard deviation values are included in the appendix.

4.4.5. PseudoAOM

Together with hylogen, pseudoAOM is the dominant kerogen group within this dataset. When the point counting method was used it comprised 39 % of the samples, and 40 % when the area measurement method was applied (Fig.4.1 and 4.2). The two column diagrams below illustrate the average amounts of pseudoAOM present in each slide together with associated standard deviation values for both methods (Figs. 4.19 and 4.20). The most significant difference observed between the two methods was found in slide BJ26 where there is a 11 % difference between the two methods, with area measurement giving the highest pseudoAOM values. For point counting the SD exceeds the point count average values 5 times in the palynological slides BJ20, BJ28, BJ32, BJ44 and BJ58. In these slides, it is worth noting that the SD barely exceeds the point counting average value. The SD from the area measurements exceeds the measured average values 7 times in the following palynological slides: BJ04, BJ20, BJ28, BJ32, BJ44, BJ48 and BJ58 indicating a that the spread in both area and count is not that big.

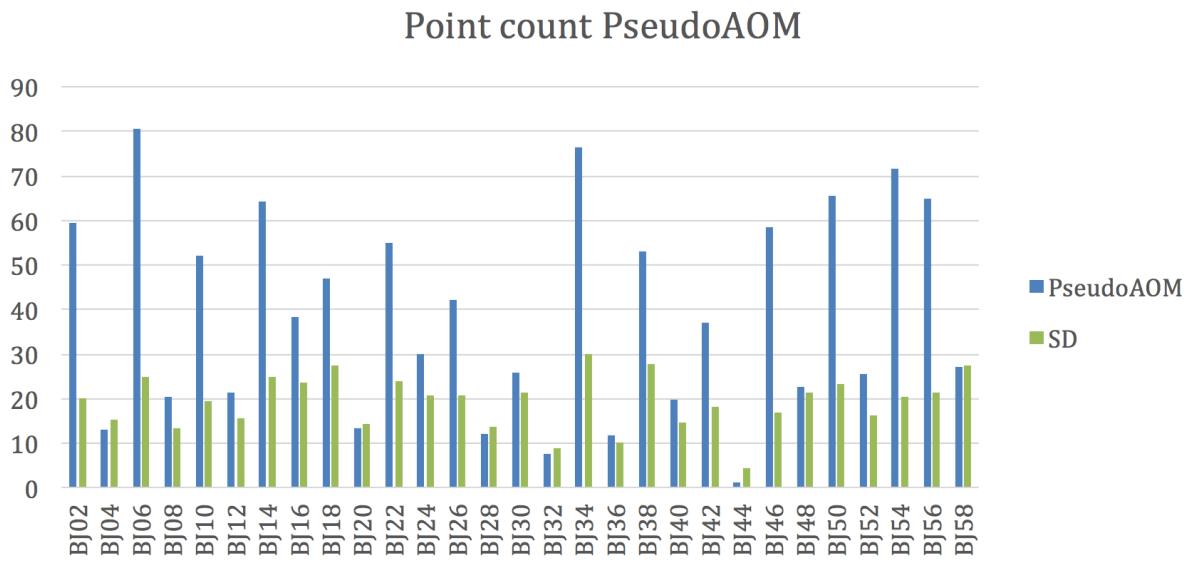

Figure 4. 19: Relative percentage of the average values of pseudoAOM for each slide using the point counting method (blue) together with adjacent standard deviation (SD) values for each slide (green). The values from the point counting are presented in table 4.1, while the standard deviation values are included in the appendix.

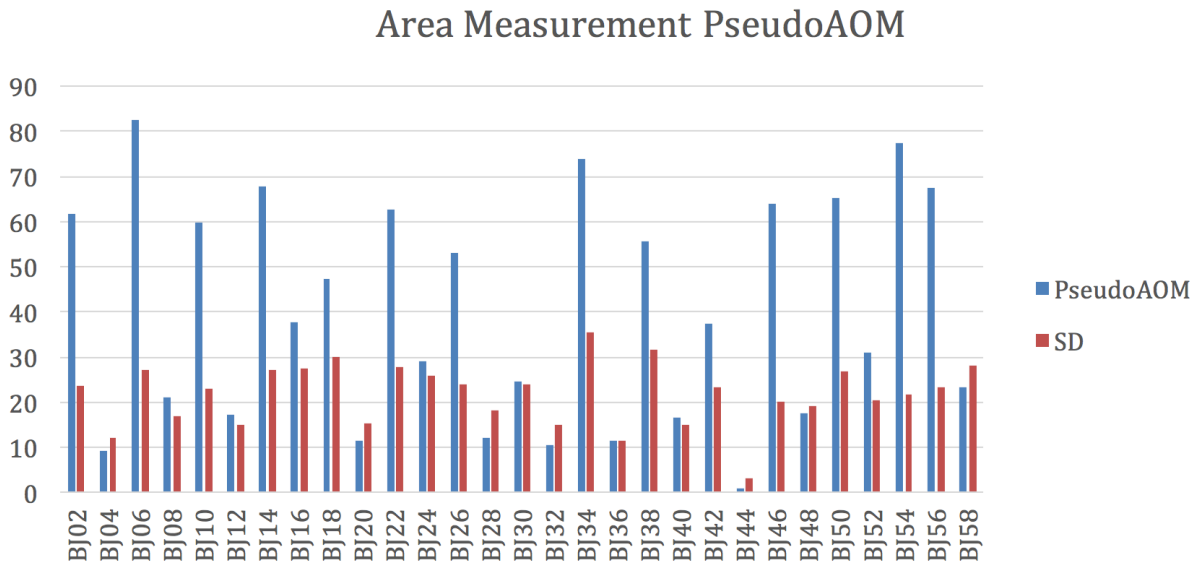

Figure 4. 20: Relative percentage of the average values of pseudoAOM using the area measurement method (blue) together with the calculated standard deviation(SD) values for each slide (red). The values from the area measurement are presented in table 4.2 while the standard deviation values are included in the appendix.

4.5 HC Source Rock Assessment Results

According to Bujak *et al*. (1977) the different types of organic matter particles in sedimentary rocks will, to some extent, affect the hydrocarbon production from the rock during maturation. The results obtained in this study could therefore also be used to analyse the hydrocarbon potential of the samples, although since that is not the primary aim of this work it must be considered as preliminary. All the *Botryococcus* counts from the fluorescence analysis of all 29 kerogen slides are presented in figure 4.21. The results from the point counting and area measurement presented in table 4.1 and 4.2 were used as input data in the software Stratabugs, to create the two charts presented in figures 4.22 and 4.23. The charts display the results as "saw-tooth" diagrams used to implicate source rock potential. All five kerogen groups (after Bujak *et al*. 1977) are presented separately with a vertical column. The samples BJ02-BJ58 are listed stratigraphically to the left. When comparing the two charts, it does not appear to be any substantial difference between the two methods, as the overall trend is similar. Regardless of the method used, hylogen and pseudoAOM are the dominant organic matter groups observed. Hylogen and pseudoAOM seem to be the dominant kerogen groups for the Hoelbreen Member (Fig.

4.22), Towards the top of the succession hylogen seems to be more dominant than pseudoAOM. PseudoAOM is also the dominating kerogen group in the Mumien Formation, with a notable increased abundance in the Birger Johnsonfjellet Member. The amount of amorphogen is as mentioned earlier, very sparse, but it is more abundant in the Hoelbreen Member, rapidly decreasing upwards in the stratigraphy. It is almost non-existent at the top of the Hoelbreen Member, and barely present in the Birger Johnsonfjellet Member. Melanogen is also very poorly represented throughout the stratigraphy, and can barely be found at the top of the Birger Johnsonfjellet Member. Phyrogen is represented throughout the succession, although the result for this kerogen group is very alternating with several excursions and the major peak observed at 231 m, slide BJ52 in the Birger Johnsonfjellet Member.

The Sporehøgda Member was not sampled, due to its lithology type being sandstone, marked by a break in the charts.

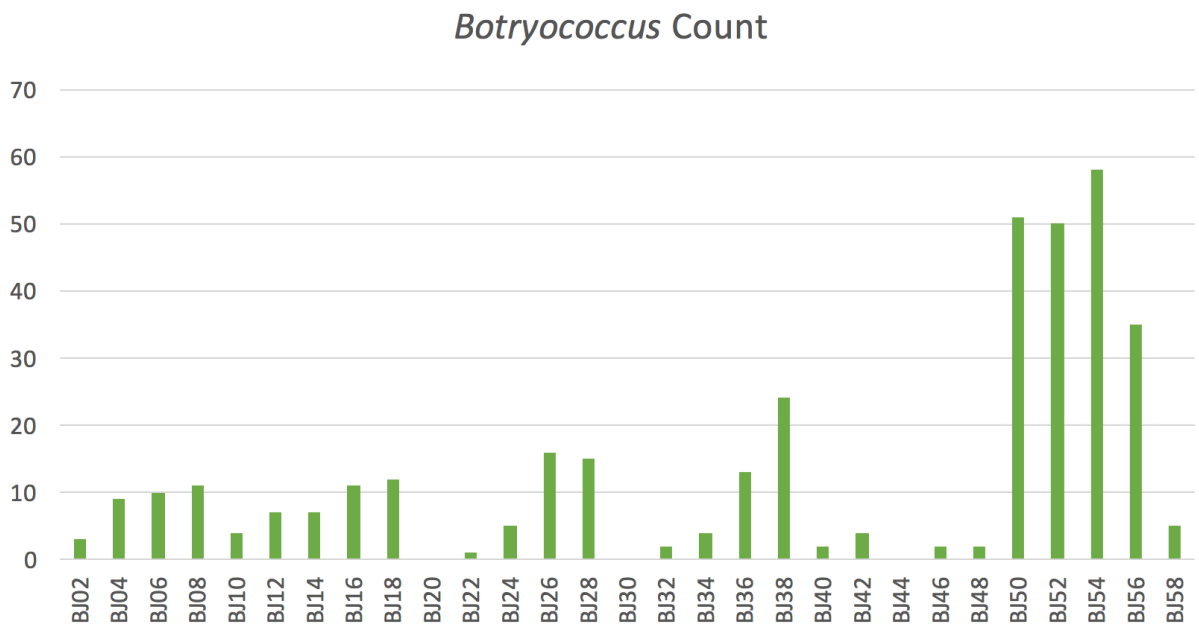

Figure 4. 21: Diagram showing the counts (y-axis) of *Botryococcus* counts along the y-axis, for all kerogen slides (x-axis).

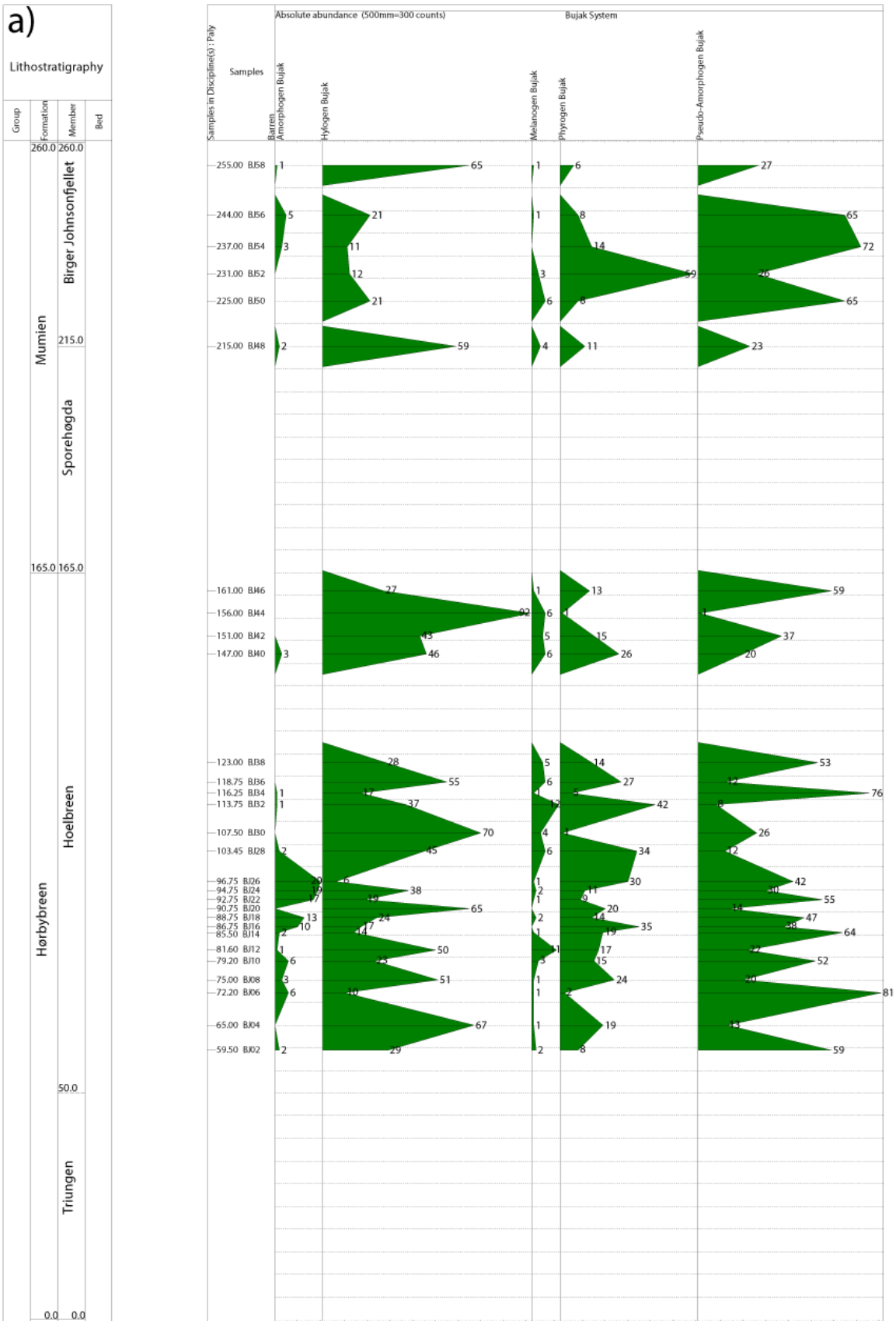

Figure 4. 22: Point counting results of the twenty-nine analysed kerogen slides, displayed as a saw tooth diagram. Each kerogen group has its own column.

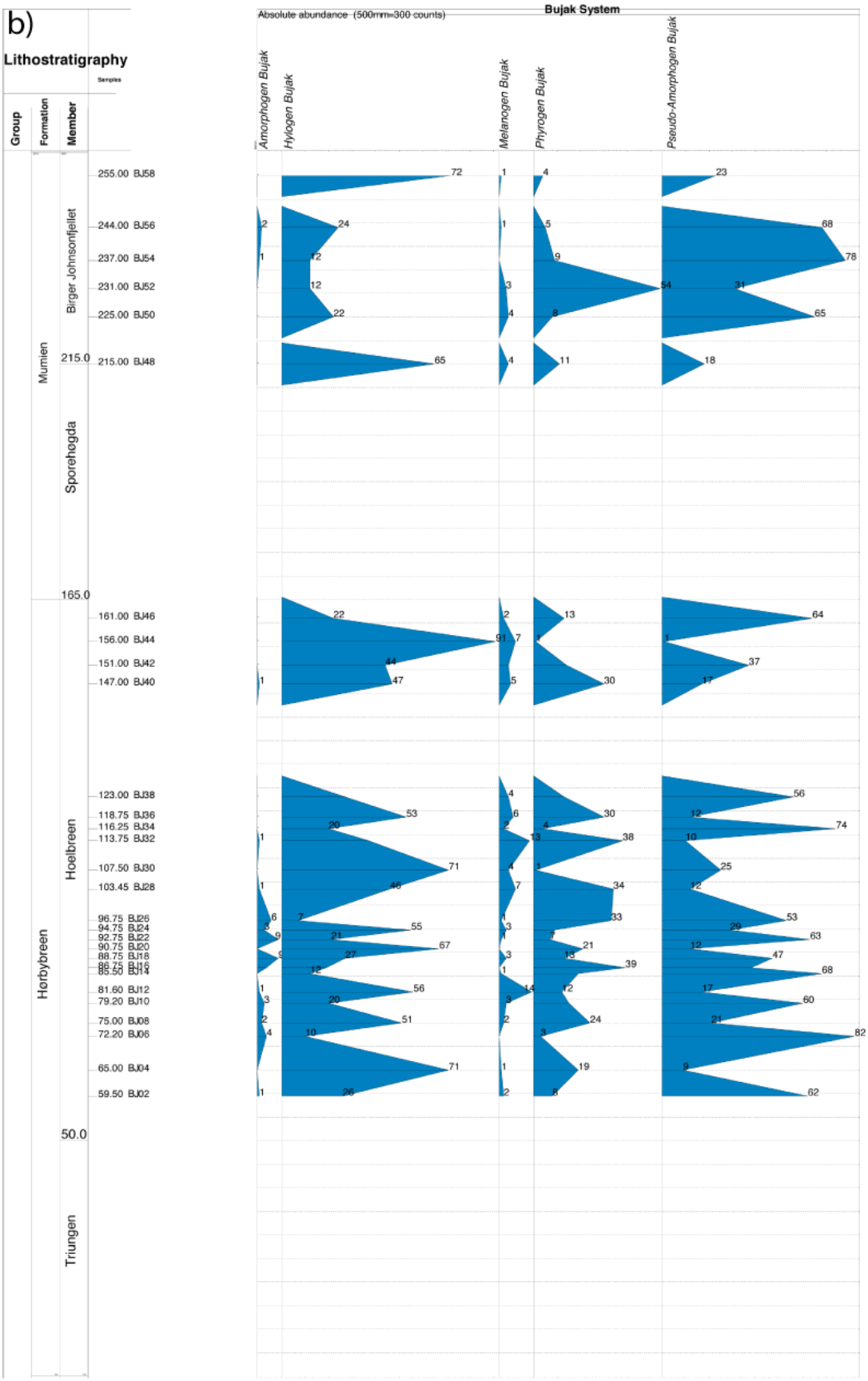

Figure 4. 23: Area measurement results of the twenty-nine analysed kerogen slides, displayed as a saw tooth diagram. Each kerogen group has its own column.

5. Discussion

For any study the choice of method is crucial. As stated by Wood *et al*. (1996), the methodology used is the foundation of palynological analysis. The main objective of this thesis was to compare two different methods for palynofacies analysis, both of which are often used. Below, the results are interpreted in a broader context and discussed in order to clarify whether the measurement of relative area based on image analysis is more accurate than point counting. Which of the two methods is more effective, and which of the methods generate less uncertainties throughout the analysis. A brief hydrocarbon source rock assessment is also conducted.

5.1 Palynofacies Techniques

The pre-study (chapter 3.5) demonstrated that most people tend to overestimate the area of particles when implementing visual area estimations. This illustrates the importance of developing more robust techniques for palynofacies analysis. As pointed out previously, point counting is the most commonly employed proxy due to its speed and low cost. The reliability of the point counting method has, however, been a subject for discussion for decades among scientists (for example Van der Plas and Tobi, 1965; Neilson and Brockman, 1977). In palynofacies analysis one potential problem includes the fact that some types of organic matter disintegrate easily. Proximity to the source area is for example an important factor for different OM types as some types of organic matter would break more easily than others, and could easily lead to an overrepresentation when the point counting is the applied method. The results from the present study collaborate this and revealed that there could be visual estimation challenges related to the kerogen group hylogen. The particles from this kerogen group can potentially be overestimated if the sample represents a location which was close to the source area, as the particles are still not broken down.

The present study revealed that the average results for each kerogen group did not show a substantial difference between the two tested methods, as illustrated in figure 5.1. This diagram combines the results presented in the pie charts in figures 4.1 and 4.2 (Sub-chapters 4.1 and 4.2). This was somewhat surprising as the hypothesis based on the pre-study considered the measurement of relative areas based on image analysis to be a more accurate method compared to point counting for estimation of relative proportions of organic matter. The present data does, in other words, not immediately support this hypothesis. However, it is important to bear in mind that there is only roughly 200 meters separating the palynological samples from the top to the base of the succession (Fig. 3.1, chapter 3.1), and different types of OM can dominate in the different facies. An average value of the entire succession will therefore not give a representative result since the samples are recorded from varying depositional facies as described in chapter 2. One advantage of this study is therefore that both methods have been tested in various facies. A limitation is, on the other hand, that analysis in the same type of facies have not been tested more than once due to time constrains in this Master project. Some intervals from the outcrop were sampled more densely, with a 2 meters sampling interval. These slides displayed a larger spread in the results, indicating that with a more densely spaced sampling program, it would have been possible to better analyse the differences in particle size within the different facies.

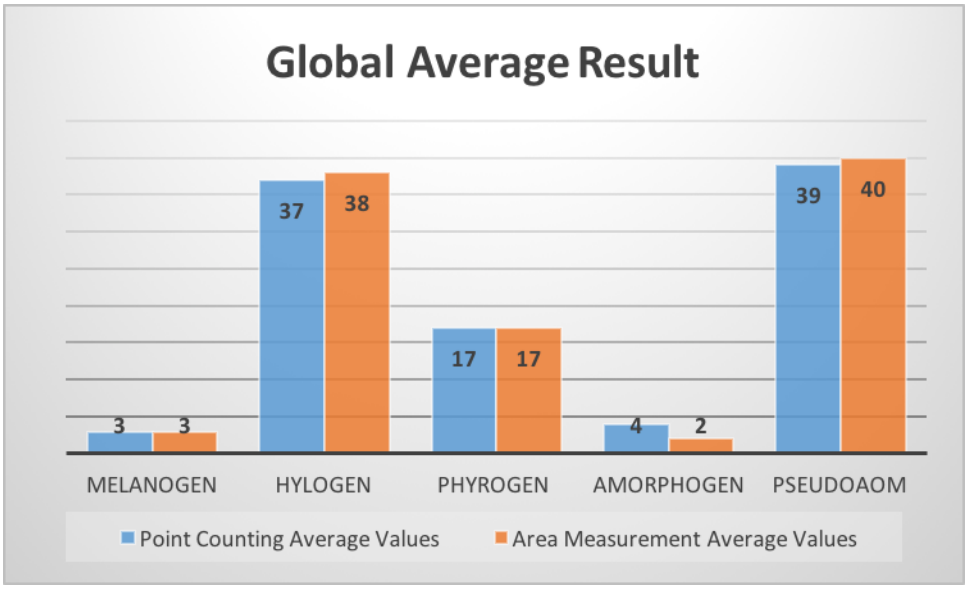

Figure 5. 1: Diagram comparing the average results from the area measurement and the point counting for all five kerogen groups after Bujak *et al*. (1977).

Despite that the average values, based on the results from the point-counting and area measurement methods, did not show any notable differences, more detailed analysis of some kerogen groups recorded more different results when comparing both methods. One difference was shown in the kerogen group amorphogen (sub-chapter 4.4.4). The results clearly demonstrated that point counting might lead to overrepresentation when the studied organic matter is highly degraded, and potentially broken down into several small fragments. The global average difference between the two methods was only 2 % (Fig. 5.1), but there was a 16 % average difference between the two methods in slide BJ24 (Table 4.8, sub-chapter 4.3.4) and in frame 24 of the same slide, 50 % differed between the two methods. This illustrates that there might be a huge spread in the results when comparing the both methods, although this is not clearly portrayed in the global average values, nor when point counting was conducted. As outlined in sub-chapter 3.8 only material recognized by the software ImageJ was included in the study. One cause for the variations in the results within this kerogen group in some samples, could be that the cut off for which material to include was set too low, incorporating particles, which should have been excluded. Amorphogen only counts for 3-4 % of the total OM content, depending on the methodology used. As this study shows, it presents some very interesting results, but this only applies to a small fraction of the total samples. This is also applicable for melanogen, which regardless of the method used, accounted for 3 % (Fig.

5.1) of the total OM in the 29 slides, with a maximum difference between those two methods of 3 % (Table 4.1 and 4.2). The occurrence is sparse, and the difference between the two methods is small. It would therefore be interesting to study these two kerogen groups more thoroughly in samples where they are more abundant.

By observing the results displayed in figure 4.7, it is clear that the size of the particles differs quite a lot within the same kerogen group. This is especially the case for the hylogen group as illustrated in figure 5.2, where two hylogen particles, each marked with an H, are presented and the size difference is clear. This assumption is supported by the large SD values indicating a great spread in the results, which potentially can lead to either over- or underrepresentation of this kerogen group. Hylogen is more common in samples with a terrestrial origin as it is comprised of fibrous plant material from woody components (Rashid, 2012). A controlling factor in the size and spread of the particles in this group is likely to be the proximity to the source of the OM (Koutsoukos, 2005).
Fluvial settings have more energy to break up particles while in a swamp environment the energy is lower and thus, material is more likely to be preserved in bigger particles (Fig 5.3).

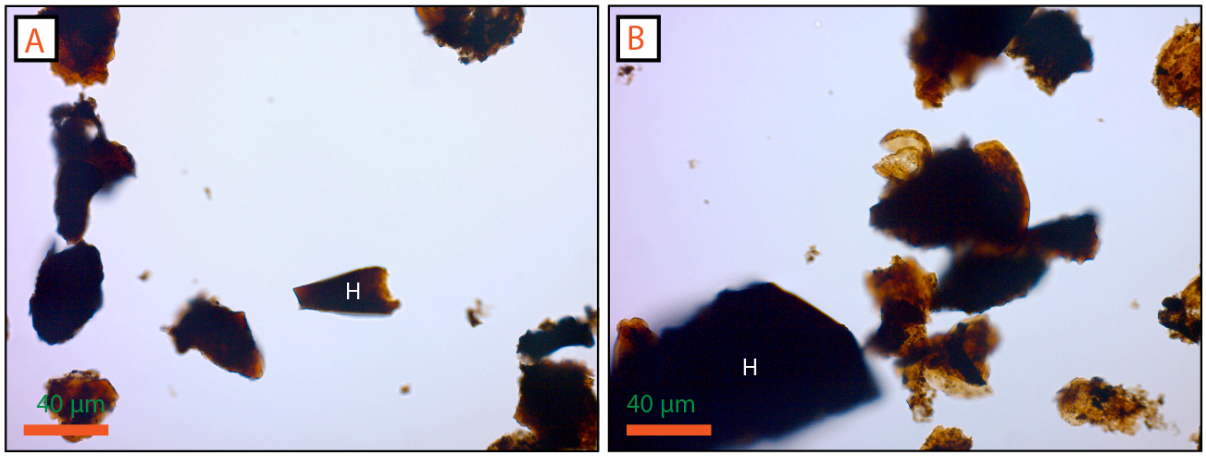

Figure 5. 2: Frame 18 and 35 in kerogen slide BJ20. In each frame a hylogen particle is marked with an "H" to illustrate the difference in size between these two particles..

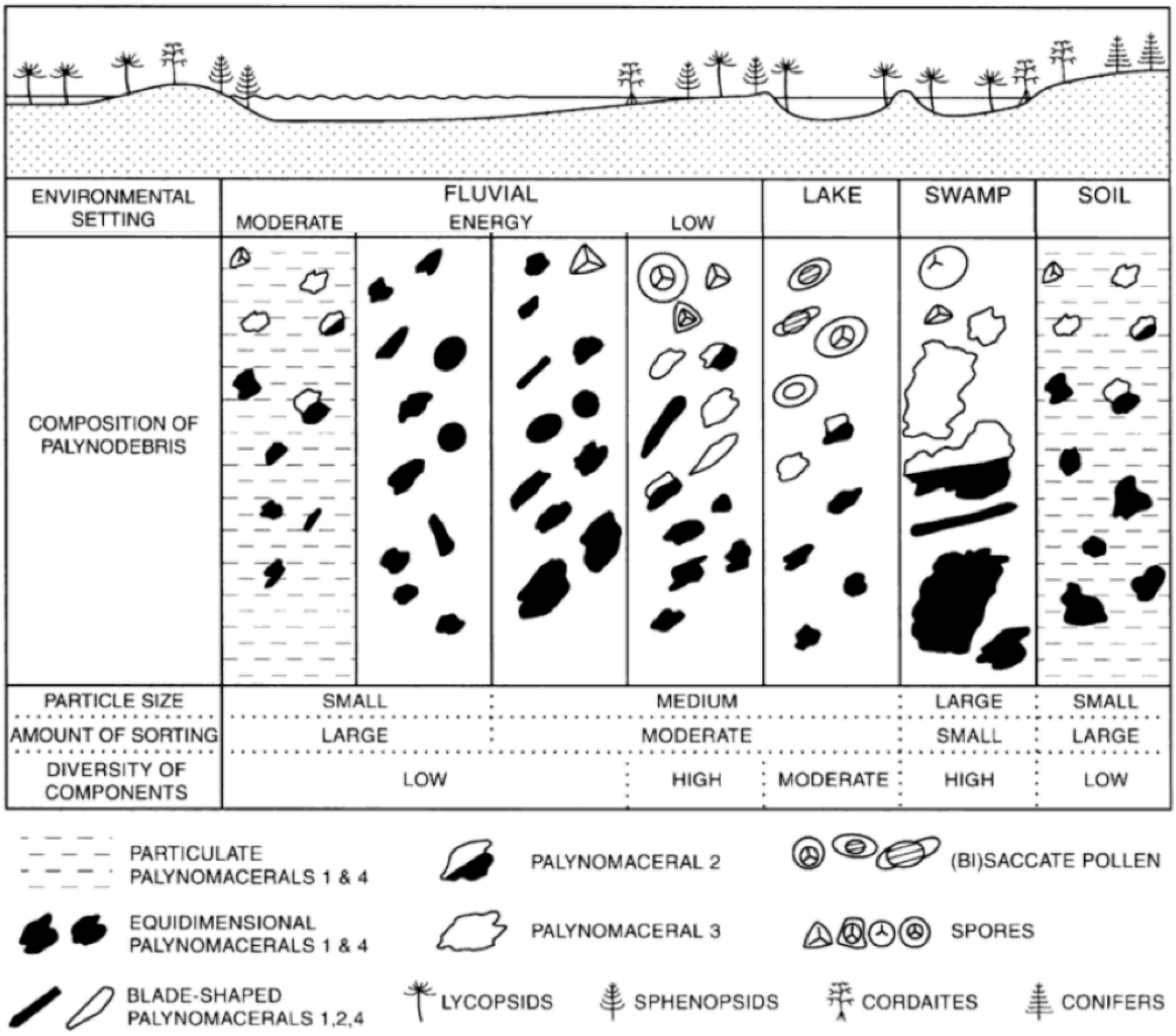

Figure 5. 3: Carboniferous non-marine palynofacies. Modified from Koutsoukos (2005), showing OM and their relative abundance in fluvial to lacustrine and terrestrial deposits.

One kerogen group were the choice of method does not seem to affect the results is phyrogen. Regardless of the applied method, the present study does not demonstrate any significant difference in the average results for this kerogen group (Fig. 5.1). The reason why this happens is not fully understood. Yet, one very likely reason is that phyrogen does not disintegrate as easily during transportation due to its particle size that, at least for material of Carboniferous age is fairly consistent and small.

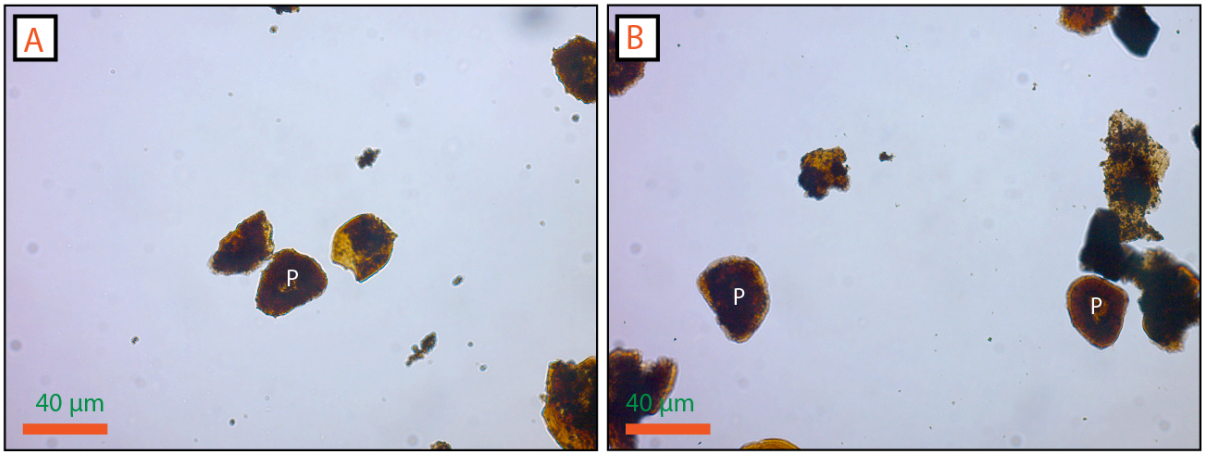

Figure 5. 4: Figure A shows frame 3 and figure B shows frame 4 from the kerogen slide BJ52, illustrating the similarity in size between the two phyrogen particles, both marked with a P.

The kerogen group, pseudoAOM showed a difference of only 1 % between the two tested methods based on the count of 6250 particles (Figs 4.1 and 5.1). For a single slide, the maximum difference between the two methods was 11 % (Slide BJ26, see sub-chapter 4.4.5). Since pseudoAOM is comprised of degraded material that originally could have been either hylogen or phyrogen, it is difficult to interpret the results from this category in terms of size, since the origin of the particles are can be quite different. The results do however point out how the size of the particles can vary, and thus the need for a proper analysis technique to be used. One challenge related to the analysis of this kerogen group was its resemblance to the algae *Botryococcus*, which were common in several of the kerogen slides. Both types of particles can seem morphological similar, but by using a fluorescence microscope they were easily distinguished. *Botryococcus* will fluoresces in bright yellow colour due to its lipid content (Tyson, 1995).

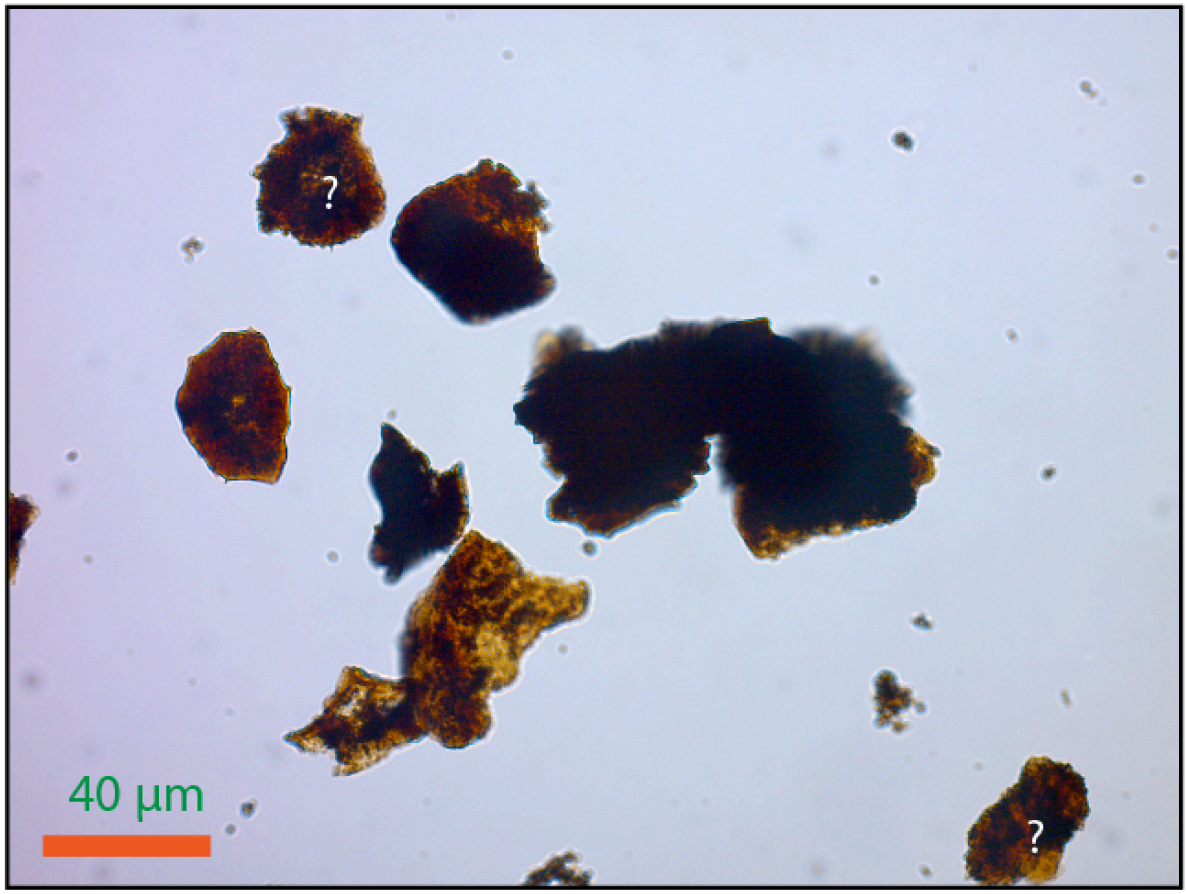

Figure 5. 5: Frame 18 from slide BJ52. The question marks indicate particles where it can be difficult to differentiate *Botryococcus* and/or pseudoAOM.

There have been several attempts to use automated softwares for palynological analysis (e.g. Charles *et al.*, 2007; Holt and Bennett, 2014). Automated point counting has showed several limitations but these programs can be further developed and maybe in the future, they can be seen as an asset. As this project has illustrated, point counting might not be the best approach when trying to determine the actual composition of a sample. The varying sizes within the different kerogen groups are simply too significant for all of them to be counted the same way, regardless of size. One of the limitations regarding the area measurement method when using a software, is that the method can be very time consuming.

In the efforts of working towards an automated point count, where software is programmed to recognise and count palynomorphs, maybe adding another feature as area measurement can be possible in the future. The method would still face the same challenges as automated point count when it comes to problems found in this project, such as overlapping, and particles at different levels in the slide, but it would provide a more representative composition of what is present in the slide.

One disadvantage with the present study is that the comparison between the two methods has only been conducted on terrestrial material. In addition, the fact that there is not much research performed on comparing these methods, can be a challenge, as there are no studies to compare the achieved results with. The findings in this study are therefore only basic assumptions. Today several commercial laboratories are offering to do palynological work on a per-sample fee basis, this is resulting in industry standards often including assessing only a couple of frames per- slide (Traverse, 2007). As demonstrated in this study by the large spread in SD values, this could highly affect the results, and the best protocol to use is to therefore to do area measurement using a software, for a more reliable result.

For future work, area measurement by image analysis should be tested in several facies. Another interesting study would be to study OM particles using z-stack imaging and SEM. This could allow the calculation of a conversion ratio that could enable the estimation of relative volumes of OM types in rocks, rather than relative areas, a more important parameter for predicting what type(s) of hydrocarbons may be generated.

5.2 HC Source Rock Potential

Batten (1982) debated the importance of palynofacies analysis as a tool to identify potential hydrocarbon source rocks. He also pointed out the importance of palynofacies results being confirmed by geochemical data, such as TOC (total organic carbon) and HI (hydrogen index), to evaluate the processes resulting in hydrocarbon accumulation in sediments. Unfortunately, geochemical data were not available for the present study, and calibration to organic analysis was not possible. Therefore, this source rock assessment should only be regarded as a preliminary study.

As noted earlier, no marine indicators were recorded throughout the study, this observation is supported by the palynological analysis obtained from the same samples by Lopes (oral communication). However, the alga *Botryococcus* dominated several samples. A flaw with the classification after Bujak *et al.* (1977) is how OM is placed in one of four (five, in this study) categories, *Botryococcus* is therefore included in phyrogen in this study, and it is not detailed in which samples it is present or more abundant. It was previously stated that one of the reasons for choosing the classification scheme after Bujak *et al.* (1977) was the relatively simple classification, which does not depend upon the analyst's experience. For future work palynomorphs indicative of certain facies should be added to the scheme as sub-groups or even a new group as was the case for pseudoAOM in this study. A fluorescence microscope was used to confirm observations of *Botryococcus* in all the slides. In this process, all occurrences of *Botryococcus* were identified visually, and these observations reflects the results presented by Abdullah *et al.* (1988). According to this study there is an increasing appearance of *Botryococcus* upwards in the succession with the most abundant records in slides BJ50-BJ56 (Fig. 4.21).

The colour of the OM studied was as stated in chapter 3, dark brown to black, with only a few occurrences of material of amber orange colour. This place all the within the red selected area in the classification scheme after Bujak *et al.* (1977), presented in figure 5.6. The colours observed are not definite, and the area marked is an approximation, which is why this assessment can only be regarded as preliminary. The colour (TAI) of the OM can be used to indicate the temperature (T) the material has been exposed to. This is not something that has been studied in detail in this study, but by looking at the selected area

within the red square in figure 5.6, the material have probably been exposed to temperatures between 150-200 ºC Due to the time constrains in the present study it was not possible to, show any substantial differences in the average values for the different methods, therefore it should not make a difference if the HC assessment is based upon the results from the point counting or the area measurement. In this study, the assessment of these samples is based upon the result from area measurement (Fig. 4.23)

The Hoelbreen Member was dominated by hylogen and pseudoAOM, hylogen is most likely in this case gas prone (Fig. 5.3). PseudoAOM is more difficult to interpret, because it is not included in the scheme after Bujak *et al.* (1977). Since pseudoAOM is either derived from hylogen or phyrogen it is assumed that the kerogen group will plot not far from its precursor, and is therefore interpreted to be gas, possibly oil prone.

The Birger Johnsonfjellet Member is dominated by pseudoAOM and to some extent phyrogen. These observations are confirmed by Abdullah *et al.* (1988) who noted an increased *Botryococcus* occurrence in the Birger Johnsonfjellet Member. Based on the recorded occurrences of pseudoAOM, together with the increased occurrence of phyrogen, this member is interpreted to be more oil prone.

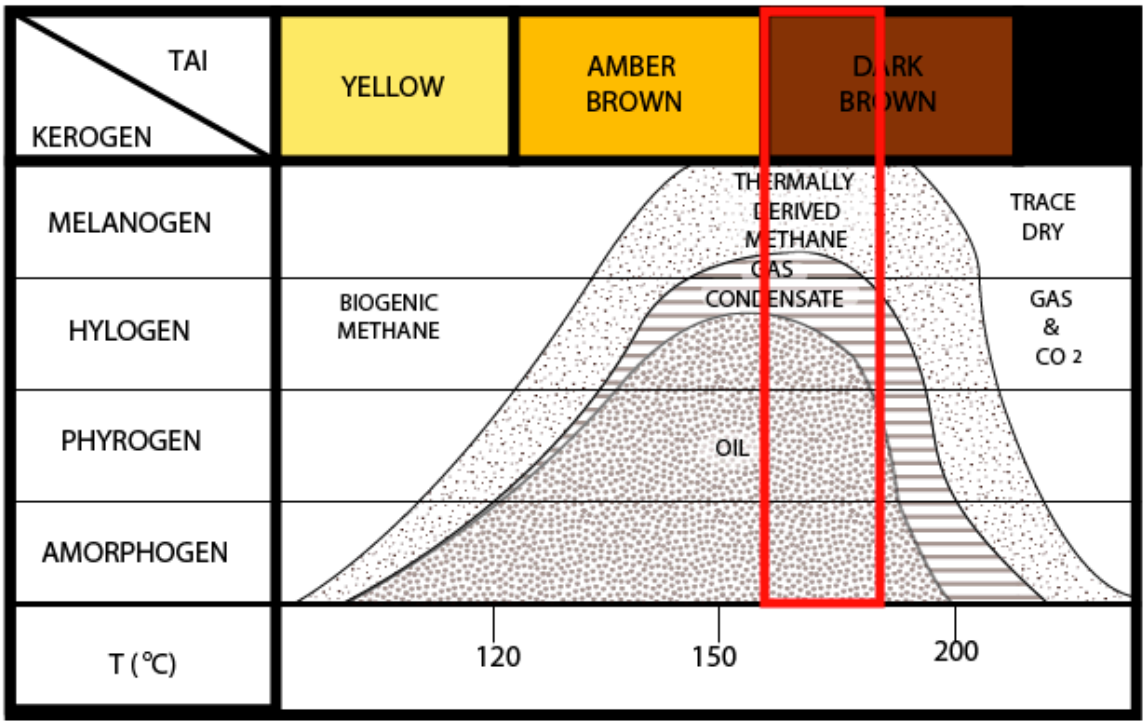

Figure 5. 6: Illustration of the relationship between kerogen type, spore colour, hydrocarbon generation and temperature. The colour of the samples analysed in this study places the OM within the selected area (Modified from Bujak *et al.*, 1977). TAI – Thermal alteration index, T – Temperature.

5.3 Possible Sources of Error

In science, various sources of error are important to be aware of and take into account, some challenges related to the present study are discussed below.
As discussed above, one of the limitations in this study is related to software accuracy. For this study, and studies of its kind, material not recognized by the software is not included although some slides did contain a lot of debris not accounted for. This can lead to inaccurate interpretation of the samples.
Another uncertainty in this type of analysis is the subjectivity of the analyst. This will probably not affect the testing of the methods, if the analyst is consistent, but misinterpretations could e.g. affect the source rock analysis. That is why calibrating the observations with geochemical data is highly recommended (Batten, 1982). The analyst experience is also a central factor, which potentially can play a big role in the results, referring to how easily misinterpretations can be done as explained with the distinction between *Botryococcus* and PseudoAOM particles.

The samples in this study are outcrop samples, and the author did not participate in the sampling. However, it has been assured that the standard precautions and protocol for palynological sampling such as avoiding weathered material with a risk of oxidation were carefully followed.

A final issue that can also be considered in the present study is the choice of the laboratory preparation technique. The palynological processing technique can affect the any palynological analysis (see for example Wood *et al,.* 1996). As stated previously the samples analysed in this study were processed using standard palynological kerogen preparation techniques after Doher (1980). This is a standardized method, and as explained by Wood *et al.* (1996), each laboratory develops its own techniques often depending on available lab equipment, mounting material, as well as their sterility and routines in order to avoid contamination (Wood *et al.,* 1996). One potential issue is how the crushing of the sample could break down the OM in smaller fragments. Several publications have presented differences in the processing technique for specified aims, including Brown (1960), (Doher, 1980) and Traverse (1988). In the case of palynofacies

analysis, avoiding oxidation and ultra-sound techniques is of outmost importance during the material preparation.

6. Conclusions

Based on the studies of the 29 kerogen slides, the analysis of 1 789 photographed frames, and a total of 16 226 particles counted and measured, the following conclusions can be drawn/made:

- The pre – study demonstrated that people's persuasions of visual estimation tend to be more subjective than desired, and overestimation of particle size often occurs.
- The average result of the kerogen estimates does not seem to be affected by the method used, as long as a satisfactory number of frames are tested per samples (in this study, 60 frames).
- Aerial estimation results of the kerogen groups amorphogen and phyrogen showed the widest range of differences based on the same samples when studying single frames. In the comparison between the two methods, differences of up to 50 % for amorphogen was observed in certain analysed frames.
- The major differences observed in the size of the hylogen particles are likely to be related to proximity to the source of the material, as energy level would influence the size of the particles.
- Phyrogen did not show a substantial difference in the size of the particles in the studied samples. This is assumed to be a combination of the acid resistant wall structure which does not break down particles easily combined with the consistency in the size of material of Carboniferous age.
- PseudoAOM did not show much difference between the two methods tested, and the maximum difference within a single frame was 11 %. It is difficult to conclude with a reason for this as the precursor for the pseudoAOM is unknown.
- The relatively high standard deviation values for all kerogen groups indicates a great spread in the size, and number of organic matter particles.
- The findings from this study suggests that area measurement is a more reliable method for palynofacies analysis than point counting based on the relatively large variations observed when comparing the results from the two methods tested herein.

- The colour of the OM studied was dark brown when compared to the scheme of Bujak *et al.* (1977), indicating that the OM is mature. The preliminary hydrocarbon assessment suggests that the Hoelbreen Member, dominated by hylogen and pseudoAOM is mainly gas prone. While the Birger Johnsonfjellet Member which had an increased amount of phyrogen as well as increased amounts of *Botryococcus*, is regarded as oil prone.

7. References

Abdullah, W., Murchison, D., Jones, J., Telnaes, N., & Gjelberg, J. (1988). Lower Carboniferous coal deposition environments on Spitsbergen, Svalbard. *Organic geochemistry, **13***, 953-964.

Batten, D. (1982). Palynofacies, palaeoenvironments and petroleum. *Journal of Micropalaeontology, **1**,* 107-114.

Batten, D., & Stead, D. (2005). Palynofacies analysis and its stratigraphic application. *Applied stratigraphy*, 203-226.

Brown, C. A. (1960). Palynological techniques. *CA Brown*.

Bujak, J. P., Barss, M. S., & Williams, G. L. (1977). Offshore eastern Canada - Part I and II: Organic type, color and hydrocarbon potential. *Oil and Gas Journal, **75***, 96-100 & 198-202.

Charles, J., Kuncheva, L. I., Wells, B., & Lim, I. (2008). Object segmentation within microscope images of palynofacies. *Computers & Geosciences, **34***, 688-698.

Combaz, A. (1964). Les palynofacies. *Revue de Micropaléontologie*, **7**, 205-218.

Cutbill, J., & Challinor, A. (1965). Revision of the stratigraphical scheme for the Carboniferous and Permian rocks of Spitsbergen and Bjørnøya. *Geological Magazine, **102***, 418-439.

Cutbill, J. L., Henderson, W. G., & Wright, N. J. R. (1976). The Billefjorden Group (Early Carboniferous) of Central Spitsbergen. *Norsk Polarinstitutt Skrifter*, **164**, 57-89.

Dallmann, W. K., Gjelberg, J. G., Harland, W. B., Johannessen, E. P., Keilen, H. B., Lønøy, A., ... & Worsley, D. (1999). Upper Palaeozoic lithostratigraphy. *Lithostratigraphic lexicon of Svalbard. Norsk Polarinstitutt, Tromsø*, 25-126.

Doher, L. I. (1980). Palynomorph preparation procedures currently used in the paleontology and stratigraphy laboratories*, US Geological Survey* (2330-5703).

Doré, A. (1991). The structural foundation and evolution of Mesozoic seaways between Europe and the Arctic. *Palaeogeography, Palaeoclimatology, Palaeoecology,* **87,** 441-492.

Doré, A. (1995). Barents Sea geology, petroleum resources and commercial potential. *Arctic*, 207-221.

Durand, B., & Monin, J. C. (1980). Elemental analysis of kerogens (C, H, O, N, S, Fe). *Kerogen: Paris, Editions Technip*, 113-142.

Ercegovac, M., & Kostić, A. (2006). Organic facies and palynofacies: Nomenclature, classification and applicability for petroleum source rock evaluation. *International Journal of Coal Geology,* **68**, 70-78.

Faleide, J. I., Gudlaugsson, S. T., & Jacquart, G. (1984). Evolution of the western Barents Sea. *Marine and Petroleum Geology,* **1**, 123-150.

Gjelberg, J. G. & Steel, R. J. (1981). An outline of Lower– Middle Carboniferous sedimentation on Svalbard: effects of tectonic, climatic and sea level changes in rift basin sequences. *Canadian Society of Petroleum Geologists Memoir,* ***7***, 543–62.

Holt, K. A., & Bennett, K. (2014). Principles and methods for automated palynology. *New Phytologist,* ***203***, 735-742.

Jakobsson, M., L. A. Mayer, B. Coakley, J. A. Dowdeswell, S. Forbes, B. Fridman, H. Hodnesdal, R. Noormets, R. Pedersen, M. Rebesco, H.-W. Schenke, Y. Zarayskaya A, D. Accettella, A. Armstrong, R. M. Anderson, P. Bienhoff, A. Camerlenghi, I. Church, M. Edwards, J. V. Gardner, J. K. Hall, B. Hell, O. B. Hestvik, Y. Kristoffersen, C. Marcussen, R. Mohammad, D. Mosher, S. V. Nghiem, M. T. Pedrosa, P. G. Travaglini, and P. Weatherall, The International Bathymetric Chart of the Arctic Ocean (IBCAO) Version 3.0, *Geophysical Research Letters*, doi: 10.1029/2012GL052219.

Jansonius, J., & McGregor, D. C (1996). Palynology, principles and applications. *American Association of Stratigraphic Palynologist Foundation,* **5**.

Jäger, H., McLean, D., (2008). Palynofacies and spore assemblage variation of upper Visean (Mississippian) strata across the southern North Sea. Rev. *Paleobotany, Palynology,* **148**, 136-153.

Koutsoukos, E. (2005). Stratigraphy: Evolution of a concept. *Applied stratigraphy*, 3-19.

Larssen, G.B., Elvebakk, G., Henriksen, L.B., Kristensen, S.E., Nilsson, I., Samuelsberg, T.J., Svånå, T.A., Stemmerik, L., Worsley, D., (2005). Upper Palaeozoic lithostratigraphy of the southern part of the Norwegian Barents Sea. Nor*. Geol. Unders*. **444**, 3–45.

McPhilemy, B. (1988). The value of fluorescence microscopy in routine palynofacies analysis: Lower Carboniferous successions from counties Armagh and Roscommon, Ireland. *Review of palaeobotany and palynology,* ***56,*** 345-359.

Mendonça Filho, J. G., Menezes, T. R., de Oliveira Mendonça, J., de Oliveira, A. D., da Silva, T. F., Rondon, N. F., & da Silva, F. S. (2012). Organic facies: palynofacies and organic geochemistry approaches *Geochemistry-Earth's System Processes*: InTech.

Mertens, K. N., Verhoeven, K., Verleye, T., Louwye, S., Amorim, A., Ribeiro, S., Deaf, A. S., Harding, I. C., De Schepper, S., & González, C. (2009). Determining the absolute abundance of dinoflagellate cysts in recent marine sediments: the Lycopodium marker-grain method put to the test. *Review of Palaeobotany and Palynology,* ***157***, 238-252.

Muller, J. (1959). Palynology of recent Orinoco delta and shelf sediments: reports of the Orinoco shelf expedition. *Micropaleontology*, **5,** 1-32.

Mørk, A., Dallmann, W. K., Dypvik, H., Johannessen, E. P., Larssen, G. B., Nagy, J., Nøttvedt, A., Olaussen, S., Pchelina, T. M., and Worsley, D., (1999). Mesozoic lithostratigraphy: Lithostratigraphic lexicon of Svalbard. Upper Palaeozoic to Quaternary bedrock. *Review and recommendations for nomenclature use*, p. 127-214.

Neilson, M., & Brockman, G. (1977). The error associated with point-counting. *American Mineralogist,* **62**, 1238-1244.

NPD, (2016), Resource Report, http://www.npd.no/en/Publications/Resource-Reports/2016/

Nøttvedt, A., Cecchi, M., Gjelberg, J. G., Kristensen, S. E., Lønøy, A., Rasmussen, A., Rasmussen, E., Skott, P. H. & van Veen, P. M. (1992a) SvalbardBarents Sea correlation: a short review. In Vorren, T. O. *et al*. (eds.): Arctic Geology and Petroleum Potential, 363-375. Norwegian Petroleum Society (NPF), Special Publication No. 2, Elsevier, Amsterdam.

Nøttvedt, A., Livbjerg, F., Midbøe, P. S. & Rasmussen, E. (1992b). Hydrocarbon potential of the Central Spitsbergen Basin. In Vorren, T. O. *et al*. (eds*.): Arctic Geology and Petroleum Potential*, 333-361. Norwegian Petroleum

Palaeos, (2002). (18.06.2017) Retrieved from http://palaeos.com/paleozoic/carboniferous/mississippian.htm

Pickard, N. A., Eilertsen, F. L. E. M. M. I. N. G., Hanken, N. M., Johansen, T. A., Lønøy, A., Nakrem, H. A., ... & Somerville, I. D. (1996). Stratigraphic framework of Upper Carboniferous (Moscovian-Kasimovian) strata in Bünsow land, central Spitsbergen: palaeogeographic implications. *Norsk Geologisk Tidsskrift*, ***76***, 169-185.

Playford, G., (1962). The Lower Carboniferous microfloras of Spitsbergen. *Palaeontology* ***5****,* 550–678.

Rashid, M. A. (2012). *Geochemistry of marine humic compounds*. Springer Science & Business Media.

Samuelsberg, T.J., Pickard, N.A.H., (1999). Upper Carboniferous to Lower Permian transgres- sive–regressive sequences on central Spitsbergen. *Geol. J.* **34**, 393–411.

Sakshaug, E., Bjørge, A., Gulliksen, B., Loeng, H., & Mehlum, F. (1994). Structure, biomass distribution, and energetics of the pelagic ecosystem in the Barents Sea: a synopsis. *Polar Biology,* **14,** 405-411.

Smelror, M., Petrov, O., Larssen, G. B., & Werner, S. (2009). Geological history of the Barents Sea. *Norges Geol. undersøkelse*, 1-135.

Staplin, F.L. (1969). Sedimentary organic matter, organic metamorphism and oil and gas occurence. *Bulletin of Canadian Petroleum Geology*, **17**, 47-66.

Terry, R. D., & Chilingar, G. V. (1955). Summary of:" Concerning some additional aids in studying sedimentary formations. *J. Sediment. Petrol, **25***, 229-234.

Tissot, B., & Welte, D. (1984). Petroleum formation and occurrence: Springer, New York.

Traverse, A., (1988). Paleopalynology, first edition*, Unwin Hyman*, Boston, 600 pp.

Traverse, A., 2007. Paleopalynology. second edition. *Springer*, Dordrecht, Netherlands, pp. 1- 813.

Tyson, R. V. (1993). Palynofacies analysis *Applied micropalaeontology* (pp. 153-191): *Springer.*

Tyson, R. V. (1995). Palynological kerogen classification Sedimentary Organic Matter (pp. 341-365): *Springer.*

Van der Plas, L., & Tobi, A. (1965). A chart for judging the reliability of point counting results. *American Journal of Science, **263*,** 87-90.

Van der Zwan, C.J., 1981. Palynology, phytogeography and climate of the Lower Carboniferous. *Palaeogeography, Palaeoclimatology*, *Palaeoecology*, **33**, 279-310.

Van der Zwan, C.J., Boulter, M.C., Hubbard, R.N.L.B., (1985). Climatic change during the Lower Carboniferous in Euramerica, based on multivariate statistical analysis of palynological data. *Palaeogeography, Palaeoclimatology, Palaeoecology, **52*,** 1-20.

Willis, K.J. and McElwain, J.C., (2014). The Evolution of Plants, second edition, *Oxford University Press, UK,* 398 p.

Wood, G. D., Gabriel, A. M., & Lawson, J. C. (1996). Palynological techniques—processing and microscopy. *Palynology: principles and applications*, **1**, 29-50.

Worsley, D. (2008). The post-Caledonian development of Svalbard and the western Barents Sea. *Polar Research,* **27**, 298-317.

Worsley D., Aga O.J., Dalland A., Elverhøi A. and Thon A. (1986). The geological history of Svalbard-evolution of an Arctic acrchipelago. *Stavanger: Statoil*

Worsley, D., Nøttvedt, A., (2008). Vast lowland plains, coal and salt — Chapter 9. In: Ramberg, I.B., Bryhni, I., Nøttvedt, A., Rangnes, K. (Eds.), *The Making of a Land: Geology of Norway.* Norwegian Geological Association, pp. 304–329.